

# **MECHANICS OF POROELASTIC GEOLOGIC MEDIA SUSCEPTIBLE TO DAMAGE**

By  
Ali Shirazi  
May, 2004

Department of Civil Engineering and Applied Mechanics  
McGill University, Montreal, QC, Canada, H3A 2K6

A thesis submitted to  
McGill University  
in partial fulfillment of the requirements for the degree of  
Doctor of Philosophy

©Copyright  
2004, A. Shirazi



Library and  
Archives Canada

Bibliothèque et  
Archives Canada

Published Heritage  
Branch

Direction du  
Patrimoine de l'édition

395 Wellington Street  
Ottawa ON K1A 0N4  
Canada

395, rue Wellington  
Ottawa ON K1A 0N4  
Canada

*Your file    Votre référence*

*ISBN: 0-494-06342-4*

*Our file    Notre référence*

*ISBN: 0-494-06342-4*

#### NOTICE:

The author has granted a non-exclusive license allowing Library and Archives Canada to reproduce, publish, archive, preserve, conserve, communicate to the public by telecommunication or on the Internet, loan, distribute and sell theses worldwide, for commercial or non-commercial purposes, in microform, paper, electronic and/or any other formats.

The author retains copyright ownership and moral rights in this thesis. Neither the thesis nor substantial extracts from it may be printed or otherwise reproduced without the author's permission.

#### AVIS:

L'auteur a accordé une licence non exclusive permettant à la Bibliothèque et Archives Canada de reproduire, publier, archiver, sauvegarder, conserver, transmettre au public par télécommunication ou par l'Internet, prêter, distribuer et vendre des thèses partout dans le monde, à des fins commerciales ou autres, sur support microforme, papier, électronique et/ou autres formats.

L'auteur conserve la propriété du droit d'auteur et des droits moraux qui protègent cette thèse. Ni la thèse ni des extraits substantiels de celle-ci ne doivent être imprimés ou autrement reproduits sans son autorisation.

---

In compliance with the Canadian Privacy Act some supporting forms may have been removed from this thesis.

Conformément à la loi canadienne sur la protection de la vie privée, quelques formulaires secondaires ont été enlevés de cette thèse.

While these forms may be included in the document page count, their removal does not represent any loss of content from the thesis.

Bien que ces formulaires aient inclus dans la pagination, il n'y aura aucun contenu manquant.

  
**Canada**

*To My Parents*

## Abstract

The classical theory of poroelasticity developed by Biot (1941) deals with the time-dependent response of the fluid-saturated porous media derived from the coupling of the mechanical deformations and the deformations of pore fluid. The classical theory of poroelasticity has been successfully applied to a range of problems of interest to geomechanics and biomechanics. The brittle poroelastic media can experience alterations in poroelasticity properties resulting from the generation and/or growth of micro-defects. The effects can be modelled by appeal to continuum damage mechanics. Damage-induced alterations can influence the consolidation behaviour of a damage-susceptible poroelastic medium. Continuum damage mechanics concepts can be incorporated within the theory of poroelasticity to model the damage-induced alterations in poroelasticity properties. This thesis deals with the development of a computational procedure for modelling the damage-induced alterations in both elasticity and hydraulic conductivity characteristics of a brittle poroelastic medium. Furthermore, the evolution of damage can also exhibit a stress state-dependency. The computational procedure has also been extended to include the stress state-dependent evolution of damage in brittle poroelastic media. The alterations in the elastic stiffness and the hydraulic conductivity are characterized through a damage evolution function with relationship to distortional strain invariant. The stress state-dependency of the damage process is governed by the state of the volumetric strains. It is assumed that an overall decrease in the volumetric strains does not result in damage evolution.

The computational procedure that accounts for damage-induced evolution of stiffness and hydraulic properties and stress state dependency in damage evolution are used to model practical problems of interest in geomechanics, applied mechanics and civil engineering. The fluid pressure development within a spheroidal fluid inclusion surrounded by a damage-susceptible poroelastic medium has been examined through the computational procedure. The computational procedure has also been used to study time-dependent translational displacements of a rock socket embedded in a damage susceptible soft rock



and the procedure has been also applied to examine the time-dependent in-plane displacements of a flat elliptical rigid anchorage. The computational results indicate that the consolidation behaviour of the brittle poroelastic media can be significantly influenced through consideration of the damage-induced alterations in both the elastic stiffness and the hydraulic conductivity, the latter property exerting a greater influence. The dependency of the evolution of damage to the state of stresses can also influence the consolidation of a poroelastic medium.

## Résumé

La théorie classique de la poroélasticité développée par Biot (1941) traite la réponse transitoire des matériaux poreux saturés à travers le couplage des déformations mécaniques et des déformations du fluide poreux. La théorie classique de la poroélasticité a été utilisée avec succès dans la résolution de plusieurs problèmes de géomécanique et de biomécanique. Le milieu poroélastique fragile peut subir des altérations dans les propriétés poroélastiques qui résultent de la génération et/ou croissance des micro-défauts. Ces altérations induites par endommagement peuvent influencer la consolidation des matériaux poroélastiques il ne peut pas être modélisé par la théorie classique de poroélasticité.

Le concept de la mécanique des milieux continus endommagés introduit par Kachanov (1985) peut être incorporée dans la théorie de la poroélasticité pour modéliser les altérations induites par endommagement aux propriétés poroélastiques. Le but de cette étude est de développer une méthode itérative par éléments finis considérant les altérations induites par endommagement aux caractéristiques élastiques et hydrauliques d'un milieu poroélastique fragile. De surcroît, l'évolution de l'endommagement peut devenir dépendante de l'état des contraintes ; la procédure de calcul a également été élargie pour inclure cette dépendance dans un milieu poroélastique fragile. Les altérations de la rigidité élastique sont caractérisées à travers une fonction d'évolution d'endommagement en relation avec l'invariant de la déformation de distorsion. Dans un contexte géomécanique, l'évolution de l'endommagement peut mener à une augmentation de la conductivité hydraulique dans les géomatériaux. Il y a peu d'observations expérimentales sur l'effet de l'endommagement sur la conductivité hydraulique des géomatériaux et son influence sur la consolidation des géomatériaux. Les altérations à la conductivité hydraulique sont caractérisées par une fonction d'endommagement basée sur les observations expérimentales disponibles. La dépendance du procédé d'endommagement sur l'état de contraintes est régie par l'état des déformations volumétriques. On considère que la compaction due à l'état des

déformations mène à une insignifiante évolution d'endommagement dans les matériaux poroélastiques susceptibles à l'endommagement. La méthode de calcul est utilisée pour résoudre des problèmes en géomécanique, mécanique appliquée ainsi qu'en génie civil. Le développement de la pression du fluide dans une inclusion fluide sphérique entourée d'un milieu poroélastique à dommage-susceptible a été examiné par cette méthode de calcul. La méthode de calcul a également été utilisée pour étudier le déplacement latéral transitoire d'une inclusion rocheuse rigide dans une matrice rocheuse élastique. Elle a également été appliquée pour examiner le déplacement d'un ancrage elliptique plat rigide.

Les résultats numériques indiquent que la consolidation d'un milieu poroélastique fragile peut être significativement influencée par les altérations induites par endommagement à la conductivité hydraulique. La dépendance de l'évolution de l'endommagement à l'état de contraintes peut également influencer la consolidation d'un milieu poroélastique.

## **Acknowledgments**

Foremost, the author praises God for giving him health, strength and patience during years of studying.

The author wishes to express his sincere gratitude to his doctoral research supervisor, Professor A.P.S. Selvadurai, William Scott Professor, Department of Civil Engineering and Applied Mechanics for suggesting the topic of research, his extensive guidance, encouragement and support during this research. His invaluable comments and extensive reviews and corrections to several drafts of the thesis are greatly appreciated.

Sincere thanks and appreciation goes to Dr. Gilles Armand for his useful discussions and advice in programming of computational procedure used in this research.

Sincere thanks and appreciation also go to Wenjun Dong, Qifeng Yu, Hani Ghiabi and Tuan Ahn Luu for creating a friendly and stimulating environment in the Computational Geomechanics Research laboratory.

Special thanks are due to Mr. Reza Shirazi for his assistance in revision of abstract of this thesis written in French.

The financial support provided by the Natural Sciences and Engineering Research Council of Canada through research grants awarded to Professor A.P.S. Selvadurai is also acknowledged.

Finally, the author is indebted to his family who always provided him with love, care and support during all stages of his study.

## Table of Contents

Abstract	iii
Résumé	v
Acknowledgments	vii
List of Figures	xii
List of Symbols	xviii
List of Publications Resulting from the Research	xxi
 1 INTRODUCTION AND LITERATURE REVIEW	 1
1.1 General	1
1.2 Theory of Poroelasticity	2
1.3 Applications of Poroelasticity	3
1.4 Non-linear Behaviour of Soil Skeleton	9
1.4.1 Continuum Damage Mechanics	12
1.5 Experimental Observations on Damage Evolution	14
1.5.1 Damage-induced Alterations in Mechanical Properties	15
1.5.2 Damage-induced Alterations in Hydraulic Conductivity Properties	17
1.6 Computational Modelling of Damage Evolution in a Saturated Brittle Geomaterial	21
1.7 Objectives and Scope of the Research	22
1.8 Statement of Originality and Contributions	24
 2 COMPUTATIONAL DEVELOPMENTS IN THE MODELLING OF POROELASTIC MEDIA	 25
2.1 Introduction	25

2.2	Classical Theories of Poroelasticity	26
2.3	Governing Equations of Poroelasticity	32
2.4	Computational Modelling of Poroelastic Media	37
2.5	Finite Element Formulations	39
2.5.1	Galerkin Weighted Residual Method	39
2.5.1.1	Galerkin Formulation for the Equilibrium Equation	40
2.5.1.2	Galerkin Formulation for the Fluid Continuity Equation	42
2.5.1.3	Time Integration and Stability	44
2.5.2	Finite Element Discretization in Space	45
2.5.3	Numerical Properties of the Discretization in Time	47
3	MECHANICS OF BRITTLE FLUID SATURATED POROELASTIC MEDIA SUSCEPTIBLE TO MICRO-MECHANICAL DAMAGE	50
3.1	Introduction	50
3.2	Continuum Damage Mechanics Concepts	53
3.2.1	The Damage Variable	56
3.2.2	The Net Stress	57
3.3	The Evolution of Damage	59
3.4	Stress State-dependency of the Evolution of Damage	60
3.5	Theoretical Observations on Damage-induced Alterations in the Poroelasticity Parameters	61
3.5.1	Damage-induced in Elastic Stiffness of the Brittle Materials	62
3.5.2	Damage-induced Alterations in Hydraulic conductivity of a Damage- susceptible Geomaterial	64
3.6	Computational Scheme for Time-dependent Response of Brittle Geomaterials Susceptible to Damage	65
3.6.1	Degradation in Elasticity Parameters	65
3.6.2	Alterations in Hydraulic conductivity	66

3.7	The Computational Procedures	66
4	ONE-DIMENSIONAL CONSOLIDATION OF POROELASTIC MEDIA	69
4.1	General	69
4.2	The One-dimensional Consolidation of a Poroelastic Layer	70
4.2.1	Analytical Solution of One-dimensional Consolidation Using Terzaghi's Theory	71
4.2.2	Analytical Solution of One-dimensional Consolidation Using Biot's Theory	72
4.2.3	Numerical Results for the Problem of One-dimensional Consolidation	73
4.3	The Problem of Consolidation of a Poroelastic Sphere	78
4.3.1	Analytical Solution for Consolidation of a Poroelastic Sphere Based on Terzaghi's Theory	79
4.3.2	Analytical Solution for Consolidation of a Poroelastic Sphere Based on Biot's Theory	80
4.4	Numerical Results for Consolidation of a Poroelastic Sphere	82
5	THE SPHEROIDAL FLUID-FILLED INCLUSIONS IN DAMAGE-SUSCEPTIBLE POROELASTIC GEOLOGIC MEDIA	85
5.1	Introduction	85
5.2	Computational Modelling and Results	87
5.2.1	The Oblate Spheroidal Fluid Inclusion	89
5.2.2	The Prolate Spheroidal Fluid Inclusion	95

6	LATERAL LOADING OF A ROCK SOCKET EMBEDDED IN A DAMAGE-SUSCEPTIBLE GEOLOGICAL MEDIUM	101
6.1	Introduction	101
6.2	Elastic Solutions for a Rigid Pile Embedded in an Elastic Half-space	105
6.3	Computational Modelling of the Laterally Loaded Rock Socket	107
6.4	Computational Results	110
7	MECHANICS OF AN IN-PLANE LOADED RIGID ANCHORAGE EMBEDDED IN A DAMAGE-SUSCEPTIBLE POROELASTIC REGION	122
7.1	Introduction	122
7.2	Elastic Solution for the In-plane Loading of a Flat Anchor Region	127
7.3	Computational Modelling	129
7.4	Computational Results and Discussion	130
8	CONCLUSIONS AND RECOMMENDATIONS	139
8.1	General	139
8.2	Summary and Concluding Remarks	139
8.3	Recommendations for Future Work	144
	REFERENCES	146



## List of Figures

Figure 1.1	Indentation of a brittle poroelastic geomaterial	12
Figure 1.2	Micro-cracks in sandstone (Modified after Gatelier <i>et al.</i> , 2002)	15
Figure 1.3	The results of uniaxial compression tests conducted on concrete (After Spooner and Dougill, 1975)	16
Figure 1.4	The results of uniaxial compression tests conducted on concrete (After Mazars and Pijaudier-Cabot, 1989)	17
Figure 1.5	The evolution of hydraulic conductivity in saturated geomaterials (a) after Zoback and Byerlee (1975) and (b) after Shiping <i>et al.</i> (1994)	19
Figure 1.6	The evolution of hydraulic conductivity in saturated geomaterials (After Souley <i>et al.</i> , 2001)	19
Figure 1.7	The evolution of hydraulic conductivity in natural salt (After Schulze <i>et al.</i> , 2000)	20
Figure 1.8	Alterations in hydraulic conductivity of the saturated geomaterials as an increase at stress levels well below the peak and as an decrease in high confining pressure (After Wang and Park, 2002)	20
Figure 2.1	Three-dimensional isoparametric element	46
Figure 3.1	Typical stress-strain curve and the damaged induced alterations in hydraulic conductivity of the brittle geomaterials	51
Figure 3.2	Representative element of (a) virgin state and (b) damaged state of brittle material	56
Figure 3.3	Schematic presentation for the hypothesis of strain equivalence	57
Figure 3.4	A cracked volume subjected to stress (a) micro-cracks (b) micro-voids	61
Figure 3.5	Computational scheme for the stress analysis of a poroelastic medium exhibiting stress state-dependent	68

	evolution of damage stress state-dependent	
Figure 4.1	Boundary conditions for the problem of one-dimensional consolidation	70
Figure 4.2	Finite element discretization of the domain considered in the problem of one-dimensional consolidation	75
Figure 4.3	A comparison between the computational results obtained by the finite element procedure and analytical results for ideal poroelasticity. (results for both loading and unloading)	76
Figure 4.4	Computational results for one-dimensional consolidation ( <i>Stress state-independent evolution of damage</i> )	76
Figure 4.5	Computational results for one-dimensional consolidation ( <i>Stress state-dependent evolution of damage</i> ) (results for both loading and unloading)	77
Figure 4.6	Computational results for two choices of computational schemes (A) only edge nodes account for pore pressure effects, (B) all nodes account for pore pressure effects	77
Figure 4.7	The problem of the consolidation of a poroelastic sphere	78
Figure 4.8.	The Mandel-Cryer effect, obtained from the experimental observations (After Gibson <i>et al.</i> , 1963)	82
Figure 4.9	Pore pressure development at the centre of a poroelastic sphere	84
Figure 5.1	Oblate spheroidal fluid inclusion in an extended poroelastic medium	90
Figure 5.2	Finite element discretization of the damage susceptible poroelastic medium bounded internally by an oblate spheroidal fluid inclusion: geometry and boundary conditions	90
Figure 5.3	Evolution of fluid pressure in the oblate spheroidal fluid inclusion in a non-isotropic far field stress field: Comparison of results for the damaged and ideal poroelasticity material responses ( $n = 0.5$ ) ( <i>Stress state-independent damage evolution</i> )	91
Figure 5.4	Evolution of fluid pressure in the oblate spheroidal	92

	fluid inclusion in a non-isotropic far field stress field : Comparison of results of the damaged and ideal poroelasticity material responses ( $n = 0.5; 1.0$ ) ( <i>Stress state-independent damage evolution</i> )	
Figure 5.5	Evolution of fluid pressure in the oblate spheroidal fluid inclusion: Influence of the geometry of the oblate spheroidal inclusion in a non-isotropic far field stress field. ( <i>Stress state-independent damage evolution</i> )	93
Figure 5.6	Evolution of fluid pressure in the oblate spheroidal fluid inclusion in a non-isotropic far field stress with different deviatoric stress ratios ( <i>Stress state-dependent damage evolution.</i> [ $R = \sigma_A / \sigma_R$ ; $n = b/a$ ; $\sigma_m = (\sigma_A + 2\sigma_R)/3$ ] )	94
Figure 5.7	Prolate spheroidal fluid inclusion in an extended poroelastic medium	96
Figure 5.8	Finite element discretization of the damage susceptible poroelastic medium bounded internally by a prolate spheroidal fluid inclusion: geometry and boundary conditions	96
Figure 5.9	Fluid pressure for prolate fluid inclusion in a non-isotropic stress field ( $n = 2.0$ ) ( <i>Stress state-independent damage evolution</i> )	97
Figure 5.10	Evolution of fluid pressure in the prolate spheroidal fluid inclusion: Influence of the geometry of the prolate spheroidal inclusion in a non-isotropic far field stress field ( <i>Stress state- independent damage evolution</i> )	98
Figure 5.11	Evolution of fluid pressure in the prolate spheroidal fluid inclusion: Influence of the geometry of the prolate spheroidal inclusion in a non-isotropic far field stress field. ( <i>Stress state- independent damage evolution</i> )	99
Figure 5.12	Evolution of fluid pressure in the prolate spheroidal fluid inclusion in a non-isotropic far field stress with	100

different deviatoric stress ratios ( *Stress state-dependent damage evolution*) [  $R = \sigma_A / \sigma_R$  ;  $n = b/a$  ;  $\sigma_m = (\sigma_A + 2\sigma_R)/3$  ]

Figure 6.1	A laterally loaded rigid pile embedded in a poroelastic geomaterial	105
Figure 6.2	Boundary conditions for a pervious interface between rock socket and geomaterial	109
Figure 6.3	Boundary conditions for an impervious interface between rock socket and geomaterial	109
Figure 6.4	Finite element discretization of the rock socket-poroelastic medium system	112
Figure 6.5	Numerical results for the time-dependent translational displacement of a rock socket ( $L/d = 1.0$ ) embedded in a brittle poroelastic half-space (pervious interface)	114
Figure 6.6	Numerical results for the time-dependent translational displacement of a rock socket ( $L/d = 1.0$ ) embedded in a brittle poroelastic half-space (impervious interface)	114
Figure 6.7	Comparison of results for the rock socket with ( $L/d = 1.0$ ) with either a pervious or an impervious interface between the rock socket and poroelastic half-space	115
Figure 6.8	Numerical results for the degree of consolidation of a laterally loaded a rock socket ( $L/d = 1.0$ ) embedded in a brittle poroelastic half-space (pervious interface)	115
Figure 6.9	Numerical results for the degree of consolidation of a laterally loaded rock socket ( $L/d = 1.0$ ) embedded in a brittle poroelastic half-space (impervious interface)	116
Figure 6.10	Numerical results for the time-dependent translational displacement of a rock socket ( $L/d = 2.0$ ) embedded in a brittle poroelastic half-space (pervious interface)	116
Figure 6.11	Numerical results for the time-dependent translational displacement of a rock socket ( $L/d = 2.0$ ) embedded	117

	in a brittle poroelastic half-space (impervious interface)	
Figure 6.12	Comparison of results for the rock socket with ( $L/d = 2.0$ ) with either a pervious or an impervious interface between the rock socket and poroelastic half-space	117
Figure 6.13	Numerical results for the degree of consolidation of a laterally loaded rock socket ( $L/d = 2.0$ ) embedded in a brittle poroelastic half-space (pervious interface)	118
Figure 6.14	Numerical results for the degree of consolidation of a laterally loaded rock socket ( $L/d = 2.0$ ) embedded in a brittle poroelastic half-space (impervious interface)	118
Figure 6.15	Numerical results for the time-dependent translational displacement of a rock socket ( $L/d = 4.0$ ) embedded in a brittle poroelastic half-space (pervious interface)	119
Figure 6.16	Numerical results for the time-dependent translational displacement of a rock socket ( $L/d = 4.0$ ) embedded in a brittle poroelastic half-space (impervious interface)	119
Figure 6.17	Comparison of results for the rock socket with ( $L/d = 4.0$ ) with either a pervious or an impervious interface between the rock socket and poroelastic half-space	120
Figure 6.18	Numerical results for the degree of consolidation of a laterally loaded rock socket ( $L/d = 4.0$ ) embedded in a brittle poroelastic half-space (pervious interface)	120
Figure 6.19	Numerical results for the degree of consolidation of a laterally loaded rock socket ( $L/d = 4.0$ ) embedded in a brittle poroelastic half-space (impervious interface)	121
Figure 7.1	A flat anchorage located in a geologic medium	123
Figure 7.2	Rigid disc inclusion surrounded with a brittle poroelastic medium (a) $b/a < 1$ , (b) $b/a > 1$	125
Figure 7.3	Boundary conditions for a rigid flat anchorage surrounded with a poroelastic medium	130

Figure 7.4	Finite element discretization for a flat rigid anchorage for cases (a) $b/a < 1$ (b) $b/a > 1$	132
Figure 7.5	A comparison between the analytical results given by Yue and Selvadurai (1995) for an impermeable circular anchorage and the computational results	134
Figure 7.6	Numerical results for a flat circular rigid inclusion disc surrounding with a brittle poroelastic medium susceptible to damage	135
Figure 7.7	Numerical results for a flat rigid inclusion disc ( $b/a = 1/2$ ) surrounding with a brittle poroelastic medium susceptible to damage	135
Figure 7.8	Numerical results for a flat rigid inclusion disc ( $b/a = 1/3$ ) surrounding with a brittle poroelastic medium susceptible to damage	136
Figure 7.9	Numerical results for a flat rigid inclusion disc ( $b/a = 1/5$ ) surrounding with a brittle poroelastic medium susceptible to damage	136
Figure 7.10	Numerical results for a flat rigid inclusion disc ( $b/a = 2$ ) surrounding with a brittle poroelastic medium susceptible to damage	137
Figure 7.11	Numerical results for a flat rigid inclusion disc ( $b/a = 3$ ) surrounding with a brittle poroelastic medium susceptible to damage	137
Figure 7.12	Numerical results for a flat rigid inclusion disc ( $b/a = 5$ ) surrounding with a brittle poroelastic medium susceptible to damage	138

## List of Symbols

### Latin Symbols

Symbol	Description
$A_0$	Initial cross sectional area
$\bar{A}$	Net cross sectional area
$B$	Skempton pore pressure parameter
$\mathbf{B}$	Strain-displacement matrix
$C_c$	Compressibility of the porous fabric
$C_w$	Compressibility of the pore fluid
$C_v$	Coefficient of consolidation
$\mathbf{C}$	Coupling matrix due to interaction between solid skeleton and pore fluid
$d$	Diameter that corresponds to either rigid pile or rock socket
$D$	Damage variable
$D_0$	Initial damage variable
$D_c$	Critical damage variable
$\mathbf{D}$	Elastic stiffness matrix
$e_c$	Error due to the discretization
$e_s$	Error due to the stability
$E$	Elastic modulus of undamaged porous skeleton
$E^d$	Elastic modulus of damaged porous skeleton
$E_p$	Elastic modulus of rigid pile or rock socket
$E_{oed}$	Oedometric modulus
$\mathbf{E}$	Compressibility matrix for the pore fluid
$\mathbf{f}$	Body force

$\mathbf{F}_i$	Vector representing the traction applied at the boundary
$\mathbf{H}$	Hydraulic conductivity matrix
$H(t)$	Heaviside step function
$I_1$	First invariant of total strain
$J_1$	First invariant of total stress
$k^0$	Hydraulic conductivity for undamaged state
$k^d$	Hydraulic conductivity for damaged state
$L$	Length of rock socket
$n$	Porosity
$\mathbf{n}$	Outward unit normal
$N$	Density function for micro-voids
$N_K^p$	Shape function for the pore pressure field
$N_K^u$	Shape function for the displacement field
$p$	Pore water pressure
$P_0$	Lateral load applied to either rock sockets or flat rigid anchorages
$\mathbf{S}$	Strain tensor
$t$	Time
$\Delta t$	Time increment
$\mathbf{T}$	Total stress tensor
$u_i$	Components of displacement vector
$\mathbf{u}$	Displacement vector in porous fabric
$U$	Degree of consolidation
$\mathbf{v}$	Specific discharge vector
$W$	Strain energy density function

#### Greek Symbols

$\alpha$	Poroelastic parameter
$\beta$	Poroelastic parameter



$\chi$	Amplification factor
$\varepsilon_{ij}$	The strain tensor
$\gamma$	Integration constant that varies between 0 and 1
$\gamma_w$	Unit weight of pore water
$\eta$	Material constant that correspond to the evolution of damage
$\lambda$	Bulk modulus of the porous skeleton
$\delta_{ij}$	Kronecker's delta function
$\mu$	Shear modulus for the undamaged porous skeleton
$\mu^d$	Shear modulus for the damaged porous skeleton
$\nu$	Drained value of Poisson's ratio
$\nu_u$	Undrained value of Poisson's ratio
$\sigma_{ij}$	The total stress tensor
$\sigma''_{ij}$	The total net stress tensor
$\sigma'_{ij}$	The effective stress tensor
$\xi_d$	Equivalent shear strain
$\xi_v$	Volumetric strain in the fluid
$\Delta$	In-plane displacement of a flat rigid anchorage
$\Delta_h$	Translational displacement of a rock socket

## List of Publications Resulting from the Research

- Selvadurai A.P.S. and A. Shirazi, 2004, 'Mandel-Cryer effects in a spheroidal fluid inclusion in damage-susceptible poroelastic geologic media', *Comput. Geotech.* (In press).
- Shirazi A. and A.P.S. Selvadurai, 2004, 'The fluid-filled spherical cavity in a damage-susceptible poroelastic medium', *Int. J. Damage Mech.* (In press).
- Shirazi A. and A.P.S. Selvadurai, 2004, 'Lateral loading of a rigid pile embedded in a damage-susceptible poroelastic solid', *Int. J. Geomech.* (Under revision).
- Selvadurai A.P.S. and A. Shirazi, 2004, 'A fluid inclusion in a poroelastic solid with void compaction', *XXI ICTAM*, 15-21 August 2004, Warsaw, Poland.
- Shirazi A. and A.P.S. Selvadurai 2003, 'Time-dependent response of the rock sockets embedded in a geomaterial susceptible to damage', *31th CSCE Conference*, June 4-8<sup>th</sup>, Moncton, NB, Canada, GCJ-187, 1-9.
- Selvadurai A.P.S. and Shirazi A., 2002, 'Pressure decay in a fluid inclusion located in a damage-sensitive poroelastic solid', *Poromechanics II*, August 26-28<sup>th</sup>, Grenoble, France (J.-L. Auriault, C. Geindreau, P. Royer, J.-F. Bloch, C. Boutin and J. Lewandowska, Eds.), A.A.Balkema, The Netherlands, 933-939.
- Shirazi A. and A.P.S. Selvadurai, 2002, 'Indentation of a poroelastic half-space susceptible to damage', *30<sup>th</sup> CSCE Conference*, June 1-4<sup>th</sup>, Montreal, QC, Canada, GES 020, 1-10.

# **CHAPTER 1**

## **INTRODUCTION AND LITERATURE REVIEW**

### **1.1. General**

In conventional treatments of the mechanics of fluid saturated porous media it is implicitly assumed that the porous fabric has an unchanging form. In certain situations, the stresses sustained by the porous fabric can lead to the alterations in its mechanical and fluid flow characteristics. The scope of this thesis relates to the study of the mechanics of fluid saturated media where micro-mechanical damage can lead to the alterations of the mechanical and fluid transport properties. In geomaterials that are characterized as brittle in their mechanical response, the micro-mechanical alterations of the porous fabric can be visualized as the development of micro-cracks or micro-voids, which can be modelled using the theory of continuum damage mechanics.

Fluid saturated porous materials, including soils, rocks and biomaterials are multiphase materials consisting of a deformable fabric, which is saturated with either incompressible or compressible pore fluids. The porous fabric can be visualized either as an assemblage of individual particles with inter-granular bonded contact or a porous medium with an interconnected network of pores. Examples of the former can include cemented sands and examples of the latter can include low porosity rocks. The mechanical behaviour of a multiphase porous material can be significantly different from that of a single-phase material (either solid or liquid) due to the interaction between the porous fabric and the pore fluid.

## 1.2. Theory of Poroelasticity

The theory of poroelasticity, which describes the mechanics of fluid-saturated porous elastic media, has its origins dating back to the classical work of Terzaghi (1923). The contributions of other researchers including Fillunger (1913) and Rendulic (1936) are now gaining acceptance and recognition. A recent review of developments in the theory of poroelasticity is given by de Boer (2000). The theory of soil consolidation proposed by Terzaghi (1923) assumes that when a saturated geomaterial is subjected to external loads, both the porous fabric, or the soil skeleton, and the pore fluid participate in carrying the applied loads. Terzaghi (1923) also postulated a theory of soil consolidation, which accounts for the time-dependent partitioning of the stresses in the pore fluid and in the soil skeleton. The time-dependent variation of the pore pressure during a consolidation process follows a diffusive pattern. According to the theory of consolidation, the externally applied loads are initially carried by the pore fluid and if the pore fluid is incompressible, the soil as a whole will not experience any initial volumetric deformations. With time, and depending upon the nature of the drainage conditions, the pore pressures will be transferred to the soil skeleton, which results in consolidation settlements. The consolidation process of saturated geomaterials is characterized by the time-dependent coupling between the deformation of the porous skeleton and the flow of pore fluid through the voids within the porous skeleton.

The original development of Terzaghi (1923) was primarily concerned with the one-dimensional behaviour of saturated soils. Terzaghi (1923) assumed that the soil skeleton is isotropic and elastic and that the pore fluid is incompressible. The individual soil particles themselves were regarded as non-deformable. The fluid flow through the porous skeleton was governed by Darcy's law (1856). Biot (1941, 1955, 1956) extended the theory of Terzaghi to include the three-dimensional effects, compressibility of both the pore fluid and the soil particles and the anisotropic behavior of the soil skeleton. The contributions made by Terzaghi (1923) and Biot (1941, 1955 and 1956) established the basis for the *classical theory of poroelasticity* for a fluid saturated medium. The classical theory of poroelasticity is now regarded as a major development in applied continuum

mechanics and provides a framework for the examination of a variety of engineering problems dealing with the mechanics of fluid-saturated porous elastic media.

### **1.3. Applications of Poroelasticity**

The classical theory of poroelasticity has been successfully applied to the study of time-dependent transient phenomena encountered in a wide range of natural and synthetic materials, including geomaterials and biomaterials (Schiffman, 1984; Whitaker, 1986; de Wiest, 1969; Detournay and Cheng, 1993; Coussy, 1995; Selvadurai, 1996, 2001; Cheng et al., 1998; de Boer, 1999, 2000; Wang, 2000). The classical theory of poroelasticity has been extensively applied to the analytical study of a large class of problems of practical interest to geotechnical engineering. The earliest of such applications is due to Mandel (1953), who examined the problem of the consolidation of a cubical element of saturated soil and made the classic observation concerning the time-dependent increase in the pore water pressure prior to its decay. This observation was confirmed by Cryer (1963) and laid the basis for the pore pressure response, which is now referred to as the Mandel-Cryer effect. de Josselin de Jong (1953) examined the time-dependent consolidation of the axial loading of a spherical cavity, located within an extended poroelastic medium. Noteworthy contributions in the study of semi-infinite domains of poroelastic media are due to McNamee and Gibson (1960 a,b). They examined the problems of the surface loading of a poroelastic half-space for axisymmetric and plane strain deformations with either permeable or impermeable surfaces. Soderberg (1962) examined the time-dependent behaviour of a rigid pile embedded in a poroelastic medium and subjected to an axial load through an approximate analytical method. Jana (1963) studied the time-dependent radial deformations around a cylindrical cavity located in a poroelastic region. Jana (1963) determined the analytical solutions for radial deformations obtained during the early stages of the consolidation process. Cryer (1963) also compared the three-dimensional theory of poroelasticity developed by Biot (1941) with the one-dimensional theory proposed by Terzaghi(1923) and applied both theories to the problem of consolidation of a poroelastic sphere. Cryer (1963) illustrated that Terzaghi's theory cannot account for the increase in pore pressure prior to its decay, which has also been

determined by Mandel (1953) for a poroelastic region with a cubic shape. Gibson *et al.* (1963) and Verruijt (1965) have confirmed the existence of the Mandel-Cryer effect through the experimental observations. de Josselin de Jong and Verruijt (1965) investigated the primary and secondary consolidation of a spherical clay sample, subjected to hydrostatic pressure at outer surface, using a double-cell apparatus containing the sample. The experimental results were compared with the analytical results, given by Cryer (1963). de Josselin de Jong and Verruijt (1965) also observed a difference between the experimental observations and analytical predictions and this was attributed to secondary consolidation resulting from creep of the porous skeleton. Schiffman and Fungaroli (1965) examined the problem of consolidation of a poroelastic half-space subjected to tangential loading, for half-spaces with free draining and impervious surfaces. Poulos and Davis (1968) examined the time-dependent behaviour of a rigid pile embedded in a poroelastic medium and subjected to an axial load. Poulos and Davis (1968) determined an approximate analytical solution and presented the results for a variety of length to diameter ratios of the rigid pile. Gibson *et al.* (1970) mathematically investigated the time-dependent settlement of both a plane strain uniform loading (infinite flexible strip footing) and an axisymmetric uniform loading (circular footing) located on a finite poroelastic layer with a smooth impervious base. The surface to which loads were applied was assumed to be free draining and the transient settlement was obtained for various ratios of the size of the load to the depth of finite poroelastic layer. Shanker *et al.* (1973) investigated analytically the plane strain consolidation of a poroelastic half-space, subjected to surface tangential loadings, for either free draining or impervious surfaces. Agbezuge and Deresiewicz (1975) investigated the problem of rigid indentation of a poroelastic half-space for the cases of either free draining or impervious indentation surface. Analytical solutions to the problem of the rigid indentation of a poroelastic half-space were proposed by Chiarella and Booker (1975) and Gaszynski and Szefer (1978). Deresiewicz (1977) also investigated the influence of alterations in Poisson's ratio of the porous fabric on the rigid indentation of a poroelastic half-space. Deresiewicz (1977) showed that a larger Poisson's ratio (within acceptable bounds) results in a faster rate of consolidation. Updated analytical studies of the rigid indentation of a poroelastic half-space and a poroelastic infinite space are given by Selvadurai and

Yue (1994) and Yue and Selvadurai (1995) respectively. Booker and Small (1975) investigated the stability of the solutions for the classical theory of poroelasticity developed by Biot (1941). Rice and Cleary (1976) obtained Navier-type equations for the consolidation process in terms of displacement components. Rice *et al.* (1978) studied the deformation field around a spherical cavity filled with a highly permeable soft material, surrounded by a poroelastic medium that was subjected to shear. The soft material can be treated as a weakened rock located at a fault zone. Rice *et al.* (1978) developed an analytical solution for the time-dependent displacement field around the spherical cavity. Randolph and Wroth (1979) developed a closed-form analytical solution for the consolidation around a driven pile in soft clay. The driving of the pile results in generation of excess pore pressure, which dissipates with time and as a result, the soft clay experiences consolidation. Randolph and Wroth (1979) assumed that the dimensions of the plastic zones can be neglected in comparison with the dimensions of the region over which consolidation occurs, which ensures the applicability of the classical theory of poroelasticity developed by Biot (1941). The results are also of interest to analysis of pressuremeter tests, used to obtain the in-situ consolidation properties primarily the coefficient of consolidation of clay. Siriwardane and Desai (1981) investigated the influence of the non-linearity in soil skeleton and fluid flow, using a finite element method. One-dimensional consolidation and axisymmetric consolidation of a poroelastic medium were examined. Siriwardane and Desai (1981) showed that the non-linearity in poroelastic parameters can have a significant influence on the consolidation behaviour of a poroelastic medium. Booker and Small (1984) examined analytically the time-dependent behaviour of a permeable flexible circular footing embedded on a fluid-saturated half-space of clay. These authors determined the time-dependent settlement of the footings and observed that the degree of consolidation of the circular footing is influenced by the rigidity of the footing. Booker and Small (1986) also extended their studies to include impermeable flexible circular footings embedded on a fluid-saturated half-space. The time-dependent deflection of a rigid circular anchor has also been examined by Small and Booker (1987) in connection with an impermeable disc anchor. Yue and Selvadurai (1994) presented an analytical study of the eccentric loading of a rigid circular foundation located at the surface of a poroelastic half-space region, with

either permeable or impermeable pore pressure boundary conditions. Kassir and Xu (1988) examined the harmonic dynamic response of a rigid strip foundation embedded in a poroelastic half-plane, which can exhibit linear hysteretic damping. Gibson *et al.* (1989) investigated the Mandel-Cryer effect for a poroelastic sphere experiencing large displacements, where natural (Hencky) strains are applicable. They observed that Mandel-Cryer effect can be influenced by the presence of the large strains. de Boer and Ehlers (1990) also investigated the influence of related mechanisms on the behaviour of poroelastic media. Detournay and Cheng (1991) presented an analytical model of the hydraulic fracture phenomenon within a poroelastic medium, resulting from the pressurization of a fluid saturated cylinder. Lan and Selvadurai (1996) analyzed the time-dependent response of two interacting rigid circular indentors, resting on a poroelastic half-space through the mathematical analysis of a mixed boundary value problem. The results also demonstrated the influence of the pore pressure boundary conditions, in the form of either free drainage or impervious free surface, on the time-dependent response of the interacting indentors. Selvadurai and Mahyari (1997) examined the process of steady crack extension in fluid saturated media. They confirmed the accuracy of the computational scheme through comparison with analytical results given by Atkinson and Craster (1991). Kanji *et al.* (2003) determined a closed form analytical solution for pore pressure and stresses generated within a pressurized hollow cylinder of transversely isotropic poroelastic material. Li (2003) investigated analytically the consolidation around a pressurized borehole in a poroelastic medium with double porosity, in the presence of a non-isotropic in-situ stress state. Li (2003) observed that the pore pressure decay in the borehole can be influenced by non-isotropy in the in-situ stress state. The mechanics of geomaterials induced as a result of the withdrawal of water or energy resources such as oil and natural gas can be also examined through the classical theory of poroelasticity. Computational schemes have been used successfully for the study of such problems. The articles by Valliappan *et al.* (1974), Schrefler and Simoni (1987) and Lewis and Schrefler (1998) give further discussions and references in this area.

The theory of fluid saturated poroelastic media has recently gained attention in its application to the modelling of thermally driven fluid flow in saturated geological media.



One important factor, which is involved in thermally driven fluid flow through a porous medium, relates to the relative compressibility between the pore fluid and both the solid material and porous skeletal fabric. A contribution in this area due to Brownell *et al.* (1977), determined the governing equations, related to the hydrothermal response of geothermal reservoirs. The formulations given by these authors can model the incremental non-linear behaviour of the porous fabric. The time-dependent pore pressure development in a fluid-saturated poroelastic region surrounding a spherical heat source has been investigated by Booker and Savvidou (1984) using an analytical approach. The problem of modelling of thermally driven consolidation of the poroelastic media has been examined by Aboustit *et al.* (1985) who use finite element methods. McTigue (1986) investigated the problem of thermally driven one-dimensional consolidation. Selvadurai and Nguyen (1995) investigated the coupled thermal-hydraulic-mechanical behaviour of fractured rocks by using a finite element procedure and applied computational methods to model the thermally driven consolidation around nuclear waste repositories. Giraud and Rousset (1996) conducted experimental observations on thermally driven consolidation in fluid-saturated porous media. The experimental observations were used to model the time-dependent behaviour of tunnels, excavated in deep clays. Zhou *et al.* (1998) mathematically examined thermal-hydraulic-mechanical response of the axisymmetric problems, including thermal cylindrical and spherical heat sources, located in poroelastic media. Pao *et al.* (2001) used the finite element procedure, applicable to coupled thermal-hydraulic-mechanical procedures to model the time-dependent behaviour of the oil-reservoirs containing two liquid phases of water and oil. A recent study by Khalili and Selvadurai (2003) developed the complete thermo-hydro-mechanical theory for a poroelastic medium exhibiting double porosity.

The classical theory of poroelasticity and its developments that include the influence of the non-linear response of the porous skeleton, irreversible deformations of the porous skeleton and other time-dependent phenomena have found applications in the study of a variety of natural and synthetic materials including biological materials such as bone, tissues, arteries, skin. A documentation of developments in this area is given by Selvadurai (1996) and Cowin (2001).

The purely mathematical approaches to the study of poroelasticity problems have limitations due to several factors. The presence of time-dependency invariably involves the application of Laplace transforms, which makes the numerical inversion procedure both complicated and computing intensive. Also the analytical approaches are more suitable for situations involving regular domains and simplified loading configurations. In order to examine configurations encountered in practical problems involving poroelastic domains, with complicated loading patterns etc., it becomes necessary to develop alternative approaches. The two computational approaches that have been widely applied to the modelling, are the finite element and boundary integral or boundary element techniques. The first application of the finite element method to the study of a problem in the consolidation of geomaterials is due to Sandhu and Wilson (1969). They applied a Galerkin technique along with a variational principle due to Gurtin (1964) to develop a computational procedure for the analysis of soil consolidation. The study by Sandhu and Wilson (1969) presents computational results for the problem of the one-dimensional consolidation and for the problem of the consolidation of a poroelastic half-space, subjected to a strip load. Christian and Boehmer (1970) applied the finite element method to investigate the plane strain problem in poroelasticity, including the consolidation of a long poroelastic cylinder subjected to hydrostatic stress at the outer surface. Ghaboussi and Wilson (1973) and Booker and Small (1975) have developed finite element methods for the analysis of problems associated with surface loading of semi-infinite poroelastic media. Selvadurai and Gopal (1986) and Schrefler and Simoni (1987) have applied mapped infinite elements to investigate the consolidation of saturated geomaterial regions of infinite extent. Noorishad *et al.* (1984) examined time-dependent behaviour of a fluid-saturated fractured porous rock using a finite element procedure developed for modelling coupled thermal-hydraulic-mechanical behaviour of porous media. Selvadurai and Nguyen (1995) also developed a finite element scheme, applicable to the modelling of thermal-hydraulic-mechanical phenomena in fractured poroelastic media filled with a compressible fluid. Selvadurai and Nguyen (1995) also applied the computational scheme to investigate transient thermally driven behaviour of fluid-saturated porous media. Cui *et al.* (1996) applied the finite element method to model the stress concentration near the wall of an inclined borehole, located in an

anisotropic poroelastic medium. They also developed a generalized finite element formulation, applicable to plane strain problems in poroelasticity and modelled the consolidation response of a poroelastic medium around a pressurized cylindrical cavity. Lewis and Schrefler (1998) give an account of the application of the finite element formulations for the study of coupled thermal-hydraulic-mechanical problems in porous media, consisting of different liquid phases (either compressible or incompressible) within the porous media. Lewis and Schrefler (1998) also gave a documentation of the possible applications of couple thermal-hydraulic-mechanical modelling to petroleum engineering and water reservoirs. Cleary (1977) gives a review of the boundary element methods that are applicable to the fluid-saturated porous media and examines the problem of a point heat source, located in a poroelastic region. A review on the boundary element formulations for poroelastic media are also given by Banerjee and Butterfield (1981) and Brebbia *et al.* (1984). Cheng and Liggett (1984a) used the boundary element technique to investigate the class of problems dealing with fracture propagation within a poroelastic region. These authors also investigated soil consolidation by using boundary element methods and applied the procedures to study the problem of consolidation of a strip load located in both a homogenous and a layered poroelastic half-space either compressible or incompressible pore fluids. Dargush and Banerjee (1991) used the boundary element method to examine the axisymmetric soil consolidation, including indentation of a rigid cylinder and consolidation around a cylindrical pile subjected to normal loadings. Dominguez (1992) used the boundary element method to investigate the behaviour of poroelastic media, subjected to a harmonic excitation. The transient response of a pressurized spherical cavity, located at a poroelastic medium was investigated by Senjuntichai and Rajapakse (1993) by considering the associated initial boundary value problems. Chopra and Dargush (1995) successfully applied the boundary element method to examine the problem of consolidation of a poroelastic sphere.

#### **1.4. Non-linear Behaviour of Soil Skeleton**

The assumption of the linear elastic response of the soil skeleton is a significant limitation when applying the classical theory of poroelasticity to brittle geomaterials,

which can exhibit a non-linear response due to a variety of processes ranging from elasto-plastic phenomena to fracture. The non-linear processes that are being investigated in this thesis focus on the evolution of micro-cracks and micro-defects, which can be addressed through a phenomenological theory of continuum damage mechanics. The generation of defects in the soil skeleton can influence geomaterial behaviour in terms of reduction in its stiffness and an attendant increase in the hydraulic conductivity. As a result, consolidation behaviour of brittle saturated geomaterials can be influenced by generation of defects in the porous soil skeleton.

The finite element approach has versatility in that the mechanical response needs no longer be restricted to the classical elasticity model. The classical theory of poroelasticity can be extended to include more complicated responses of the porous fabric. These can include elasto-plastic and viscoplastic behaviour of the skeletal response (Desai and Siriwardane, 1984). The boundary element techniques, due to the more mathematical nature of their formulations and the extensive use of Green's function techniques in the computation, are largely suited to the computational modelling of problems in classical poroelasticity.

The notion of development of micro-mechanical damage is entirely phenomenological when considering the fact that the deformable fabric of the fluid saturated medium is in itself a porous medium. The scales at which the defects that contribute to damage evolution should be such that the constitutive behaviour of the porous fabric in the damaged state can still be described through a classical continuum mechanics formulation. For example, the pore scale of rock such as sandstone can be of the order of  $0.0001 \text{ mm}$  and the continuum damage evolution can result in distributed defects of the order of  $0.001 \text{ mm}$  and the continuum notion applicable to the damaged state will be realistic provided the dimension of the representative volume element is within the order of  $0.01 \text{ mm}$ . Admittedly, these are not rigorous limits for the various scales, but intended to illustrate the ranges of relative length scales that would make the modelling meaningful. The damage evolution in the porous skeleton is therefore interpreted in a

phenomenological sense, where the porous skeleton will experience both alterations in the elasticity and fluid transmissivity properties as a result of micro-mechanical damage.

Brittle geomaterials can experience both continuum damage and discrete fracture simultaneously. Observations made by Bazant (1991) point to the generation of micro-defects in the region around the crack, which is referred to as a process zone. There are several factors influencing the dominant mode of flaw generation and flaw development in brittle geomaterials. Factors that control the flaw evolution include the stress state, the rate of loading, the microstructure of the geomaterial, the presence of stress singularities (e.g. crack tips) and the capability of a flaw to either extend or to remain closed. For this reason, establishing one universal criterion cannot be regarded as basis for the determination of the mode of flaw generation that governs the elastic behaviour of brittle geomaterials in a damaged state. In many instances, the characteristics of the brittle response can be determined only through experimental observations. The concept of continuum damage mechanics is more relevant to the description of the mechanical behaviour of semi-brittle geomaterials such as soft rocks, overconsolidated clays and other porous geological media that can exhibit reductions of the elastic stiffness at stress levels well below the peak or failure stress. The progressive reduction in elastic stiffness prior to the peak stress is assumed to be a result of the growth of existing micro-defects or generation of new micro-defects. The process of discrete cracking is more related to predominantly brittle geomaterials such as competent rocks (e.g. granite or basalt) subjected to low confining pressure (See Figure 1.1). This research focuses on defect generation as a result of micro-mechanical damage in semi-brittle geomaterials (e.g. sandstone) that are subjected to stress levels well below the peak stress levels. Experimental observations (Cheng and Dusseault, 1993) confirm the presence of this type of phenomenon in brittle geomaterials such as sandstone. At these stress levels, brittle geomaterials behave as continua and continuum damage evolution is expected. The influence of development of micro-defects during the damage evolution process in a saturated geomaterial can be examined by incorporating the concept of continuum damage mechanics introduced by Kachanov (1958) within the framework of the classical theory of poroelasticity developed by Biot (1941). The alterations in both the

deformability of the damaged material and the evolution of its hydraulic conductivity properties with damage are considered to be the topics of primary interest to geomechanics.

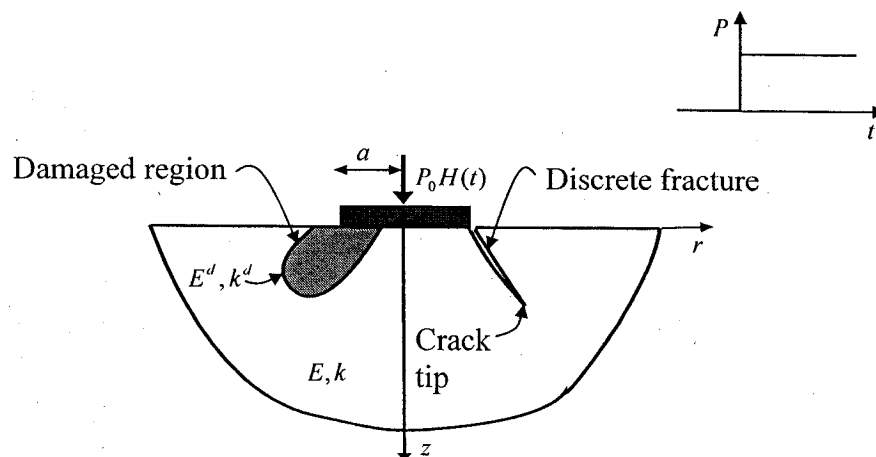


Figure 1.1 Indentation of a brittle poroelastic geomaterial.

#### 1.4.1. Continuum Damage Mechanics

The concept of continuum damage mechanics was first proposed by Kachanov (1958) in his classical studies pertaining to the modelling of the creep response of materials. The theory examines the development of micro-defects such as micro-cracks and micro-voids and their influence on the behaviour of materials prior to the development of macro-cracks such as fractures. The theory of continuum damage mechanics has been widely used to examine the non-linear behaviour of a variety of materials including metals, concrete, composites, ice, biomaterials, frozen soil and other geological materials. Accounts of continuum damage mechanics and its applications are given in the articles by Krajcinovic (1984, 1996), Lemaitre (1984), Bazant (1986), Nemes and Speciel (1996), Wohua and Valliappan (1998 a,b) and Voyiadjis *et al.* (1998). Krajcinovic and Fonseka (1981 a,b) used the concept of continuum damage mechanics to model the uniaxial tension and compression response of concrete as a brittle material susceptible to damage. Simo and Ju (1987) also used the concept of continuum damage mechanics to model the

response of concrete at stress levels well below the failure using the experimental observations by Wang (1977). Chow and Wang (1987) developed a tensorial form of continuum damage mechanics, applicable to anisotropic damage in damage-susceptible materials. The application of continuum damage mechanics to concrete has been investigated by Mazars and Pijaudier-Cabot (1989 a,b). Ju (1990) investigated the evolution of damage variables in damage-susceptible materials, associated with the continuum damage mechanics approach by using approaches derived from micro-mechanics. Selvadurai and Au (1991) applied continuum damage mechanics in the presence of visco-plasticity to model the indentation of a polycrystalline solid. Their results were applied to model the behaviour of ice at temperatures significantly below the freezing point. Cheng and Dusseault (1993) used the experimental observations from tests conducted on sandstone, to model the mechanical behaviour of a brittle geomaterial such as sandstone. They applied the resulting developments to examine the response of a strip footing, resting on a half-space consisting of sandstone. Tinawi and Ghrib (1994) investigated the response of concrete gravity dams by using continuum damage mechanics applicable to anisotropic damage. Selvadurai and Hu (1995) modelled the behaviour of frozen soils exhibiting tertiary creep by using the concept of continuum damage mechanics. Mahyari and Selvadurai (1998) proposed an iterative finite element procedure that accounts for the evolution of damage within a damage-susceptible poroelastic medium and applied the computational scheme to the problem of the axisymmetric indentation of a damage-susceptible poroelastic half-space by a rigid cylinder with a smooth, impermeable flat base. Mahyari and Selvadurai (1998) utilized the experimental observations for damage-induced alterations in poroelasticity parameters, given by Cheng and Dusseault (1993) (related to the damage-induced decrease in elastic stiffness) and Shiping *et al.* (1994) (related to the damage-induced alterations in hydraulic conductivity of poroelastic materials) to conduct the computational modelling. Valliappan *et al.* (1996) used continuum damage mechanics to model the seismic response of gravity dams through a damage evolution function, based on the consideration of tensile principal strains. Valliappan *et al.* also (1999) used a similar methodology to model the seismic response of arch dams. Shao and Lydzba (1999) applied the concept of damage mechanics to model the evolution of isotropic

damage within poroelastic media using microstructure parameters. Bart *et al.* (2000) studied mechanics of fluid-saturated brittle rock in connection with the anisotropic form of continuum damage mechanics. These authors modelled the experimental results from triaxial test conducted on brittle rocks. Lee *et al.* (2000) introduced a fatigue model, using continuum damage mechanics, applicable to the evaluation of the life cycle of asphalt pavements. Planas and Elices (2003) used damage mechanics to examine damage evolution in concrete due to cooling at very low temperatures. Selvadurai (2004) introduced the concept of “stationary damage” to develop alternative techniques for examining the mechanics of poroelastic media susceptible to damage. In the stationary damage concept the evolution of stiffness and hydraulic conductivity at the start of the poroelastic process is maintained in the remainder of the transient process. The technique was applied to the modelling of indentation of a damage susceptible poroelastic half-space.

The non-linear behaviour of materials due to generation of micro-mechanical damage can be developed by introducing a set of parameters referred to as local damage variables. Damage variables reflect average material degradation at a scale normally associated with the classical continuum formulations. Therefore, the introduction of the damage variable makes it possible to adopt and extend any classical continuum theory applicable to material behaviour, to the domain of damage mechanics. Instances where this approach has been successfully applied, are given by Sidoroff (1980), Krajcinovic (1984), Lemaitre (1984), Chow and Wang (1987) and Lemaitre and Chaboche (1990). (See also Voyiadjis *et al.*, 1998).

### **1.5. Experimental Observations on Damage Evolution**

The non-linear behaviour of most brittle materials in the pre-peak load range results from the growth of existing micro-defects or generation of new micro-defects (see Simo and Ju, 1987). A typical micro-crack generated in a brittle geomaterial (sandstone) is shown in Figure 1.2 (Gatelier *et al.*, 2002). The evolution of micro-cracks and micro-voids even at damage levels well below those required for material failure is assumed to be the



essential mechanisms that can lead to alterations in elastic stiffness and hydraulic conductivity in porous brittle materials (see Cheng and Dusseault, 1993 and Shiping *et al.*, 1994). The experimental basis for the assumption is provided through a number of investigations.

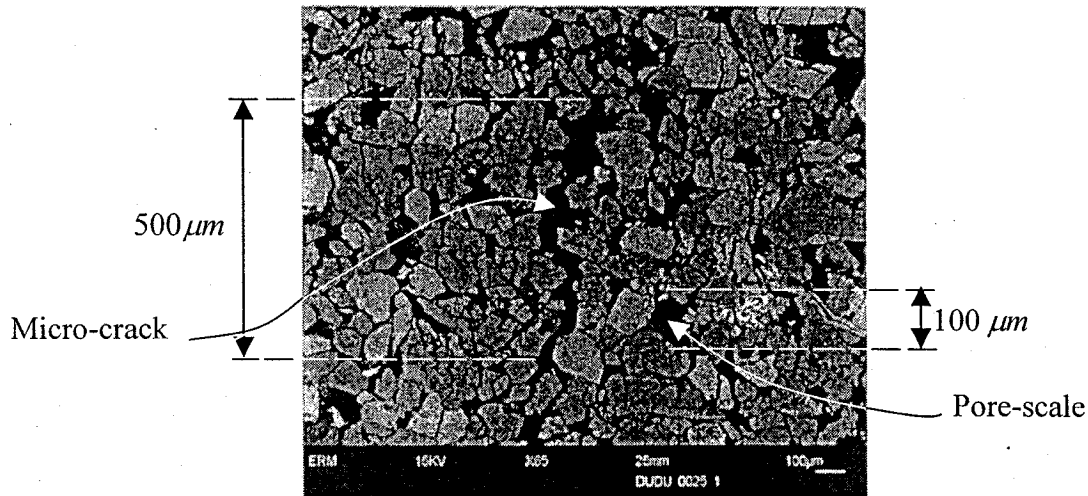


Figure 1.2 Micro-cracks in sandstone (Modified after Gatelier *et al.*, 2002).

### 1.5.1. Damage-induced Alterations in Mechanical Properties

Cook (1965) investigated the reduction in elastic stiffness through the changes in elastic energy concepts introduced by Griffith (1921). The reduction in elastic stiffness of brittle rocks is also theoretically demonstrated by Cook (1965). The uniaxial tension and compression tests, conducted by Cook (1965) on Tennessee Marble also point to the reduction in the elastic stiffness. Bieniawski *et al.* (1967) conducted experimental investigations on South African hard rocks, described as Norite, using uniaxial compression tests and observed that the elastic stiffness reduced as a result of development of micro-defects. The degradation in mechanical properties of concrete as a brittle material even at stress levels well below the peak has been observed by Spooner and Dougill (1975) (Figure 1.3). This degradation has also been observed by Mazars and Pijaudier-Cabot (1989) for concrete (Figure 1.4). Cheng and Dusseault (1993) investigated the degradation in mechanical properties of sandstone as a result of evolution

of damage. Cheng and Dusseault (1993) proposed a damage evolution function for soft rocks through the application of continuum damage mechanics theories to experimental observations conducted by Cheng (1987) on sandstone samples subjected to uniaxial compression. The damage evolution function proposed by Cheng and Dusseault (1993) has also been used in the computational modelling used by Mahyari and Selvadurai (1998) to determine time-dependent response of damage-susceptible fluid-saturated poroelastic media.

The evolution of damage is expected to be highly stress state-dependent. The investigations conducted by Hunsche and Hampel (1999) illustrate the stress state-dependency of the damage-induced alterations in mechanical properties of rock salt. Hunsche and Hampel (1999) also observed that in the absence of expansion within the element of damage-susceptible material, no significant damage-induced alterations in mechanical properties are expected. This observation has also been supported by Schulze *et al.* (2001) through their research conducted on rock salt.

From the results of experimental investigation discussed, we may conclude that the degradation in mechanical properties occurs as a result of the evolution of damage within the damage-susceptible materials. Furthermore, the alterations can also be influenced by the stress state-dependency.

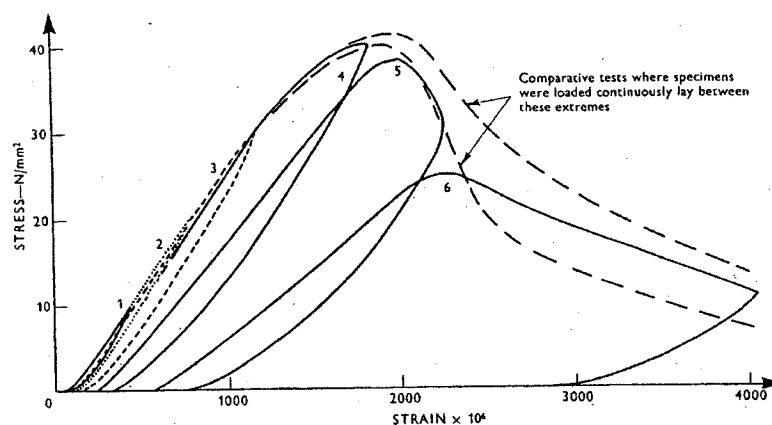


Figure 1.3 The results of uniaxial compression tests conducted on concrete (After Spooner and Dougill, 1975)

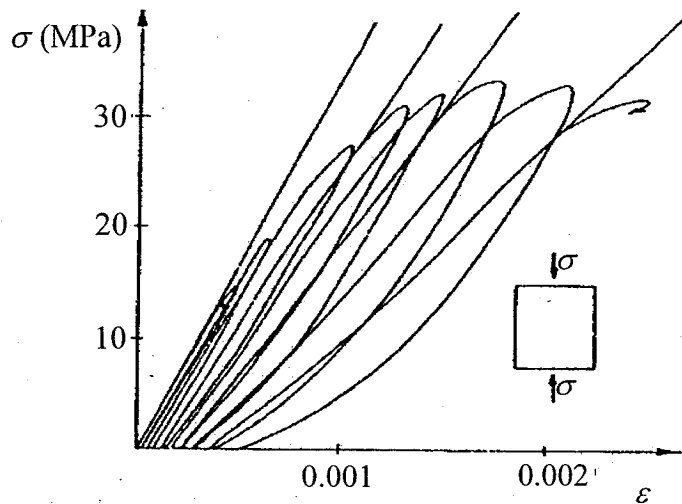


Figure 1.4 The results of uniaxial compression tests conducted on concrete (After Mazars and Pijaudier-Cabot, 1989)

### 1.5.2. Damage-induced Alterations in Hydraulic Conductivity Properties

A review of the damage-induced alterations in the fluid transmissivity characteristics of brittle geomaterials is given in a recent article by Selvadurai (2004). The damage-induced alterations in the hydraulic conductivity of saturated geomaterials have been investigated by Zoback and Byerlee (1975) through experiments conducted on granite (Figure 1.5). The experiments indicate the increase in the hydraulic conductivity by up to a factor of four at stress levels within 50% of the peak stress. The results of experiments conducted by Shiping *et al.* (1994) on sandstone indicate that for different stress states, the hydraulic conductivity is increased by an order of magnitude (Figure 1.5). Results of triaxial tests conducted on anisotropic granite reported by Kiyama *et al.* (1996) also indicate the trend towards an increase in hydraulic conductivity due to the evolution of micro-defects. A phenomenological relationship for the evolution of hydraulic conductivity due to damage process in claystone has also been proposed by Skoczylas and Shao (1996). The micro-mechanical damage-induced increases in hydraulic conductivity has also been reported by Coste *et al.* (2002) in connection with experiments conducted on rocks and claystone. These authors have observed an increase in hydraulic conductivity of up to two-orders of magnitude. Investigations of hydraulic conductivity alterations in excavation-damage

zones have also been reported by Zhang and Dusseault (1997), who used simple constant head borehole tests to evaluate the alterations in hydraulic conductivity. Souley *et al.* (2001) examined the excavation damage-induced alterations in hydraulic conductivity of granite of the Canadian Shield; an increase in hydraulic conductivity of four orders of magnitude was observed in the damaged zone (Figure 1.6). Experimental results given by Samaha and Hover (1992) show an increase in the hydraulic conductivity of concrete subjected to compression. The study conducted by Gawin *et al.* (2002) also shows an increase in the hydraulic conductivity of concrete at high temperatures due to generation of thermo-mechanical damage. This study also presented a set of empirical relationships to determine alterations in hydraulic conductivity of concrete as a function of temperature and damage. Bary *et al.* (2000) conducted an experimental study of the evolution of hydraulic conductivity in concrete gravity dams subjected to fluid pressures. They presented experimental results that investigate the evolution of hydraulic conductivity of concrete subjected to axial stress.

The evolution of hydraulic conductivity in natural salt has also been investigated by a number of researchers including Stormont and Daemen (1992) and Schulze *et al.* (2001). An increase in permeability has been observed as a result of evolution of micro-mechanical damage due to applied stresses (Figure 1.7). It should be noted that natural salt is susceptible to creep; therefore, elastic damage is only a minor component of the overall mechanical response. With reference to damage evolution it should be noted that not all stress states will induce such an increase in hydraulic conductivity of geomaterials. The studies conducted by Brace *et al.* (1978) and Gangi (1978) indicate that hydraulic conductivity of granite can be reduced by increasing confining stresses. Similar observations have been made by Patsouls and Gripps (1982) for chalk and by Wang and Park (2002) for sedimentary rocks and coal. Experimental data given by Zhu and Wong (1997) point to the decrease of hydraulic conductivity due to an increase in the deviator stress levels; however, these studies deal mainly with the behaviour of geomaterials at post-peak stress levels and applicable to the stress-softening range. These

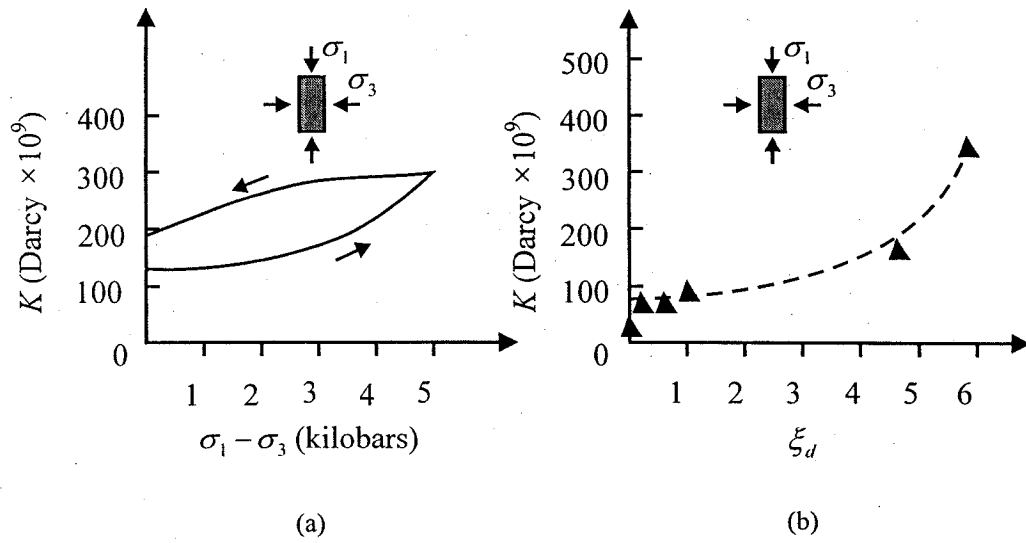


Figure 1.5. The evolution of hydraulic conductivity in saturated geomaterials (a) after Zoback and Byerlee (1975) and (b) after Shiping *et al.* (1994).

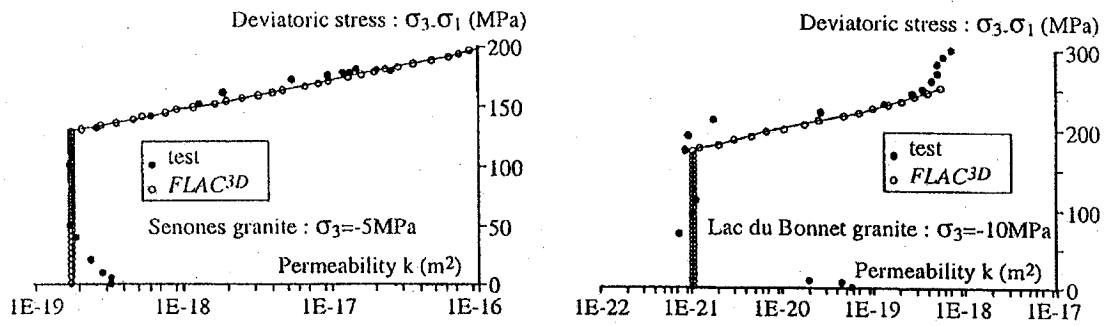


Figure 1.6 The evolution of hydraulic conductivity in saturated geomaterials (After Souley *et al.*, 2001)

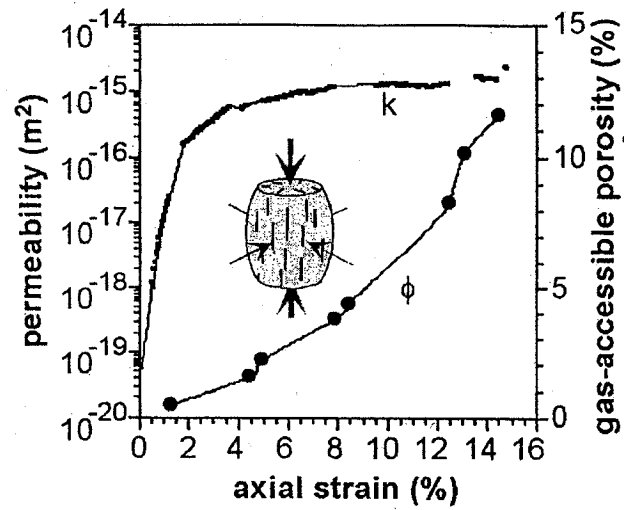


Figure 1.7 The evolution of hydraulic conductivity in natural salt (After Schulze *et al.*, 2000).

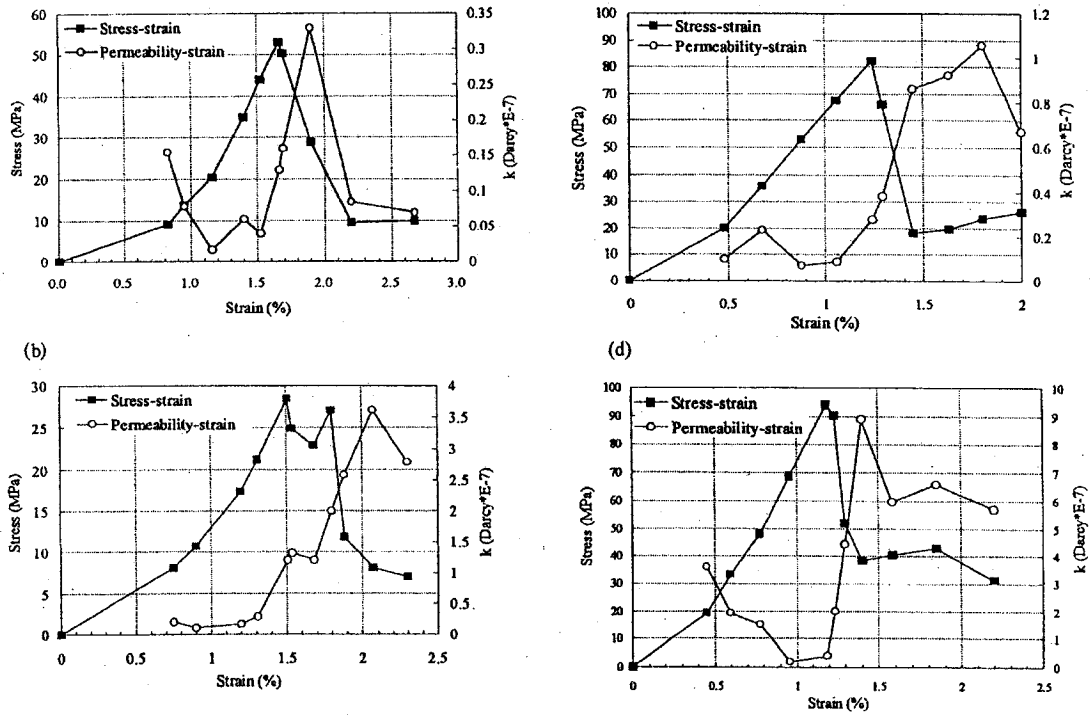


Figure 1.8 Alterations in hydraulic conductivity of the four different geomaterials as an increase at stress levels well below the peak and as a decrease in high confining pressure (After Wang and Park, 2002)

effects are not within the scope of this research, which mainly deals with hydraulic conductivity evolution during damage in the stress levels that maintain the elastic character of the poroelastic material (Figure 1.8). It should also be mentioned that the phenomenon of a reduction in the hydraulic conductivity as a result of an increase in deviator stress in the presence of high confining pressure can be relevant to certain classes of geomaterials that can exhibit pore closure during shearing.

In the context of stress state-dependency of the damage process, Schulze *et al.* (2001) observed that, in the absence of dilation, the hydraulic conductivity of rock salt cannot be increased significantly. According to the experimental observations discussed previously, it can be concluded that damage-induced alterations can occur in the hydraulic conductivity of geomaterials and that for certain materials, these alterations can also be stress state-dependent.

#### **1.6. Computational Modelling of Damage Evolution in a Saturated Brittle Geomaterial**

The computational modelling of damage evolution in a brittle geomaterial taking into consideration alterations in both the deformability and the hydraulic conductivity characteristics of the material has been investigated by only a limited number of researchers. Mahyari and Selvadurai (1998) proposed a computational scheme as an iterative finite element technique that accounts for alterations in both the elasticity and hydraulic conductivity characteristics of a saturated brittle geomaterial through the updating the governing material parameters. They successfully applied the computational scheme to examine the axisymmetric problem of the indentation of a brittle geomaterial such as saturated sandstone. The computational scheme proposed by Mahyari and Selvadurai (1998) provides a basic framework that can be extended to examine three-dimensional problems in general, and further modified to take into consideration the stress state-dependency in the damage evolution process. Shao *et al.* (1998) developed a one-dimensional finite element technique to examine the influence of damage-induced

alterations in poroelastic parameters on the consolidation of claystone, which was modelled as a brittle poroelastic material. These authors used the experimental observations conducted on claystone reported by Skoczylas and Shao (1996). The computational scheme has also been applied to the study of problems with a simple geometry and to the analysis of deep cavities. The computational scheme has been used for examining unsaturated geomaterials of a multiphase nature, accounting for solid, liquid and air components. This makes it possible to computationally model effects of drying in fluid-saturated media, particularly when thermo-hydro-mechanical problems involving heating of the material are examined. Bary *et al.* (2000) investigated hydro-fracture of concrete by adopting a damage model that considers the alterations in hydraulic conductivity of concrete due to the damage process. A computational study has also been conducted by Tang *et al.* (2002) in order to examine the alterations in hydraulic conductivity of sedimentary rocks. The basis of the computational scheme proposed by Wang and Park (2002) is essentially identical to that proposed *originally* by Mahyari and Selvadurai (1998); the damage evolution function used for incorporating the alterations in the hydraulic conductivity, however, is a rather complicated one with certain terms that could be determined only by appeal to micro-mechanical considerations. This is a significant limitation for use of the computational scheme in general problems in geomechanics with both complex geometries and complicated boundary conditions. The damage evolution function used by Tang *et al.* (2002) can model the dependency of the evolution of damage on the applied confining pressure but it cannot address stress state-dependent evolution of damage with reference to a general three-dimensional principal stress space. Wang and Park (2002) have also examined the damage-induced alterations in hydraulic conductivity of sedimentary rocks through the computational modelling procedure presented in their studies.

### **1.7. Objectives and Scope of the Research**

Brittle geomaterials can experience non-linear elastic responses due to the generation of micro- mechanical defects. In geomaterials with pore space that is saturated with a pore fluid, the growth of existing micro-defects or the generation of new micro-defects can



also lead to alterations in fluid transport characteristics. The alterations in hydraulic conductivity can be significant even at stress levels well below the peak and rupture stress levels. The alteration in the hydraulic conductivity can influence the time-dependent consolidation response of fully saturated brittle geomaterials. The alterations in the hydraulic conductivity can exert a greater influence on the consolidation behaviour even at low stress levels, than the reduction in elastic stiffness. In a multiphase material, the influence of the damage-induced alterations in the mechanical and hydraulic conductivity behaviour of the geomaterial can be greater than those for a single-phase brittle solid susceptible to damage. One of the objectives of this research is to examine the influence of damage-induced alterations on time-dependent behaviour of a fluid-saturated brittle geomaterials through a computational scheme that accounts for alterations in both elasticity and hydraulic conductivity characteristics. The computational scheme is applied to study a number of problems in geomechanics, which are not only of fundamental interest but also have applications potential in engineering and geomechanics. The accomplishments of the research can be summarized as follows:

- (i) Extension of the computational scheme proposed by Mahyari and Selvadurai (1998) for axisymmetric problems to the study of three-dimensional problems. This enables the application of proposed computational developments to the modelling and study of practical problems in geomechanics.
- (ii) Examination of the stress state-dependency on the evolution of damage by using a computational scheme, which accounts for the influence of the “sense” of stress on the damage process. It is assumed that no significant damage evolves as a result of compaction of geomaterials due to the applied stress states. This is supported through the experimental observations available in the literature.
- (iii) Application of the computational scheme to the study of problems of interest in geomechanics including the modelling of pore pressure decay in a fluid inclusion embedded in a brittle geomaterial, which is relevant to engineering geology and petroleum engineering; the study of a laterally loaded rigid pile embedded in a brittle geomaterial with applications to foundation engineering and the modelling

of the mechanics of an anchor embedded in a brittle geomaterial, with possible applications to foundation engineering, tunneling and hydraulic structures.

- (iv) Other applications include the study of the indentation of a damage susceptible poroelastic half-space by a rigid cylindrical indenter, which is reported in a publication (Shirazi and Selvadurai, 2002).

### **1.8. Statement of Originality and Contributions**

- (1) The work presented in this thesis extends existing studies dealing with the mechanics of damage susceptible fluid-saturated media to include damage-induced alterations in both elasticity and hydraulic conductivity characteristics and to develop a computational methodology that can examine three-dimensional problems. To the author's knowledge, these extensions are considered to be novel and specific problems that model general three-dimensional approach are considered to be original.
- (2) This thesis presents a methodology for examining the stress state-dependent damage evolution in fully saturated brittle geomaterials through a computational scheme that accounts for such damage process. This development is also considered to be novel and highly original.
- (3) The developments presented in this thesis have significant applications potential in geomechanics, geotechnical engineering, foundation engineering, petroleum engineering and engineering geology. The extension of the studies to include applications to biomechanics merits further investigation.
- (4) The contributions resulting from the thesis have been published or accepted for publication in leading international journals and referred conference proceedings with a high degree of selectivity and standards in the general areas of computational geomechanics, applied mechanics and civil engineering.

## CHAPTER 2

### COMPUTATIONAL DEVELOPMENTS IN THE MODELLING OF POROELASTIC MEDIA

#### 2.1. Introduction

In this research, the classical theory of three-dimensional poroelasticity developed by Biot (1941, 1955, 1956) is used for the computational modelling of linear, isotropic, elastic porous media saturated with an incompressible pore fluid. The relevance of this idealization to the modelling of geomaterials can be established by examining certain typical examples of poroelastic behaviour involving fluid saturated geomaterials. Consider for example, an over-consolidated clay with an elastic modulus in the range of 10 MPa . For such a material the pore fluid, which has a bulk modulus of 23 GPa can be regarded as an incompressible fluid. In contrast, when considering a porous granite with a skeletal elastic modulus of the order of 10 GPa , the pore fluid must be regarded as being compressible. These limiting assumptions can be established by appeal to Skempton's pore pressure parameters  $B = 1/(1 + nC_w / C_c)$ , where  $n$  is the porosity and  $C_w$  and  $C_c$  are the compressibility factor of pore fluid and porous fabric, respectively, which relates the pore pressure development to the compressibility of the constituents of the fluid saturated medium (Skempton, 1954). As the compressibility ratio  $nC_w / C_c$  approaches zero, the fluid can be regarded as being incompressible. In geomechanics, the pore fluid is usually water and the assumption pertaining to either the compressibility or incompressibility of pore water can be made only through consideration of the relative compressibility characteristics of the deformable porous solid to that of the pore fluid. This chapter presents the partial differential equations governing the classical theory of

poroelasticity. The essential features of the classical theories of poroelasticity are reviewed with an emphasis on the physical and mathematical features of the theory of poroelasticity developed by Biot (1941), which is the standard theory used by most researchers for studying time-dependent behaviour of poroelastic media. The basic material parameters that describe the behaviour of poroelastic media saturated with incompressible fluids are also discussed.

The Chapter also presents a brief review of the finite element approach for the computational treatment of the partial differential equations governing classical poroelasticity. The focus of the presentation is on Galerkin's finite element technique that is used to develop the computational scheme. The formulations are presented for the general three-dimensional domain to model the problems with complex geometries and boundary conditions. The twenty-node isoparametric brick element is utilized for discretization of the three-dimensional domain. A Cartesian tensor notation is used in the presentation with Einstein's summation convention applied to repeated indices. In addition the following sign conventions are adopted: tensile stresses in the solid skeleton are considered positive and compressive pore fluid pressures are considered negative; the shear stresses follow the sign convention that is used in solid mechanics and geomechanics (Fung, 1965; Davis and Selvadurai, 1996, 2002).

## **2.2. Classical Theories of Poroelasticity**

The mathematical formulation and analysis of consolidation behaviour of a fluid-saturated porous medium is generally attributed to Terzaghi (1923). A consequence of the theory is the introduction of the concept of effective stress in the theories of soil mechanics. Terzaghi (1923) proposed a fundamental approach to the study of a fully saturated soil and developed the one-dimensional theory of soil consolidation through a model of a porous medium that experiences small deformations. The basic assumptions of Terzaghi's theory are as follows: (i) The porous skeleton of the soil is considered to be mechanically and hydraulically isotropic and homogeneous. (ii) The fluid flow through pores and mechanical deformations are one-dimensional. (iii) The strains are small. (iv)

The mechanical response of the porous skeleton is governed by a linear isotropic elastic Hookean law and pore fluid flow is governed by an isotropic form of Darcy's law. (v) The pore fluid is incompressible in comparison with the porous fabric. The soil layer is subjected to a total vertical stress  $\sigma$  and it is assumed that mechanical deformation and fluid flow through the layer are one-dimensional. The flow through the element is governed by Darcy's law as follow as:

$$v_z = ki = -k \frac{\partial h}{\partial z} \quad (2.1)$$

where  $k$  is hydraulic conductivity of soil and  $h$  is the total fluid head. The pore fluid pressure is also related to the total fluid head in the following form:

$$p = \gamma_w h \quad (2.2)$$

where  $p$  is the pore pressure and  $\gamma_w$  is the unit weight of water. Substituting (2.2) in (2.1), (2.1) takes the form:

$$v_z = -\frac{k}{\gamma_w} \frac{\partial p}{\partial z} \quad (2.3)$$

The equation of continuity, associated with quasi-static fluid flow in the deforming porous skeleton is:

$$\frac{d\varepsilon_v}{dt} = \frac{dv_z}{dz} = -\frac{k}{\gamma_w} \frac{\partial^2 p}{\partial z^2} \quad (2.4)$$

where  $\varepsilon_v$  is the volumetric strain of the porous skeleton. For an isotropic poroelastic medium experiencing one-dimensional straining, the rate of volumetric strain can be expressed in terms of one-dimensional modulus of the soil skeleton in the following form:

$$\frac{d\varepsilon_v}{dt} = \frac{1}{E_{oed}} \frac{\partial \sigma'}{\partial t} \quad (2.5)$$

where  $E_{oed} = \frac{E(1-\nu)}{(1+\nu)(1-2\nu)}$  is the oedometric modulus,  $E$  is elastic modulus,  $\nu$  is Poisson's ratio. The effective stress  $\sigma'$  for one-dimensional consolidation of a poroelastic medium, saturated with an incompressible fluid takes the form:

$$\sigma' = \sigma - p \quad (2.6)$$

where  $\sigma$  is the total stress, which is identical to the total vertical external stress, for one-dimensional consolidation and  $p$  is pore pressure. If we assume that the externally applied stress  $\sigma$  is constant in time, then

$$\frac{\partial \sigma'}{\partial t} = -\frac{\partial p}{\partial t} \quad (2.7)$$

Combining (2.4), (2.5) and (2.7), we obtain:

$$\frac{\partial p}{\partial t} = C_v \frac{\partial^2 p}{\partial z^2} \quad (2.8)$$

where the coefficient of consolidation  $C_v$  takes the form:

$$C_v = \frac{k(1-\nu)E}{(1+\nu)(1-2\nu)\gamma_w} \quad (2.9)$$

and indicates that the pore pressure within the poroelastic layer has a diffusive pattern. The result (2.8) was first derived by Terzaghi (1923) to examine the time-dependent pore pressure decay in the one-dimensional consolidation of a poroelastic layer.

Terzaghi's theory of one-dimensional consolidation has been widely applied to the analysis of practical problems and became a standard procedure in the geotechnical analysis of the effects of consolidation. Many conventional methods for predicting the magnitude and the rate of settlements beneath the foundations use this theory (Harr, 1966; Lambe and Whitman, 1969).

A generalization of the Terzaghi's theory to include three-dimensional effects was suggested by Rendulic (1936). This theory is based on the assumption that during the process of soil consolidation, the first invariant of the total stress remains constant during the dissipation of excess pore pressure. This hypothesis leads to Terzaghi-Rendulic theory for soil consolidation. In this theory, the total stress field in the soil medium is treated independently and usually accomplished through the assumption that it is governed by a time-independent elastic analysis of the elastic medium.

The three-dimensional form of the continuity equation, which is identical to (2.4), takes the following form:

$$\frac{\partial \varepsilon_v}{\partial t} = -\frac{k}{\gamma_w} \left( \frac{\partial^2 p}{\partial x^2} + \frac{\partial^2 p}{\partial y^2} + \frac{\partial^2 p}{\partial z^2} \right) \quad (2.10)$$

The rate of volumetric changes can be expressed in the following form:

$$\frac{\partial \varepsilon_v}{\partial t} = \frac{1}{\lambda} \frac{\partial \sigma'_v}{\partial t} \quad (2.11)$$

where  $\lambda$  is the bulk modulus of the soil skeleton and  $\sigma'_v$  takes the form:

$$\sigma'_v = \frac{1}{3}(\sigma_{xx} + \sigma_{yy} + \sigma_{zz}) - p = \frac{1}{3}J_1 - p \quad (2.12)$$

where,  $J_1$  is the first invariant of total stress. Rendulic (1936) assumed that the first invariant of total stress ( $J_1$ ) remains constant with time within the poroelastic medium. This results in the following equation, which is identical to Equation (2.7) for the one-dimensional theory of consolidation developed by Terzaghi (1923);

$$\frac{\partial \sigma'_v}{\partial t} = -\frac{\partial p}{\partial t} \quad (2.13)$$

Substituting (2.13) and (2.11) in to (2.10), we obtain

$$C_v \left( \frac{\partial^2 p}{\partial x^2} + \frac{\partial^2 p}{\partial y^2} + \frac{\partial^2 p}{\partial z^2} \right) = \frac{\partial p}{\partial t} \quad (2.14a)$$

or

$$C_v \nabla^2 p = \frac{\partial p}{\partial t} \quad (2.14b)$$

where,  $\nabla^2$  is Laplace's operator. The pore pressure, obtained from (2.14) again has a diffusive pattern. The coefficient of consolidation ( $C_v$ ) for the Terzaghi-Rendulic theory has the following form:

$$C_v = \frac{\lambda k}{\gamma_w} = \frac{kE}{3\gamma_w(1-2\nu)} \quad (2.15)$$

Rendulic (1936) also conducted experimental observations on samples, subjected to triaxial states of stress and compared those with the theoretical results, obtained from Equation (2.14). Rendulic (1936) observed that the coefficient of consolidation ( $C_v$ ) is not a constant parameter and depends on the dimensionality of the problem (see e.g.



Terzaghi, 1943). Therefore, the coefficient of consolidation, defined by (2.15) should be considered as a variable that takes the form:

$$C_v = \frac{kE}{\gamma_w f(x, y, z)} \quad (2.16)$$

where,  $f(x, y, z)$  relates the rate of volumetric changes to the state of effective stresses within the poroelastic medium.

One of the serious drawbacks of the above mentioned theories is the absence of a correct form of coupling between the time-dependent deformation of the soil skeleton and the flow of the pore fluids. As a result of this deficiency, some special features of the consolidation process, such as the Mandel-Cryer effect (Mandel, 1950 and 1953; Cryer, 1963) do not appear in the two uncoupled theories proposed by Terzaghi (1923) and Rendulic (1936). This aspect of the appropriate form of the coupling between the mechanical deformations and pore fluid pressure is a major development of the theory of three-dimensional soil consolidation proposed by Biot (1941) (see e.g. Schiffman *et al.*, 1969).

The theory of three-dimensional linear poroelasticity for a saturated medium was formulated by Biot (1941, 1955, 1956) to model more realistically the mechanical behaviour of saturated soils and rocks. In this theory, the soil skeleton is modelled as deformable, linear, elastic, porous medium saturated with either an incompressible or a compressible pore fluid. A set of partial differential equations was formulated by Biot (1941, 1955, 1956) to describe the coupled mechanical behaviour of saturated porous media. Biot's theory of poroelasticity results in a completely self-consistent set of boundary conditions and a well-posed initial boundary value problem.

Biot's theory accounts for the time dependent interaction of the soil skeleton and pore fluid (i.e. the coupling between the deformation of the porous skeleton and the deformation of the pore fluid). The coupled mechanical state is described by mechanical

variables (effective stresses and the excess pore pressure) and kinematic variables (displacement of the porous skeleton and fluid velocity) applicable to each phase. The mechanical and kinematic variables are time-dependent. Four of these variables are independent and account for the coupling behaviour of the governing equations. They are the three displacement components and the excess pore pressure. Consequently, four independent boundary conditions (three for solid phase and one for pore fluid phase) should be applied to formulate boundary and initial value problems for saturated porous media. The four independent boundary conditions correctly match the situations encountered in many practical problems associated with fully saturated soils and rocks. Biot's theory is sufficiently general in that both the Terzaghi's classical one-dimensional consolidation theory and the Terzaghi-Rendulic theory can be recovered as special cases, but has the additional advantage that phenomena such as the Mandel-Cryer effect can be observed in the pore pressure response.

### 2.3. Governing Equations of Poroelasticity

The three-dimensional theory of poroelasticity developed by Biot (1941) that accounts for the time-dependent response of consolidation of porous media is based on the following assumptions: (i) the mechanical behaviour of the porous fabric is isotropic, (ii) the constitutive behaviour of the porous fabric is governed by Hookean elasticity, (iii) strains are infinitesimal, (iv) fluid flow through the pores is governed by an isotropic form of Darcy's law, (v) the mechanical and hydraulic behaviour of the poroelastic medium is uninfluenced by the deformations of the medium.

Based on Biot's (1941, 1955, 1956) original formulation (which has also been followed by Rice and Cleary (1976) and Detournay and Cheng (1993)) the basic mechanical variables are considered to be the total stress dyadic  $\mathbf{T}$  (see Selvadurai, 2000 b) and the scalar excess pore pressure  $p$ . The corresponding kinematic quantities include the strain dyadic  $\mathbf{S}$ , displacement vector  $\mathbf{u}$  in porous fabric, the volumetric strain in the fluid  $\xi_v$  and specific discharge vector  $\mathbf{v}$  in the pore fluids. The strain energy density function  $W$  can be expressed in the following form:

$$W = \frac{1}{2}(\mathbf{T} : \mathbf{S} + p\xi_v) \quad (2.17)$$

The mechanical response of the porous fabric is governed by a Hookean linear isotropic elasticity relationship of the form:

$$\mathbf{T} = 2\mu\mathbf{S} + \lambda\varepsilon_v\mathbf{I} + \alpha p\mathbf{I} \quad (2.18)$$

where  $\mu$ ,  $\lambda$  are the shear modulus and the bulk modulus applicable to the porous fabric, respectively,  $\alpha$  poroelastic parameter introduced by Biot and Willis (1957),  $\mathbf{I}$  is a unit tensor and  $\varepsilon_v$  is the volumetric strain of porous fabric, which takes the form

$$\varepsilon_v = \nabla \cdot \mathbf{u} \quad (2.19)$$

The pore pressure generated in the pores is given by the relationship

$$p = \beta(\xi_v + \alpha\varepsilon_v) \quad (2.20)$$

where  $\beta$  is also a poroelastic parameter, introduced by Biot and Willis (1957). The result (2.20) indicates that the generated pore pressure is related to both volumetric strain of porous fabric and volumetric variation of the fluid content. The compressibility of pore fluid is reflected in two poroelastic parameters  $\alpha$ ,  $\beta$  introduced by Biot and Willis (1957). For the case of an incompressible pore fluid  $\alpha = 1.0$  and  $\beta \rightarrow +\infty$ . The effective stress dyadic takes the form:

$$\mathbf{T}' = \mathbf{T} + \alpha p\mathbf{I} \quad (2.21)$$

The additional equations, including equilibrium, the strain displacement relation, Darcy's law and continuity equation are required to complete the theory of poroelasticity. The quasi-static equilibrium equations in the dyadic form are

$$\nabla \cdot \mathbf{T} + \mathbf{f} = \mathbf{0} \quad (2.22)$$

where  $\mathbf{f}$  is the body force vector and  $\nabla$  is the vector differential operator (see Selvadurai, 2000 a), which takes the form

$$\nabla = \mathbf{e}_1 \frac{1}{H_1} \frac{\partial}{\partial x_1} + \mathbf{e}_2 \frac{1}{H_2} \frac{\partial}{\partial x_2} + \mathbf{e}_3 \frac{1}{H_3} \frac{\partial}{\partial x_3} \quad (2.23)$$

with in Cartesian coordinates, the vector differential operator takes the form:

$$(x_1 \mathbf{e}_1, x_2 \mathbf{e}_2, x_3 \mathbf{e}_3) = (x \mathbf{e}_x, y \mathbf{e}_y, z \mathbf{e}_z), \quad (H_1, H_2, H_3) = (1, 1, 1) \quad (2.24)$$

Result (2.24) can be re-written in the following notation  $H_j$  ( $j = 1, 2, 3$ ), which are the components for the coordinates.

The strain dyadic is related to the displacement vector in the following form:

$$\mathbf{S} = \frac{1}{2} (\nabla \mathbf{u} + \mathbf{u} \nabla) \quad (2.25)$$

The isotropic form of Darcy's law for quasi-static pore fluid flow takes the form:

$$\mathbf{v} = -\frac{k}{\gamma_w} \nabla p \quad (2.26)$$

where  $k$  is the hydraulic conductivity and  $\gamma_w$  the unit weight of water. The continuity equation of fluid flow follows as:

$$\frac{\partial \xi_v}{\partial t} + \nabla \cdot \mathbf{v} = 0 \quad (2.27)$$

Results (2.17) to (2.27) form a system of linear partial differential equations that can model the three-dimensional response of the poroelastic medium, and the formulation of specific problems can be completed through the assignment of appropriate boundary and initial conditions. The partial differential equations that govern the time-dependent behaviour of a poroelastic medium take the forms:

$$\mu \nabla \cdot \nabla \mathbf{u} + (\mu + \lambda) \nabla \nabla \cdot \mathbf{u} + \alpha \nabla p + \mathbf{f} = \mathbf{0} \quad (2.28a)$$

$$\frac{\partial p}{\partial t} - \frac{k}{\gamma_w} \beta \nabla \cdot \nabla p + \alpha \beta \frac{\partial \varepsilon_v}{\partial t} = 0 \quad (2.28b)$$

The system of equations (2.28) can be formulated in Cartesian coordinates and  $\mu, \lambda$  can also be replaced with elasticity parameters  $\mu, \nu$ , where  $\nu$  is Poisson's ratio. In the absence of body forces, the system of equations in Cartesian coordinates take the forms:

$$\mu \nabla^2 u_i + (\mu + \lambda) \varepsilon_{kk,i} + \alpha p_{,i} = 0 \quad (2.29a)$$

$$\frac{k}{\gamma_w} \beta \nabla^2 p - \frac{\partial p}{\partial t} + \alpha \beta \frac{\partial \varepsilon_{kk}}{\partial t} = 0 \quad (2.29b)$$

The poroelastic parameters  $\alpha, \beta$ , which define respectively, the compressibility of the pore fluid and the compressibility of the soil fabric that were introduced by Biot and Willis (1957) can be expressed in the following forms;

$$\alpha = \frac{3(\nu_u - \nu)}{B(1 - 2\nu)(1 + \nu_u)} \quad ; \quad \beta = \frac{2\mu B^2 (1 - 2\nu)(1 + \nu_u)^2}{9(\nu_u - \nu)(1 - 2\nu_u)} \quad (2.30)$$

where  $\nu_u$  is the undrained Poisson's ratio, and  $B$  can be identified with the pore pressure parameter introduced by Skempton (1954). The parameter  $B$  is defined as the ratio of the

induced pore water pressure to the changes in total isotropic stress, measured under undrained conditions.

The bounds for the constitutive parameters, governing time-dependent behaviour of the fluid-saturated poroelastic media can be obtained by consideration of the requirements for a positive definite strain energy potential defined by (2.17) (Rice and Cleary, 1976). The bounds for the parameters take in the following forms:

$$\mu > 0; \quad -1 < \nu < \nu_u \leq 0.5; \quad k > 0; \quad B \neq 0. \quad (2.31)$$

In geomechanics, the lower limit of  $-1$  for  $\nu$  and  $\nu_u$  can be replaced by the realistic limit of zero. Consequently, the bounds for geomaterials take the forms:

$$0 \leq \nu < \nu_u \leq 0.5; \quad 0 < B \leq 1 \quad (2.32)$$

In the case of a poroelastic medium, which is saturated with an incompressible pore fluid, the poroelastic parameters take the forms:

$$\nu_u = 0.5; \quad B = 1 \quad (2.33)$$

In this case  $\xi_v = \varepsilon_{kk}$ ,  $\alpha = 1$ ,  $\beta \rightarrow \infty$  and the governing equations reduce to:

$$\mu \nabla^2 u_i + \frac{\mu}{(1-2\nu)} \varepsilon_{kk,i} + p_{,i} = 0 \quad (2.34a)$$

$$\frac{\partial \varepsilon_{kk}}{\partial t} = \frac{2k\mu(1-\nu)}{\gamma_w(1-2\nu)} \nabla^2 \varepsilon_{kk} \quad (2.34b)$$

The boundary and initial conditions on the variables  $u_i$ ,  $p$  and/or on their derivatives can be prescribed, for a well-posed problem. Aspects of uniqueness of the classical

poroelasticity problem as posed by Biot (1941) are given by Coussy (1995) and Altay and Dokmeci (1998).

In this research attention will be restricted to theories of poroelasticity, which are largely applicable to the brittle geomaterials that are fully saturated with water. The pore fluid is considered to be incompressible. This results in the assumption of incompressibility of both solid particles constituting the porous fabric and pore fluid; consequently the governing partial differential equations of classical theory of poroelasticity, developed by Biot (1941) can be reduced to the system of equations defined by (2.34). The formulation of classical theory of poroelasticity for this case has been documented by a number of researchers including, Desai and Christian (1977), Detournay and Cheng (1993) and Lewis and Schrefler (1998).

## **2.4 Computational Modelling of Poroelastic Media**

The finite element technique is now regarded as a well-established computational approach for examining a variety of problems in the engineering sciences (Bathe, 1996; Zienkiewicz and Taylor, 2000). This technique is based on subdividing the domain into discrete finite elements. The elements are connected at nodal points and continuity of displacement and pore pressure fields are prescribed at the element boundaries. The values of the field variables within the elements are interpolated by polynomials of their nodal values. The governing partial differential equations of the classical theory of poroelasticity can be represented as a system of linear matrix equations by using a variational principle to obtain the system of integral relationships. The Galerkin technique is applied to solve the system of integral formulas. The computational modelling of the classical problem in poroelasticity through finite element techniques is first attributed to Sandhu and Wilson (1969). They applied the variational principles introduced by Gurtin (1964) to the classical theory of poroelasticity developed by Biot (1941) to model the consolidation behaviour of a poroelastic region saturated with an incompressible pore fluid. Sandhu and Wilson (1969) also successfully applied the finite element scheme to model the problem of one-dimensional consolidation and the

consolidation of a strip foundation, resting on a poroelastic half-space. In work that followed, Ghaboussi and Wilson (1973) applied Gurtin's variational principle to model the consolidation behaviour of a poroelastic region saturated with either compressible or an incompressible pore fluid. Ghaboussi and Wilson (1973) applied the finite element technique to model the consolidation behaviour of the problem of an axisymmetric sand drain and the problem of consolidation of a poroelastic half-space, subjected to an axisymmetric flexible load. The investigations by Booker and Small (1975) and Sandhu *et al.* (1977) focus on different spatial interpolation schemes and temporal approximations for the study of the poroelasticity problem. Topics of related interest are also given by Turska and Schrefler (1993) and Lewis and Schrefler (1998).

Booker and Small (1975) have applied the finite element technique to examine problems associated with surface loading of a poroelastic half-space. Selvadurai and Gopal (1986) and Schrefler and Simoni (1987) have also applied the finite element technique to determine consolidation behaviour of a poroelastic half-space using special infinite elements. A paper of particular interest to this research is by Mahyari and Selvadurai (1998) who used an iterative finite element procedure to examine the mechanics of indentation of a fluid-saturated poroelastic half-space susceptible to damage.

Finite element technique has a greater appeal to the modelling of engineering problems, particularly those dealing with transient time-dependent problems, problems related to non-linear material behaviour and problems with general three-dimensional configurations, which are generally too complex to attempt a solution based on the analytical solution of the governing equations. In this research, a Galerkin finite element technique is adopted to formulate iterative computational procedures to examine the poroelasticity problems, related to initiation and evolution of damage in fluid-saturated poroelastic media.



## 2.5 Finite Element Formulations

The numerical procedure introduced by Galerkin (1915) can be applied to approximate the partial differential equations of the classical theory of poroelasticity (2.29 a, b) and to reduce them to a set of linear matrix equations. The detail of the procedure is well documented by Sandhu and Wilson (1969), Christian and Boehmer (1970), Ghaboussi and Wilson (1973), Aboustit *et al.* (1985), Schrefler and Simoni (1987), Lewis and Schrefler (1998) and Zienkiewicz and Taylor (2000). The finite element formulation of the thermal consolidation of porous media is also documented by Selvadurai and Nguyen (1995), Giraud and Rousset (1996) and Pao *et al.* (2001).

A brief review of the Galerkin technique and the finite element approximation of classical theory of poroelasticity, is given in the following sections.

### 2.5.1 Galerkin Weighted Residual Method

The formulation of the finite element procedure applicable to three-dimensional consolidation is derived for the general case without referring to any specific element types. In the absence of body forces the governing equations take the form:

$$\mu \nabla^2 u_i + (\mu + \lambda) \varepsilon_{kk,i} + \alpha p_{,i} = 0 \quad (2.29a)$$

$$\frac{k}{\gamma_w} \beta \nabla^2 p - \frac{\partial p}{\partial t} + \alpha \beta \frac{\partial \varepsilon_{kk}}{\partial t} = 0 \quad (2.29b)$$

The initial boundary value problem to be solved should satisfy the governing equations (2.29a) and (2.29b) and initial conditions within the domain  $R$  and the associated boundary conditions satisfied on the boundary  $S$  of the domain. Applying Galerkin's technique, the governing equations can be transformed into matrix equations where variables are the nodal displacements and pore pressures. Sandhu and Wilson (1969) and Ghaboussi and Wilson (1973) have shown that for ensuring the stability of the solution, the nodal displacements are assigned an order different (higher) from the stresses and

pore pressures. Let  $u_{ij}$  ( $i=1,2,3; J=1,...,N$ ) be the nodal displacements for  $N$  discrete points in  $R$  and  $p_K$  ( $K=1,...,n$ ) the nodal pore pressures in  $n$  nodes at an arbitrary time  $t$ . The displacement vector and pore pressure for any arbitrary point with coordinates  $x_j$  in the domain  $R$  are approximated in the following form:

$$u_i = u_i(x_j, t) = N_J^u u_{iJ} \quad (2.35)$$

$$p = N_K^p p_K \quad (2.36)$$

where  $N_J^u$  and  $N_K^p$  are, respectively, shape functions for the displacement and pore pressure field;  $J=1,...,N$  and  $K=1,...,n$ ;  $u_{iJ}$  is the displacement of the solid skeleton at node  $J$  in the  $i^{\text{th}}$  direction. The indices in capital letters (e.g.  $J$  and  $K$ ) refer to the nodal values and the indices in small letters (e.g.  $i$  and  $j$ ) refer to the coordinate directions. The summation convention on repeated indices is also adopted. Generally,  $N_J^u$  and  $N_K^p$  can be different but both  $N_J^u$  and  $N_K^p$  must exhibit  $C^0$  continuity.

### 2.5.1.1 Galerkin Formulation for the Equilibrium Equation

Applying Galerkin's weighted residual method to the equilibrium equations (2.29a) we obtain

$$\int_R N_I^u \left[ \mu \frac{\partial^2 u_i}{\partial x_j \partial x_j} + (\mu + \lambda) \frac{\partial^2 u_j}{\partial x_i \partial x_j} + \alpha \frac{\partial p}{\partial x_i} \right] dR = 0 \quad (2.37)$$

where  $I=1,...,N$ . Applying Green's theorem, (2.37) can be rewritten in terms of surface and domain integrals in the forms

$$\begin{aligned}
& \int_S N_i'' \left( \frac{\partial u_i}{\partial x_j} + \frac{\partial u_j}{\partial x_i} \right) n_j dS - \int_R \mu \left( \frac{\partial u_i}{\partial x_j} + \frac{\partial u_j}{\partial x_i} \right) \frac{\partial N_i''}{\partial x_j} dR + \\
& \int_S N_i'' \left( \lambda \frac{\partial u_j}{\partial x_j} + \alpha p \right) n_i dS - \int_R \left( \lambda \frac{\partial u_j}{\partial x_j} + \alpha p \right) \frac{\partial N_i''}{\partial x_i} dR = 0
\end{aligned} \tag{2.38}$$

where  $S$  is the boundary that corresponds to  $R$ . Substituting the representations (2.35) and (2.36) into (2.38) and making use of the strain-displacement representation of the constitutive relationships,

$$\sigma_{ij} = \mu \left( \frac{\partial u_i}{\partial x_j} + \frac{\partial u_j}{\partial x_i} \right) + \left( \lambda \frac{\partial u_k}{\partial x_k} + \alpha p \right) \delta_{ij} \tag{2.39}$$

We can rewrite (2.38) in the form

$$\begin{aligned}
& \int_R \left[ \mu \frac{\partial N_i''}{\partial x_j} \left( \frac{\partial N_j''}{\partial x_j} u_{ij} + \frac{\partial N_j''}{\partial x_i} u_{ji} \right) + \lambda \frac{\partial N_j''}{\partial x_i} \frac{\partial N_j''}{\partial x_j} u_{ji} \right] dR + \\
& \int_R \alpha \frac{\partial N_i''}{\partial x_i} N_K^p p_K dR = \int_S N_i'' \sigma_{ij} n_j dS
\end{aligned} \tag{2.40}$$

The matrix form of equation (2.40) can be written in the form

$$[\mathbf{K}]\{\delta\} + [\mathbf{C}]\{\mathbf{p}\} = \{\mathbf{F}_i\} \tag{2.41}$$

where  $\{\delta\}$  and  $\{\mathbf{p}\}$  are the vectors of the nodal displacements and pore pressures:

$$\begin{aligned}
\{\delta\}^T &= \{\{u_{11} \ u_{21} \ u_{31}\} \ \dots \ \{u_{1N} \ u_{2N} \ u_{3N}\}\}^T \\
\{\mathbf{p}\}^T &= \{p_1 \ \dots \ p_n\}^T
\end{aligned} \tag{2.42}$$

$\{\mathbf{F}_i\}$  corresponds to the vectors representing the traction applied at the boundary  $S$ . The components of the coupling matrix  $[\mathbf{C}]$  due to the interaction between the solid skeleton and the pore fluid are given in the following form:

$$[\mathbf{C}] = \alpha \int_R \frac{\partial N_i''}{\partial x_i} N_K^p dR \quad (2.43)$$

The stiffness matrix  $[\mathbf{K}]$  applicable to the porous skeleton takes the form:

$$[\mathbf{K}] = \int_R [\mathbf{B}]^T [\mathbf{D}] [\mathbf{B}] dR \quad (2.44)$$

where  $[\mathbf{D}]$  is the stiffness matrix corresponding to the isotropic elastic behaviour of the porous skeleton. For a material that exhibits isotropic linear elastic response, The stiffness matrix  $[\mathbf{D}]$  only depends on two elastic constants  $\mu$  and  $\lambda$ . The strains are related to the nodal displacements through the matrix  $[\mathbf{B}]$ , which depends on the shape functions  $N_i''$ .

### 2.5.1.2 Galerkin Formulation for the Fluid Continuity Equation

Applying the Galerkin method to the flow continuity equation (2.29b), its weighted residual equivalent can be obtained in the form of:

$$\int_R N_i^p \left[ \frac{k}{\gamma_w} \frac{\partial^2 p}{\partial x_i \partial x_j} - \frac{1}{\beta} \frac{\partial p}{\partial t} + \alpha \frac{\partial}{\partial t} \left( \frac{\partial u_i}{\partial x_i} \right) \right] dR = 0 \quad (2.45)$$

Applying Green's theorem to (2.45), we can rewrite it in terms of boundary and domain integrals in the form

$$\begin{aligned}
& \int_S N_I^p \frac{k_{ij}}{\gamma_w} \frac{\partial p}{\partial x_j} n_i dS - \int_R \frac{\partial N_I^p}{\partial x_i} \frac{k_{ij}}{\gamma_w} \frac{\partial p}{\partial x_j} dR \\
& - \int_R \frac{N_I^p}{\beta} \frac{\partial p}{\partial t} dR + \int_R \alpha N_I^p \frac{\partial}{\partial t} \left( \frac{\partial u_i}{\partial x_i} \right) dR = 0
\end{aligned} \tag{2.46}$$

Substituting (2.35) and (2.36) in to (2.46), we obtain:

$$\begin{aligned}
& \int_R \alpha N_I^p \frac{\partial N_J^p}{\partial x_i} \frac{du_{ij}}{dt} dR - \int_R \frac{\partial N_I^p}{\partial x_i} \frac{k_{ij}}{\gamma_w} \frac{\partial N_K^p}{\partial x_j} p_K dR \\
& - \int_R N_I^p \frac{1}{\beta} N_K^p \frac{dp_K}{dt} dR = - \int_S N_I^p \frac{k_{ij}}{\gamma_w} \frac{\partial p}{\partial x_j} n_i dS
\end{aligned} \tag{2.47}$$

The matrix form of (2.47) can be expressed in the form

$$[\mathbf{C}]^T \left\{ \frac{d\boldsymbol{\delta}}{dt} \right\} - [\mathbf{H}] \{\mathbf{p}\} - [\mathbf{E}] \left\{ \frac{d\mathbf{p}}{dt} \right\} = \{\mathbf{F}_q\} \tag{2.48}$$

where the hydraulic conductivity matrix  $[\mathbf{H}]$  takes the form:

$$[\mathbf{H}] = \int_R \frac{\partial N_I^p}{\partial x_i} \frac{k_{ij}}{\gamma_w} \frac{\partial N_K^p}{\partial x_j} dR \tag{2.49}$$

The compressibility matrix for the pore fluid  $[\mathbf{E}]$  takes the form :

$$[\mathbf{E}] = \int_R N_I^p \frac{1}{\beta} N_K^p dR \tag{2.50}$$

The inward fluid flux through the boundary  $S$  is  $\{\mathbf{F}_q\}$ . The matrix equations (2.41) and (2.48) conclude the finite element approximations of the classical theory of poroelasticity.

### 2.5.1.3 Time Integration and Stability

An incremental form of the governing equation is necessary to model the non-linear behaviour of materials resulting from evolution of damage or plasticity phenomena. (see Lewis and Schrefler, 1998 and Zienkiewicz and Taylor, 2000). Through differentiation of the equilibrium equation (2.41), the system of incremental coupled equations takes the form:

$$\begin{bmatrix} \mathbf{K} & \mathbf{C} \\ \mathbf{C}^T & -\mathbf{E} \end{bmatrix} \frac{d}{dt} \begin{Bmatrix} \delta \\ \mathbf{p} \end{Bmatrix} + \begin{bmatrix} 0 & 0 \\ 0 & -\mathbf{H} \end{bmatrix} \begin{Bmatrix} \delta \\ \mathbf{p} \end{Bmatrix} = \begin{Bmatrix} \frac{d\mathbf{F}_t}{dt} \\ \mathbf{F}_q \end{Bmatrix} \quad (2.51)$$

The matrices in (2.51) relate the increments of responses ( $d\{\delta\}, d\{\mathbf{p}\}$ ) to the increments of external driving forces ( $d\mathbf{F}_t$  and  $\mathbf{F}_q$ ). The matrices are dependent on the current state ( $\{\delta\}, \{\mathbf{p}\}$ ) in the system.

The system of coupled equations in (2.51) is discretized in the time domain using the following finite difference scheme applicable to any variable  $X$  in the system:

$$X^\gamma = (1 - \gamma)X^0 + \gamma X^1 \quad (2.52)$$

$$\frac{dX}{dt} = \frac{X^1 - X^0}{\Delta t} \quad (2.53)$$

Where  $\Delta t$  is time increment,  $X^0$ ,  $X^1$ ,  $X^\gamma$  are the values of  $X$  at different times  $t$ ,  $t + \Delta t$ ,  $t + \gamma\Delta t$  respectively;  $\gamma$  is a value that varies between 0 and 1. When  $\gamma = 0$ , the finite difference scheme is termed fully explicit; for  $\gamma = 1$  the finite difference scheme is referred to as fully implicit and when  $\gamma = 0.5$ , the finite difference scheme is referred to as the Crank-Nicholson scheme.

Applying the finite difference scheme to  $d\{\delta\}/dt$  and  $d\{p\}/dt$  in (2.51) results in the following discretized matrix equation:

$$\begin{bmatrix} \mathbf{K} & \mathbf{C} \\ \mathbf{C}^T & \{-\gamma\Delta t\mathbf{H} + \mathbf{E}\} \end{bmatrix} \begin{Bmatrix} \mathbf{u}_{t+\Delta t} \\ p_{t+\Delta t} \end{Bmatrix} = \begin{bmatrix} \mathbf{K} & \mathbf{C} \\ \mathbf{C}^T & \{(1-\gamma)\Delta t\mathbf{H} + \mathbf{E}\} \end{bmatrix} \begin{Bmatrix} \mathbf{u}_t \\ p_t \end{Bmatrix} + \{\mathbf{F}\} \quad (2.54)$$

where

$\mathbf{K}$  = stiffness matrix of the porous skeleton;

$\mathbf{C}$  = stiffness matrix due to interaction between porous skeleton and pore fluid;

$\mathbf{E}$  = compressibility matrix of the pore fluid;

$\mathbf{H}$  = hydraulic conductivity matrix;

$\mathbf{F}$  = force vectors due to external traction;

$u_t, p_t$  = nodal displacements and pore pressures at time  $t$ ;

$\Delta t$  = time increment

$\gamma$  = time integration constant and  $( )^T$  denotes the transpose.

and the time integration constant  $\gamma$  varies between 0 and 1.

### 2.5.2 Finite Element Discretization in Space

Using a standard finite element approach, the three-dimensional domain  $R$  is discretized into a number of finite elements. The element selected to discretize the poroelastic domain is the twenty-node isoparametric element, the displacements within the element are interpolated as functions of the 20 nodes, whereas the pore pressures are interpolated as functions of only the eight corner nodes (Figure 2.1). This type of element can be used to model the transient time-dependent response of poroelastic medium with a sufficient accuracy for problems that investigate consolidation behaviour of a poroelastic medium under general three-dimensional conditions. Abousit *et al.* (1985) and Lewis and Schrefler (1998) indicated that less spatial oscillation in the solution occur for the case

where the pore pressure field is interpolated at lower number of nodes than the number associated with displacements field, in a finite element where all degrees of freedom are interpolated at all nodes. This choice of element characteristics are considered necessary, especially when computational modelling is used to examine the limit of undrained behaviour. The case of limiting undrained response is achieved by setting the hydraulic conductivity and compressibility matrices to be zero. Therefore, the diagonal terms of (2.54) become zero. The physical meaning of this spatial oscillation can be explained as follows: The fluid pressure has the same dimension as the stress, and strain is directly related to stress through the elasticity parameters  $\mu$  and  $\nu$ . Since the strain is expressed in terms of the spatial derivatives of the displacement field, the polynomials used, as interpolation functions for fluid pressure should be one order lower than the functions that are used for the displacement field. Such a procedure will satisfy the consistency of fields of variables.

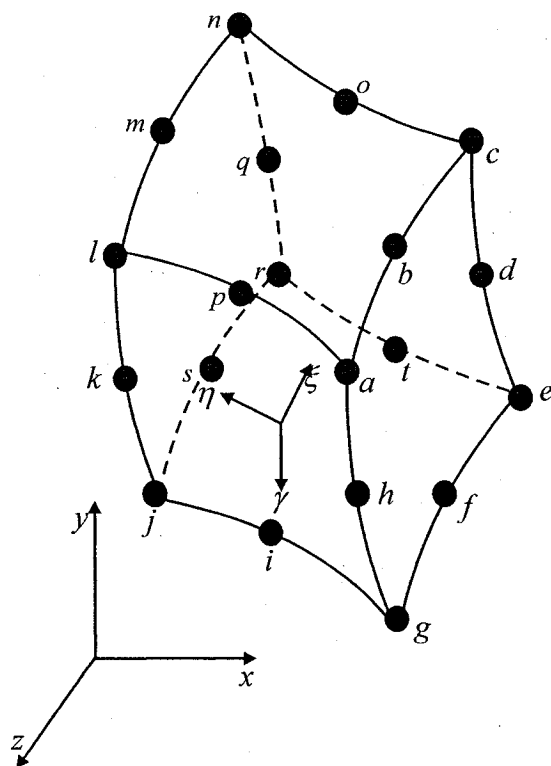


Figure 2.1 Three-dimensional isoparametric element.



### 2.5.3 Numerical Properties of the Discretization in Time

The basic requirements of modelling a differential equation through a computational scheme are consistency and stability of the approximate computational solution. Consistency ensures that the computational solution converges to the exact solution and the stability ensures that the round off errors of the initial values do not grow during the solution process. In contrast to ordinary differential equations, the partial differential equations governing initial boundary value problems, including those of the classical theory of poroelasticity, may result in a stable approximate solution that converges to the solution of a different system of equations, and consequently the computational scheme will exhibit inconsistency (see Farhat and Sobh, 1990 and Lewis and Schrefler, 1998).

It is assumed that the application of a proper choice of an element can result in consistency and convergence of the finite element discretization in space. It therefore remains to establish the convergence of the discretization scheme in time. The total error of a computational scheme is determined by the evaluation of the difference between the exact solution  $X(t_{n+1})$  and the computational solution  $\tilde{X}_{n+1}$  that corresponds to a time instant  $t_{n+1}$ , which takes the form:

$$\text{Total error} = e_c + e_s \quad (2.55)$$

where,  $e_c = X(t_{n+1}) - X_{n+1}$  corresponds to the error due to the discretization of (2.54) and  $e_s = X_{n+1} - \tilde{X}_{n+1}$  corresponds to the error due to the stability. The total error can be considered to be negligible, when the norm of the two types of errors is negligible.

Lewis and Schrefler (1998) determined the error  $e_c$  for (2.54), which takes the form:

$$e_c = \frac{1}{2}(1-2\gamma)O(\Delta t^2) + \frac{1}{2}\gamma^2 O(\Delta t^3) \quad (2.56)$$

where  $O(\Delta t)$  corresponds to the order of error. In order to examine the stability of the solution, Turska and Schrefler (1993) also performed a stability analysis. To aid the analysis, the amplification factor  $\chi$  is taken in the form:

$$X_{n+1} = \chi X_n \quad (2.57)$$

The amplification factor  $\chi$  should be determined to be a nontrivial solution of (2.54) for  $\mathbf{F} = \mathbf{0}$  if the following condition is satisfied:

$$|\chi| < 1 \quad (2.58)$$

This results in the stability of the system of equations (2.54) and the error  $\|e\| \rightarrow 0$  when  $n \rightarrow \infty$ . Then, a modal decomposition of equation (2.54) is performed, for the case where  $\mathbf{F}$  is set to zero (See Lewis and Schrefler, 1998). We assume that  $\mu_1, \mu_2, \dots, \mu_m$  correspond to the distinct complex eigenvalues of the solution and  $m$  is the rank of the matrix that leads to the solution. The homogeneous form of (2.54) decomposes into  $m$  equations:

$$(1 + \gamma \Delta t \mu_j) X_{n+1}(j) = (1 - (1 - \gamma) \Delta t \mu_j) X_n(j) \quad (2.59)$$

where  $j = 1, 2, \dots, m$  and  $X_n(j)$  denotes the scalar values, obtained by solving (2.54) through the computational scheme. The condition corresponding to (2.58) can be written as

$$\left| \frac{1 - (1 - \gamma) \Delta t \mu_j}{1 + \gamma \Delta t \mu_j} \right| < 1 \quad (2.60)$$

Substituting,  $\text{Re}[\mu_j] = \mu_R$  and  $\text{Im}[\mu_j] = \mu_I$ , the inequality (2.60) takes the form:

$$-2\mu_R < (2\gamma - 1)(\mu_R^2 + \mu_I^2)\Delta t \quad (2.61)$$

Assuming that  $\gamma > 1/2$  and  $\mu_R > 0$ , the inequality (2.61) is satisfied for all values of  $\Delta t$  and  $\mu_I$ ; consequently, this ensures that (2.54) exhibits unconditional stability if  $\gamma > 1/2$ . If  $\mu_R \leq 0$ , the inequality (2.61) results in a conditional stability with a requirement that the time step  $\Delta t$  should satisfy the requirement

$$\Delta t > \frac{-2}{2\gamma - 1} \frac{\mu_R}{(\mu_R^2 + \mu_I^2)} \quad (2.62)$$

The inequality (2.62) results in the lower bounds for the time step  $\Delta t$ . Assume that  $\gamma < 1/2$ ; Conditional stability is achieved by determining an upper bound for the time step  $\Delta t$  in the following form:

$$\Delta t < \frac{2}{1 - 2\gamma} \frac{\mu_R}{(\mu_R^2 + \mu_I^2)} \quad (2.63)$$

The solution of (2.54) is unstable, only when  $\mu_R \leq 0$ .

The criteria for the stability of the time-integration scheme for solving (2.54) are also given by other investigators. Booker and Small (1975) suggest that unconditional stability is assured when  $\gamma \geq 1/2$ . According to Nguyen (1995), Selvadurai and Nguyen (1995) and Mahyari (1997) the stability of solution can generally be achieved with the values of  $\gamma$  close to unity.

## **CHAPTER 3**

### **MECHANICS OF BRITTLE FLUID SATURATED POROELASTIC MEDIA SUSCEPTIBLE TO MICRO-MECHANICAL DAMAGE**

#### **3.1 Introduction**

The partial differential equations governing the classical theory of poroelasticity were developed by Biot (1941) by assuming a linear elastic behaviour of the porous skeleton. This assumption is a significant limitation in the application of the classical theory of poroelasticity to brittle geomaterials that could exhibit degradation in elastic stiffness and other non-linear effects resulting from the stress transfer from the pore fluid to the porous skeleton, during the consolidation process. Such non-linear behaviour and irreversible phenomena can be due to development of micro-defects such as micro-cracks and/or micro-voids in the porous skeleton, which can also lead to alterations in the hydraulic conductivity characteristics of the porous medium. The classical theory of continuum damage mechanics introduced by Kachanov (1958) can be incorporated within the classical theory of poroelasticity to model damage phenomena in brittle fluid-saturated porous materials. Experimental evidence shows that the process of evolution of damage in a brittle geomaterial is a stress state-dependent phenomenon; therefore any damage model has to account for the stress state-dependency for the development of micro-mechanical damage. This Chapter deals with the development of a finite element approach for modelling the influence of damage-induced alterations in both elasticity and hydraulic conductivity characteristics of the porous skeleton on the time-dependent behaviour of brittle fluid saturated poroelastic media.

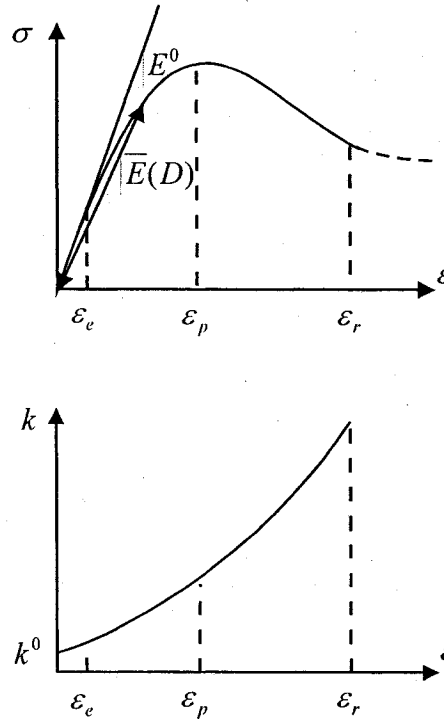


Figure 3.1 Typical stress-strain curve and the damaged induced alterations in hydraulic conductivity of the brittle geomaterials.

Classical continuum damage mechanics accounts phenomenologically for the influence of *micro-cracks* on material behaviour prior to the development of *macro-cracks* (i.e. fractures). At the level of micro-cracks development, the material is assumed to behave as a continuum. Therefore, damage can be interpreted phenomenologically as a reduction in the elastic stiffness of the material due to the generation of micro-defects. The focus of this research is restricted primarily to modelling of the brittle elastic behaviour of geomaterials to which a continuum description is applicable during the damage evolution process and the stress states are substantially lower than those required to initiate failure in the form of material yield and/or macro-crack formation (Figure 3.1). The development of damage invariably results in anisotropy in the internal structure of the porous medium. In this thesis, however, attention is restricted to the consideration of isotropic damage evolution, which can be defined by appeal to a single scalar variable.

The time-dependent behaviour of brittle fluid saturated geomaterials can be influenced by the evolution of damage in the porous skeleton. The notion of continuum damage relates to brittle geomaterials such as soft rocks, overconsolidated clays, etc., which exhibit progressive degradation in stiffness in an elastic sense due to the generation of micro-cracks and micro-voids. The generation of these defects can also lead to alterations in hydraulic conductivity characteristics that can influence the time-dependent poroelastic behaviour of the saturated geomaterial. With the class of materials examined in this thesis, the coupling of both alterations in elasticity and hydraulic conductivity characteristics is considered to be significant even at stress levels well below the peak stress. Figure 3.1 illustrates the typical idealized behaviour of a brittle fluid saturated geomaterial that experiences damage in the porous skeleton. In this figure  $\varepsilon_e$  refers to the strain that corresponds to the limit of the linear elastic response;  $\varepsilon_p$  refers to the strain that corresponds to the peak stress and  $\varepsilon_r$  refers to the strain that corresponds to a residual strain.

The influence of micro-mechanical damage on the time-dependent poroelastic behaviour of brittle saturated geomaterials can be examined by incorporating continuum damage concepts within the classical theory of poroelasticity. This can be achieved by altering the elastic stiffness and hydraulic conductivity characteristics of the porous medium with the state of damage in the material. Based on experimental observations conducted on sandstone, Cheng and Dusseault (1993) have proposed an anisotropic damage criterion for the degradation of stiffness due to damage evolution. Their treatment of damage in poroelastic media, however, does not take into account the alterations in hydraulic conductivity characteristics of the geomaterials that can result from the generation of micro-cracks and micro-voids. Such an extension was first proposed by Mahyari and Selvadurai (1998) who considered alteration in the hydraulic conductivity characteristics of the material experiencing damage by introducing a relationship for the isotropic damage-induced alterations in hydraulic conductivity. The proposals of Mahyari and Selvadurai (1998) were based on experimental observations made by Shiping *et al.* (1994) on sandstone. Furthermore, Mahyari and Selvadurai (1998) also proposed an iterative finite element scheme for examining the time-dependent behaviour of brittle

fluid saturated geomaterials by considering simultaneous alterations in both elasticity and hydraulic conductivity characteristics of porous skeleton. They applied the computational scheme to examine the problem of indentation of a brittle geomaterial half-space by a rigid smooth impermeable indenter with a flat base. The finite element formulation proposed by Mahyari and Selvadurai (1998) was applicable to only axisymmetric problems. One of the developments of this thesis is an extension of the work of Mahyari and Selvadurai (1998) to include generalized three-dimensional behaviour of the poroelastic material with isotropic damage process. Experimental observations (e.g. Schulze *et al.*, 2001) also indicate that the damage evolution is highly stress state-dependent. This research also extends the original concepts developed by Mahyari and Selvadurai (1998) to include stress state-dependency of the damage evolution process.

The computational scheme developed in connection with this research accounts for the isotropic damage-induced alterations in the elasticity and hydraulic conductivity characteristics. The isotropic damage evolution functions, which are used to model the reduction in the elastic stiffness and the increase in the hydraulic conductivity, are related to the distortional strain invariant. Admittedly, the damage process is expected to be highly anisotropic and could be restricted to localized zones. The stress state-dependency of the evolution of damage is also taken into consideration through constraints applicable to the first invariant of the effective strain tensor. The three-dimensional finite element formulations developed in connection with the research are used to examine problems with generalized loadings and three-dimensional states of deformation. In the ensuing chapters, the extended computational scheme is applied to examine problems of importance to geomechanics.

### **3.2 Continuum Damage Mechanics Concepts**

The origin of the concept of continuum damage mechanics (CDM) is attributed to Kachanov (1958), in recognition of his initial studies into the phenomenological modelling of tertiary creep in engineering materials. Classical continuum damage mechanics models the effect of internal degradation of materials prior to the development

of macro-cracks, which results in fracture. Continuum damage mechanics has been widely used to predict the non-linear behaviour of a variety of materials including metals, concrete, composites, ice, frozen soils and geological materials. Krajcinovic and Fonseka (1981) used the concept of damage mechanics in connection with the energy function for a damaged material and developed a damage function to account for the evolution of damage under uniaxial loadings. Bazant (1986) investigated the evolution of micro-mechanical damage around crack tips. Mazars and Bazant (1989) document the evolution of both macro-defects and micro-defects in concrete. Simo and Ju (1987) applied the concept of continuum damage mechanics to model the evolution of damage in concrete through comparison with the experimental observations, conducted on concrete by Wang (1977). The work of Ju (1990) examines the theoretical concepts of postulating continuum damage mechanics in the general tensorial form. Selvadurai and Au (1991) examined the problem of indentation of a polycrystalline solid through application of continuum damage mechanics in connection with viscoplasticity. Cheng and Dusseault (1993) applied the concept of continuum damage mechanics to modelling of soft rocks including sandstone, and proposed a damage evolution function, applicable to soft rocks. Selvadurai and Hu (1995) examined the mechanics of frozen soils using the concept of continuum damage mechanics. They applied damage modelling to examine the mechanics of a pipe section embedded in a frozen soil and experiencing uplift. Shao *et al.* (1997) investigated the time-dependent behaviour of brittle geomaterials by using continuum damage mechanics and modelled the experimental observations conducted on brittle rocks. Shao *et al.* (1998, 1999) investigated the behaviour of brittle soft rocks through a computational scheme that accounts for the evolution of damage. These authors also applied the concepts to examine damage-induced alterations in the Lac du Bonnet Granite encountered at the Canadian Underground Research Laboratory (URL) in Pinawa, Manitoba. Mahyari and Selvadurai (1998) investigated the time-dependent behaviour of the damage-susceptible poroelastic media through a computational scheme that accounts for damage-induced alterations in both elasticity and hydraulic conductivity characteristics of poroelastic media. Aubertin *et al.* (2000) investigated the evolution of damage in connection with plasticity, using results of experiments, conducted on brittle soft rocks including rock salt and Lac du Bonnet Granite. Souley *et al.* (2001) also



examined the damage-induced alterations in hydraulic conductivity of Lac du Bonnet Granite through the application of the concept of continuum damage mechanics within a computational scheme. The studies by Tang *et al.* (2002) examine the damage-induced alterations in hydraulic conductivity of granite by using continuum damage mechanics concepts, which is incorporated into a finite element approach. Planas and Elices (2003) studied the evolution of damage as a result of the process of cooling of concrete, by using continuum damage mechanics. Literature related to developments in damage mechanics in general are documented in the review articles and texts by Lemaitre and Chaboche (1990), Krajcinovic (1984 and 1996) and Voyiadjis *et al.* (1998).

Physically, damage can be regarded as the development of defects in the form of micro-cracks or micro-voids. The process of damage evolution begins from the virgin state of a material and ends with fracture of the material region. The non-linear behaviour of most brittle materials can result from either the initiation of new micro-defects and/or the growth of existing micro-defects. This can be modelled by introducing local damage variables. Damage variables reflect the average material degradation at a scale, which is normally associated with classical continuum concepts. This facilitates the adaptation of the *damage mechanics concepts* within any theory associated with classical continuum mechanics (i.e. elasticity, plasticity, viscoelasticity, creep, etc.). The coupling of elasticity and continuum damage mechanics has been investigated by a number of researchers. Sidoroff (1980) investigated the incorporation of anisotropic damage mechanics into the elasticity. Mazars (1982) investigated the application of continuum damage mechanics to analyze the response of the concrete structures. Chow and Wang (1987) presented a general tensorial form of the damage formulation, applicable to classical elasticity. Mazars and Pijaudier-Cabot (1989a,b) used continuum damage mechanics to model the behaviour of concrete structures susceptible to micro-mechanical damage. Eskandari and Nemes (1999) represented the damage variable in terms of fourth rank isotropic tensors and applied it to model the experimental observations conducted on quartzite rock under uniaxial compression loading.

### 3.2.1 The Damage Variable

Continuum damage mechanics is based on the definition of the variables that relate the average degradation as a result of micro-scale discontinuities to phenomenological representations at macro-scale level associated with classical continuum mechanics. Kachanov (1958) was the first to introduce a continuous variable related to density of such discontinuity defects.

Figure 3.2 shows a representative volume element of damaged material that is large enough to contain many defects and small enough to be considered as a material point within the concepts associated with formulations in continuum mechanics (see Davis and Selvadurai, 1996). The overall initial cross sectional area  $A_0$  is defined in relation to the outward unit normal  $\mathbf{n}$ . When damage evolves,  $A_0$  is reduced to the net area  $\bar{A}$ . The damage variable  $D$  associated with the surface on which tractions  $\mathbf{T}$  act is defined by

$$D = \frac{A_0 - \bar{A}}{A_0} \quad (3.1)$$

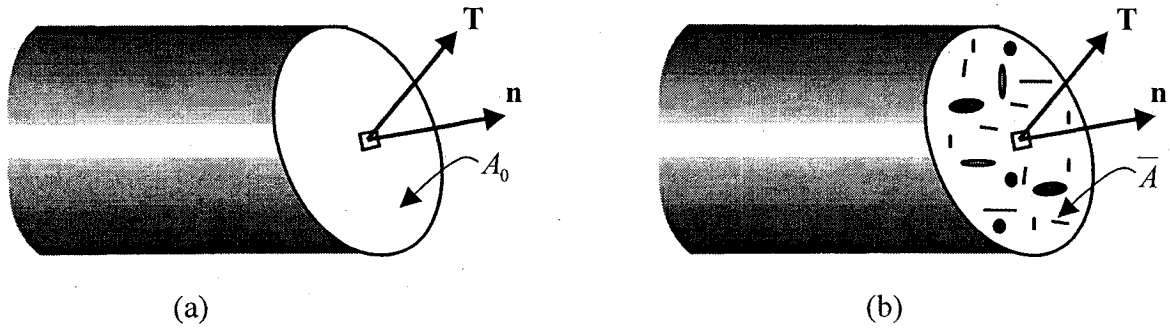


Figure 3.2 Representative element of (a) virgin state and (b) damaged state of brittle material.

The damage variable varies from zero, which corresponds to the virgin state to a critical value  $D_c$ , which corresponds to the fracture of material. In the general case, the micro-

defects are oriented and the damage variable  $D$  is a function of the vector  $\mathbf{n}$ . In such a case the damage variable has a tensorial form (Lemaitre, 1984; Chow and Wang, 1987). In the theory that assumes isotropic damage, the damage process is assumed to result in the development of micro-voids with no dominant directional dependency (i.e. nearly spherical shape) and in the case where damage evolution is due to generation of micro-cracks, the orientation of the cracks is assumed to have no preferred orientation. In these circumstances the damage evolution can be defined by appeal to a single scalar damage variable  $D$ .

### 3.2.2 The Net Stress

The introduction of a scalar damage variable  $D$  leads directly to the concept of a net stress that corresponds to the stress related to the net area. For isotropic damage, the net stress tensor  $\sigma_{ij}''$  is related to the stress tensor  $\sigma_{ij}$  in the undamaged state follows as:

$$\sigma_{ij}'' = \frac{\sigma_{ij}}{1-D} \quad (3.2)$$

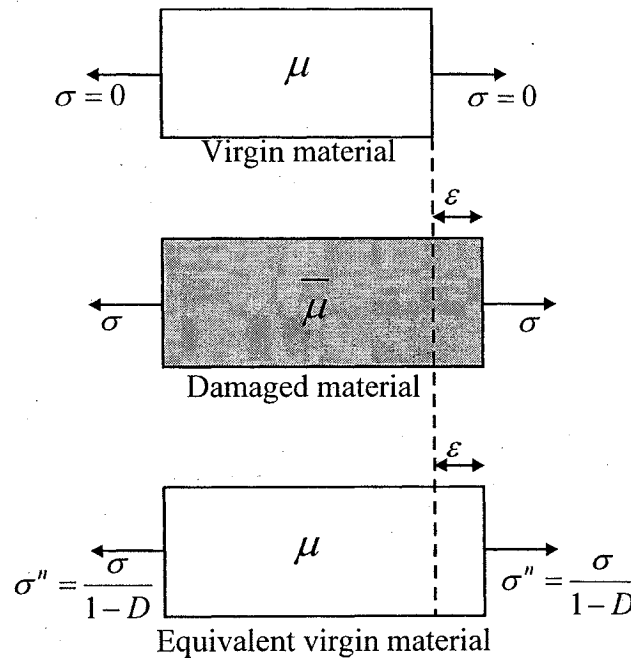


Figure 3.3 Schematic presentation for the hypothesis of strain equivalence.

The determination of parameters for the damaged material is possible through the use of the equivalency between the damaged state and the corresponding virgin state. The equivalency hypothesis, which is used most often, is the *strain equivalency* between the damaged and the undamaged state, first introduced by Lemaitre (1984). The hypothesis can be stated as follows: *A damaged volume of material under the applied stress  $\sigma$  exhibits the same strain response as the virgin state subjected to the net stress  $\sigma^*$*  (Figure 3.3). This hypothesis ensures that the forms of the constitutive laws applicable to the virgin material are also applicable to the damaged material, with the measure of stress applicable to the damaged state being represented by the net stress. The constitutive equation for the damaged material that exhibits isotropic damage and elastic isotropy takes the form:

$$\sigma_{ij} = 2\mu^d \varepsilon_{ij} + \frac{2\mu^d \nu^d}{1 - 2\nu^d} \varepsilon_{kk} \delta_{ij} \quad (3.3)$$

where  $\mu^d = \mu(D)$ ,  $\nu^d = \nu(D)$  are the variable damage-dependent shear modulus and Poisson's ratio, respectively. Using the *hypothesis of strain equivalence*, the elastic parameter  $\mu^d$  can be determined by altering the elastic parameter corresponding to the virgin state, and takes the form:

$$\mu^d = (1 - D)\mu \quad (3.4)$$

The strain equivalency hypothesis assumes that Poisson's ratio remains constant during the damage process; i.e.,  $\nu^d = \nu$ . Other forms of equivalencies can be established and examples of such relationships are given by Wohua and Valliapan (1998a). For the purposes of this research, we shall adopt the equivalency relationships derived from the postulate given by Lemaitre (1984).

### 3.3 The Evolution of Damage

The development of damage in the form of generation of new micro-defects or growth of existing micro-defects results in gradual degradation of material properties. The damage variable is therefore an evolving internal variable that varies from an initial value  $D_0$  ( $D_0 = 0$  for undamaged virgin material) to the critical value  $D_c$  corresponding to the stage at which macro-cracks are initiated (i.e. fracture). For a given state of stress, the evolution of damage is an intrinsic property of the material, which is characterized by a damage evolution function. The damage evolution function can either be postulated using a micro-mechanics approach or determined explicitly using experimental results.

Using experimental results derived from tests conducted on soft rocks, such as sandstone, Cheng and Dusseault (1993) assumed that the damage is a function of the shear strain energy and proposed a damage evolution function for soft rocks, which can be expressed as

$$\frac{dD}{d\xi_d} = \eta \frac{\alpha \xi_d}{1 + \alpha \xi_d} \left( 1 - \frac{D}{D_c} \right) \quad (3.5)$$

where  $\xi_d$  is the equivalent shear strain defined by

$$\xi_d = (e_{ij} e_{ij})^{1/2} = (3\gamma_{oct})^{1/2} \quad ; \quad e_{ij} = \varepsilon_{ij} - \frac{1}{3} \varepsilon_{kk} \delta_{ij} \quad (3.6)$$

In (3.6)  $\gamma_{oct}$  is the octahedral shear strain (see e.g. Davis and Selvadurai, 1996) and  $\alpha$ ,  $\eta$  are material constants. The critical damage variable  $D_c$  is associated with macro-cracks and rupture.

### 3.4 Stress State-dependency of the Evolution of Damage

With brittle geomaterials, the behaviour under tensile stress states can be significantly different from the behaviour under compressive stress states. This implies that the evolution of damage should take into consideration the distinction between tensile stress states and compressive stress states. In this thesis, we refer to the “sense” of the stress states to distinguish between these two types of responses. It is likely that the development of the micro-defects in the porous skeleton can be enhanced for the case of tensile tri-axial stress states. On the other hand, the compressive tri-axial stress state can suppress the development of such effects. Any arbitrary combination of principal stresses including tensile and compressive stress state can induce different magnitudes of damage evolution. The influence of various stress states on the evolution of damage requires the experimental determination of the material response due to different stress paths. The experimental observations of the stress state-dependent damage evolution in brittle geomaterials are relatively scarce; therefore, they are insufficient to develop a comprehensive stress space-dependent theory applicable to the brittle geomaterials. The limited experimental data available show that the evolution of damage is enhanced in a brittle geomaterial that experiences volumetric expansion (see e.g. Schulze *et al.*, 2001). Using these observations it is postulated that damage can initiate only when the strain state satisfies the criterion

$$I_1 = \text{tr} \boldsymbol{\varepsilon} > 0 \quad (3.7)$$

where the tensile strains are considered to be positive.

In contrast to the reduction in elastic stiffness as a result of material degradation during the evolution of damage under tensile stresses, the enhancement of the elastic stiffness is also possible as a result of void reduction or void closure due to compressive stresses. Such phenomena have also been observed during experiments conducted on geomaterials including granite (Zhu and Wong, 1997). The enhancement of elastic properties is most likely to occur when the micro-defects have an elongated form such as micro-cracks or

flattened cavities. This would also require paying attention to the influence of the effects of oriented defects, which is beyond the scope of this research. Since this research is focused on the isotropic idealization of damage modelling, attention is restricted to the evolution of damage for the states of strain that satisfy (3.7) and it is assumed that the porous skeleton remains intact for any other state of strain. Admittedly, this is only a plausible approximation and since the intention of the study is to obtain some insight into the stress state-dependency of the evolution of damage and the relevant influence on time-dependent behaviour of the fully saturated brittle geomaterials, the simplified assumption of (3.7) is justifiable.

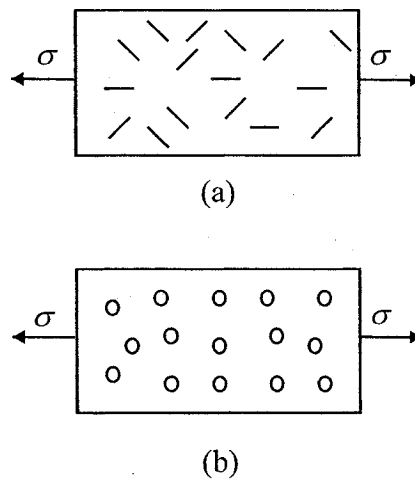


Figure 3.4 A cracked volume subjected to stress (a) micro-cracks (b) micro-voids.

### 3.5 Theoretical Observations on Damage-induced Alterations in the Poroelasticity Parameters

The existence of the damage-induced alterations in both elasticity and hydraulic conductivity properties is also supported by the theoretical studies, mainly related to micro-mechanics. In this section, a brief review of evidence related to the damage-induced alterations in brittle material properties is presented. This includes a

documentation of the relationships, associated with micro-mechanics in order to demonstrate the influence of the development of micro-defects on material properties.

### 3.5.1 Damage-induced Alterations in the Elastic Stiffness of Brittle Materials

Cook (1965) investigated the damage-induced alterations of elasticity parameters in brittle geomaterials, experiencing damage in the form of micro-cracks (Figure 3.4a). Cook (1965) related the average elastic modulus of a medium containing a random distribution of micro-cracks to the virgin elastic modulus in the following form:

$$\frac{E_{\text{cracked}}}{E} = \frac{1}{1 + 2\pi(1 - \nu^2)C^2n} \quad (3.8)$$

where  $C$  is a function of micro-cracks orientation,  $n > 0$  is a function of the density of micro-cracks and  $\nu$  is Poisson's ratio. Since for elastic geomaterial  $0 < \nu < 1/2$ , therefore  $(1 - \nu^2) > 0$ . The relationship (3.8) indicates a reduction in the elastic modulus of a cracked region. The result (3.8) can be rewritten in a form identical to the conventional result (3.4) developed in continuum damage mechanics,

$$E_{\text{cracked}} = (1 - D)E \quad (3.9a)$$

where  $D$  takes the form

$$D = \frac{2\pi(1 - \nu^2)C^2n}{1 + 2\pi(1 - \nu^2)C^2n} \quad (3.9b)$$

Equation (3.9) indicates that the elastic stiffness is reduced due to the evolution of damage in the form of a random distribution of micro-cracks.

The damage-induced alterations in the deformability characteristics as a result of micro-voids generation has also been investigated by Budiansky and O'Connell (1976) (Figure



3.4b). Budiansky and O'Connell (1976) determined the average elastic modulus of brittle materials susceptible to micro-voids, which takes the form:

$$\frac{E_{\text{cracked}}}{E} = 1 - \frac{2N(a^3)}{15} [3f(\nu) + 2g(\nu, \beta)] \quad (3.10)$$

where  $E_{\text{cracked}}$  and  $E$  are the elastic moduli of the damaged and virgin material, respectively,  $\nu$  is the Poisson's ratio,  $f$  and  $g$  are dimensionless micro-voids shape factors that depend on Poisson's ratio  $\nu$  and the orientation of micro-voids,  $N$  is a function of the density of the micro-voids and  $a$  is the average size of the micro-voids. Result (3.10) can be interpreted in relation to the conventional result (3.4) that accounts for the damage-induced alterations in the elastic stiffness. Using the conventional form, we can rewrite (3.10) as

$$E_{\text{cracked}} = (1 - D)E \quad (3.11a)$$

where  $D$  now takes the form

$$D = 1 - \frac{2N(a^3)}{15} [3f(\nu) + 2g(\nu, \beta)] \quad (3.11b)$$

These results indicate that the average elastic stiffness is reduced due to the evolution of damage in the form of micro-voids.

Although, equations (3.9) and (3.11) cannot predict the damage-induced alterations in the elastic stiffness, precisely, they point to the trend regarding the deterioration in elasticity parameters, resulting from the evolution of micro-defects.

### 3.5.2 Damage-induced Alterations in Hydraulic Conductivity of a Damage-susceptible Materials

The damage-induced alterations in the hydraulic conductivity of brittle geomaterials such as the Lac du Bonnet Granite have been investigated by Souley *et al.* (2001) using a semi-empirical method. Souley *et al.* (2001) postulated that the relationship for hydraulic conductivity generation during damage in brittle geomaterials can be expressed in the form

$$\log\left(\frac{k}{k_0}\right) = C\left(\frac{a^3}{a_0^3}\right); \text{ when } \frac{a^3}{a_0^3} > l_{rat}^3 \quad (3.12a)$$

$$k = k_0; \text{ when } \frac{a^3}{a_0^3} < l_{rat}^3 \quad (3.12b)$$

where  $a$  and  $a_0$  are the average size of the elongated micro-cracks and the average of the grain size, respectively,  $l_{rat}$  is the ratio between the crack length at the percolation flow threshold and  $C$  is a function of micro-crack density. The result (3.12) confirms the evolution in hydraulic conductivity after a specific average size of micro-cracks propagate within a damage-susceptible geomaterial.

An identical set of results is obtained by Cernuschi *et al.* (2004) for the evolution of thermal conductivity of brittle ceramics. It should be noted that in view of the mathematical similarity between Fourier's law for heat conductivity and Darcy's law for fluid flow through porous medium, the changes in thermal conductivity during cracking of a brittle geomaterial can be interpreted in terms of the evolution of hydraulic conductivity during cracking.

### 3.6 Computational Scheme for Time-dependent Response of Brittle Geomaterials Susceptible to Damage

The influence of damage-induced alterations in elasticity and hydraulic conductivity characteristics in a fully saturated brittle geomaterial can be examined by incorporating continuum damage mechanics within the classical theory of poroelasticity. This can be achieved by allowing the material parameters to evolve during the damage process. The damage functions relate the damage variable obtained from a continuum damage mechanics basis to the altered poroelastic parameters. The ensuing sections present the damage evolution functions for isotropic damage-induced alterations in the elasticity and hydraulic conductivity characteristics of the brittle geomaterials and adopt the functions based on the available experimental observations for sandstone as the test case for examining the mechanics of soft rocks experiencing micro-mechanical damage. Finally, the iterative computational scheme used in this research is documented.

#### 3.6.1 Degradations of Elasticity Parameters

The constitutive parameters applicable to an isotropic elastic material experiencing micro-mechanical damage can be determined as a function of intact elastic properties using the hypothesis of strain equivalence. The elastic shear modulus for a brittle material that exhibits isotropic damage can be taken form

$$\mu^d = (1 - D)\mu \quad (3.13)$$

where  $\mu$  is the shear modulus applicable to virgin elastic material. Based on the hypothesis of strain equivalence, the Poisson's ratio is assumed to be constant. The damage evolution function can specify the variation of the damage variable  $D$  with the state of strain in a material. The damage evolution function proposed by Cheng and Dusseault (1993) is used in this study to account for the degradation in elastic stiffness in a brittle material. Integrating (3.5), the damage evolution function takes the form,

$$D = \int_0^{\xi_d} \eta \frac{\alpha \xi_d}{1 + \alpha \xi_d} \left( 1 - \frac{D}{D_c} \right) d\xi_d = D_c - (D_c - D_0)(1 + \alpha \xi_d)^{\eta / \alpha D_c} \exp(-\eta \xi_d / D_c) \quad (3.14)$$

where  $D_0$  is the initial value of the damage variable corresponding to the intact state of a material ( $D_0 = 0$  for the virgin state).

### 3.6.2 Alterations in Hydraulic Conductivity

The establishment of damage functions that account for the alterations in hydraulic conductivity for a fully saturated brittle geomaterial is essential to developing any computational approach for brittle geomaterials susceptible to damage. In this research, a phenomenological relationship for the damage evolution function is postulated based on the results of experiments conducted on granite and sandstone by Zoback and Byerlee (1975) and Shiping *et al.* (1994), respectively (Figure 1.5). Based on experimental evidence, the hydraulic conductivity is assumed to have a quadratic variation with respect to the equivalent shear strain  $\xi_d$ . This relationship takes the form,

$$k^d = (1 + \beta \xi_d^2) k^0 \quad (3.15)$$

where  $k^d$ ,  $k^0$  are the hydraulic conductivity applicable to the damaged material and the virgin material, respectively and  $\beta$  is a damage related material constant.

### 3.7 The Computational Procedures

The concept of continuum damage mechanics is incorporated within the finite element procedure developed in connection with this research. The computational procedures developed are capable of examining the influence of alterations in the elasticity and hydraulic parameters resulting from damage evolution. The damage criteria related to evolution of these properties are based on the relationships (3.14) and (3.15). Two approaches for the evolution of damage within a brittle geomaterial have been adopted.

The first approach models stress state-independent damage evolution (i.e. stress state-independent). The scalar damage variable is first obtained, using (3.14) at the twenty-seven Gauss points within the three-dimensional finite element. The shear modulus  $\mu^d$  and the hydraulic conductivity  $k^d$  are then updated at these locations to account for damage evolution. The discretized governing equations are then solved to obtain the set of strains at each integration point using the updated poroelastic parameters  $\mu^d$  and  $k^d$  using an incremental analysis. The coupling between the state of strain and state of damage at each time step is solved by an iteration process. The standard Newton-Raphson technique (see e.g. Smith and Griffiths, 1988) is used as the iteration algorithm in the computational procedure. In the second approach, the stress state-dependency of evolution of damage is incorporated. It is assumed that damage can be initiated only for stress states where the brittle geomaterial satisfies the constraint (3.7). The basic computational algorithm used in this research, which also incorporates the concept of stress state-dependency in the damage evolution is shown in Figure 3.5.

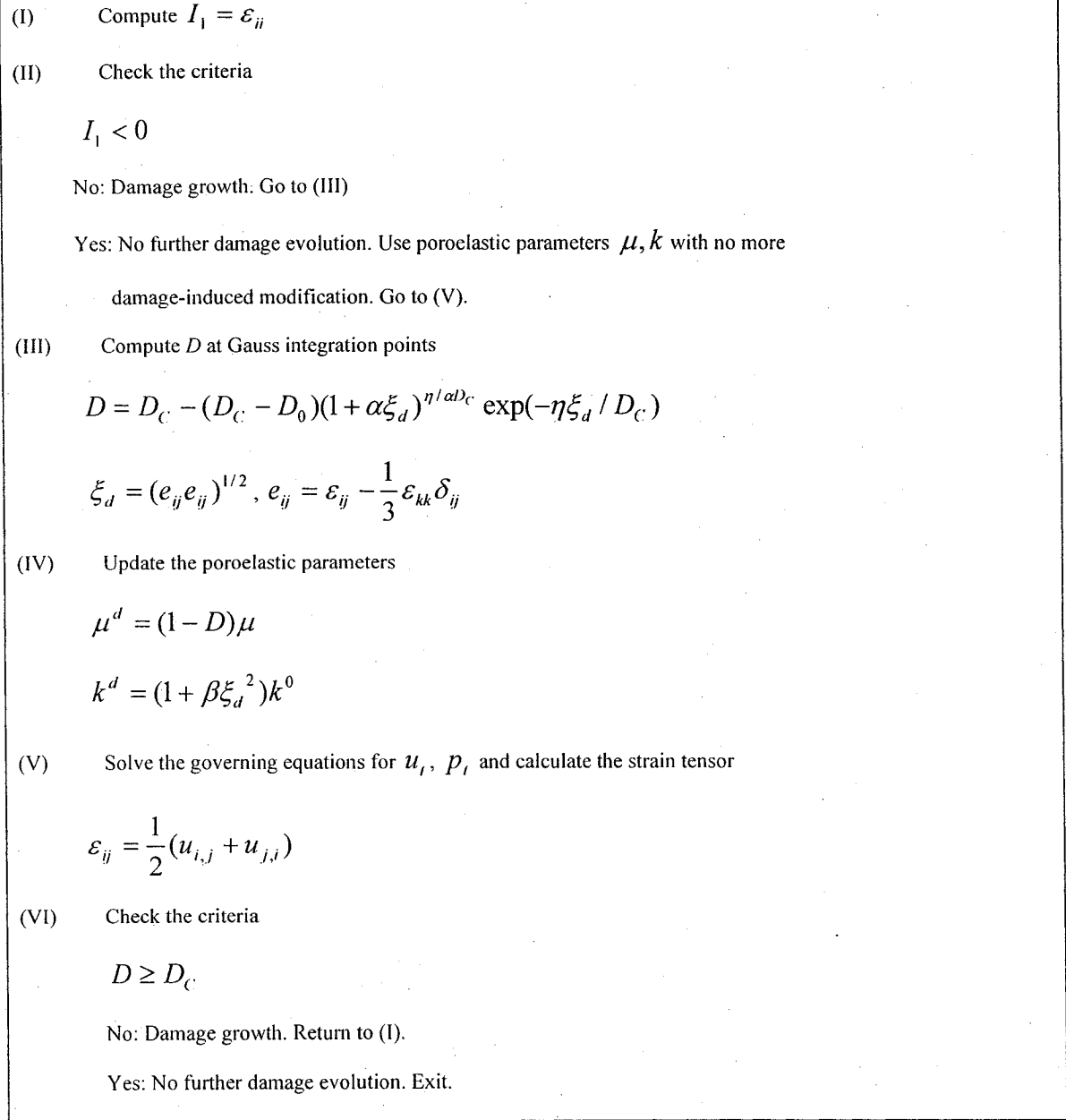


Figure 3.5 Computational scheme for the stress analysis of a poroelastic medium exhibiting stress state-dependent evolution of damage.

## **CHAPTER 4**

### **ONE-DIMENSIONAL CONSOLIDATION OF POROELASTIC MEDIA**

#### **4.1 General**

In poroelasticity, the problem dealing with one-dimensional consolidation is an important fundamental problem. It can be used as an illustrative problem to verify the validity of the computational scheme, proposed in Chapter 3. The geometry and boundary conditions of a three-dimensional problem can be confirmed in such a way that a fully constrained-one-dimensional state can be induced in any element within the region. Therefore, the problem of one-dimensional consolidation can be used as verification for the stress state-dependent criteria, proposed for this research. Furthermore, the problem of consolidation of a poroelastic sphere can also be treated as a special case of spatially one-dimensional consolidation involving spherical symmetry. The appropriate form of the coupling between time-dependent deformation of the solid skeleton and pore fluid pressure is an essential point in connection with behaviour of a poroelastic sphere, where an increase in pore pressure followed by decay is observed in analytical results. This phenomenon, which is referred to as Mandel-Cryer effect has been analytically proved by Mandel (1953) and Cryer (1963) in connection with the mathematical analysis of the consolidation of a poroelastic sphere. The absence of the Mandel-Cryer effect is a main drawback for the Terzaghi's theory of consolidation, whereas the general three-dimensional theory of consolidation introduced by Biot (1941) accounts for this effect.

This Chapter deals with the analytical and computational modelling of the consolidation of an one-dimensional poroelastic element. As a special case of one-dimensional consolidation, the problem of consolidation of a poroelastic sphere will be discussed with reference to the theories of poroelasticity developed by Terzaghi (1923) and Biot (1941). Finally, the choice of element required to ensure the stability of the finite element procedure developed in connection with research is investigated for the problem of one-dimensional consolidation.

## 4.2 The One-dimensional Consolidation of a Poroelastic Layer

We examine the problem of one-dimensional consolidation of a soil column of length  $H$ , which rests on an impermeable base (Figure 4.1). The boundary conditions applicable to displacements and pore pressures are also shown in Figure 4.1. The column is subjected to an external vertical stress  $\sigma_0$  in the form of a Heaviside step function of time.

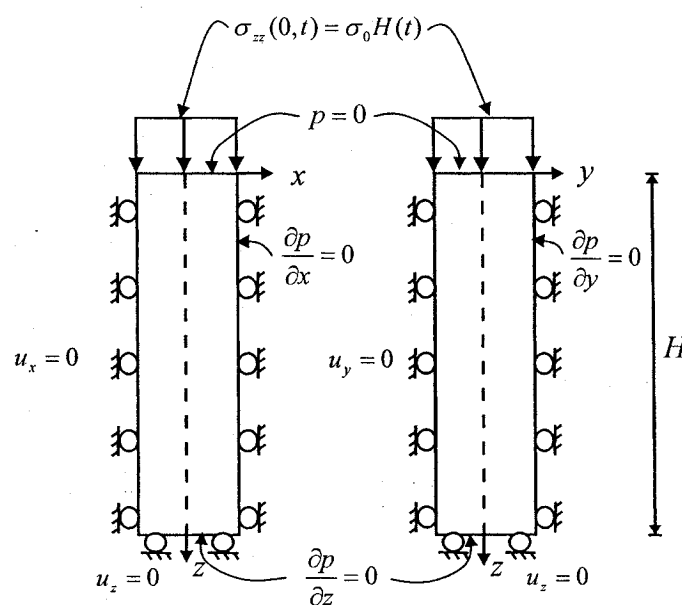


Figure 4.1. Boundary conditions for the problem of one-dimensional consolidation



#### 4.2.1 Analytical Solution of One-dimensional Consolidation Problem: Terzaghi's Theory

The analytical solution for the time-dependent development of the pore pressure within the soil column shown in Figure 4.1 was first given by Terzaghi (1923), although through an analogy with the transient heat conduction equation, the origin of the solution dates back to Fourier (1822). The partial differential equation governing one-dimensional consolidation is given by

$$\frac{\partial p}{\partial t} = C_v \frac{\partial^2 p}{\partial z^2} \quad ; \quad z \in (0, H) \quad ; \quad t \geq 0 \quad (4.1)$$

where, coefficient of consolidation ( $C_v$ ) takes the form:

$$C_v = \frac{k(1-\nu)E}{(1+\nu)(1-2\nu)\gamma_w} \quad (4.2)$$

It is assumed that the total stress is applied instantaneously and at the beginning of the consolidation process ( $t = 0^+$ ) this stress will be completely carried by the pore fluid. This results in an initial condition of the following form:

$$p(z,0) = \sigma_0 \quad \text{for} \quad 0 \leq z \leq H \quad \text{when} \quad t = 0^+ \quad (4.3)$$

The solution for the time-dependent pore pressure, developed at any location  $z$  is in the following form (see Terzaghi, 1943):

$$\frac{p(z,t)}{\sigma_0} = \sum_{m=1}^{\infty} \frac{2}{M} \left( \sin \frac{Mz}{H} \right) \exp(-M^2 T) \quad (4.4)$$

where  $M = \frac{\pi}{2}(2m+1)$  for  $m = 1, 2, \dots$  and  $T$  is referred to as a time factor, which can be expressed in,

$$T = \frac{C_v t}{H^2} \quad (4.5)$$

#### 4.2.2 Analytical Solution of One-dimensional Consolidation Problem: Biot's Theory

The equations governing Biot's theory of consolidation for a poroelastic medium, saturated with an incompressible pore fluid take the forms,

$$\mu \nabla^2 u_i + \frac{\mu}{(1-2\nu)} \varepsilon_{kk,i} + p_{,i} = 0 \quad (2.34a)$$

$$\frac{\partial \varepsilon_{kk}}{\partial t} = \frac{2k\mu(1-\nu)}{\gamma_w(1-2\nu)} \nabla^2 \varepsilon_{kk} \quad (2.34b)$$

For one-dimensional consolidation, the total stress can be written as;

$$\sigma_{zz} = 2\mu \varepsilon_{zz} + \frac{2\mu\nu}{1-2\nu} \varepsilon_{zz} + p = \frac{2\mu}{1-2\nu} \varepsilon_z + p \quad (4.6)$$

For the one-dimensional consolidation problem, equilibrium considerations require that the total axial stress  $\sigma_{zz}$  remains constant in the poroelastic element and equal to the externally applied stress  $\sigma_0$ : i.e.

$$\sigma_0 = \frac{2\mu}{1-2\nu} \varepsilon_{zz} + p = \text{const.} \quad (4.7)$$

Furthermore, for one-dimensional consolidation,  $\varepsilon_{xx} = \varepsilon_{yy} = 0$  and the volumetric strain is given by,

$$\varepsilon_{kk} = -\varepsilon_{zz} \quad (4.8)$$

Using (4.7) and (4.8), we can obtain the derivatives of the volumetric strain with respect to time and  $z$  to give,

$$\frac{2\mu}{1-2\nu} \frac{\partial \varepsilon_{kk}}{\partial t} = \frac{\partial p}{\partial t} \quad (4.9a)$$

$$\frac{2\mu}{1-2\nu} \nabla^2 \varepsilon_{kk} = \frac{\partial^2 p}{\partial z^2} \quad (4.9b)$$

Substituting (4.9a) and (4.9b) in the (2.34b), the partial differential equations governing the one-dimensional pore pressure response associated with the theory of poroelasticity developed by Biot (1941) can be written as;

$$\frac{\partial p}{\partial t} = \frac{kE(1-\nu)}{\gamma_w(1-2\nu)(1+\nu)} \frac{\partial^2 p}{\partial z^2} \quad (4.10)$$

The result (4.10) is identical to the result (2.8) or (4.1) determined through Terzaghi's theory. Therefore, the Biot's theory and Terzaghi's theory result in identical formulations for the one-dimensional consolidation of a poroelastic column or element saturated with an incompressible pore fluid.

#### 4.2.3 Numerical Results for the Problem of One-dimensional Consolidation

The problem of one-dimensional consolidation is examined in order to validate the finite element procedure developed for this research. The computational modelling takes into account the following aspects: (i) the ideal poroelastic response without any damage-induced alterations in poroelastic properties, (ii) the evolution of stress state-independent damage and its influence on both elasticity and hydraulic conductivity properties, (iii) the

evolution of stress state-dependent damage and its influence on both elasticity and hydraulic conductivity characteristics. For one-dimensional consolidation, it is expected that the response for stress state-dependent evolution of damage be identical to ideal poroelasticity due to the compressive state of stress applied to the entire region, in the absence of any damage. The computational results include the influence of both loading and unloading responses. Figure 4.2 illustrates the finite element discretization of the domain subjected to one-dimensional consolidation. The material parameters used for the computational modelling are those for sandstone given by Cheng and Dusseault (1993) and Shiping *et al.* (1994); i.e.

Elasticity parameters:  $E = 8300 \text{ MPa}$  ;  $\nu = 0.195$  ;  $\nu_u = 0.4999$

Fluid transport parameter:  $k^0 = 10^{-6} \text{ m/s}$

Failure parameters:  $\sigma_c = 30 \text{ MPa}$  (compressive);  $\sigma_t = 3 \text{ MPa}$  (tensile)

Damage parameters:  $\gamma = \eta = 130$  ;  $D_c = 0.75$  ,  $\beta = 3.0 \times 10^5$

The depth of the layer is assumed to be  $100(m)$  and the total stress, applied to the layer is  $100\text{kPa}$ .

Figure 4.3 presents a comparison of computational results, obtained from the finite element procedure discussed in Chapter 3 and analytical results. Figures 4.4 and 4.5 present the computational results for one-dimensional consolidation with evolution of damage in the sense of either stress state-independency or stress state-dependency. The damage-induced alterations in the hydraulic conductivity increases the rate of consolidation as a result of faster dissipation of the excess pore water pressure. Furthermore, no damage evolution exists when the stress state-dependent criteria for the evolution of damage within the region are utilized. A compressive state of stress results in no alteration in the poroelastic properties of the column.

The computational scheme is also applied to examine the influence of the choice of the assignment of the dependent variables, namely the displacements and pore fluid pressures

to the nodal locations on the stability of the results. To examine this, the following choices of element configurations are considered: (i) a twenty-node element, where all nodes are assigned the displacements and pore pressures and (ii) a twenty-node element, where all the nodes are assigned the displacement and only the edge nodes account for the pore pressure. Figure 4.6 presents the computational results for those choices of elements. Figure 4.6 indicates that at early times, instability occurs, in situation where all nodes account for the displacements and pore pressures in finite element discretization.

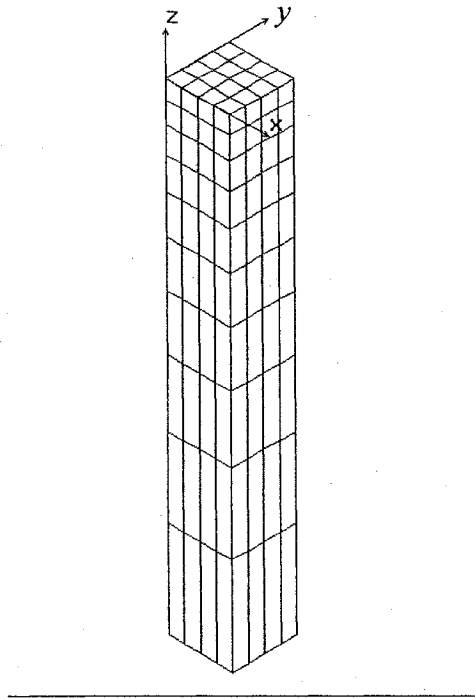


Figure 4.2 Finite element discretization of the domain considered in the problem of one-dimensional consolidation.

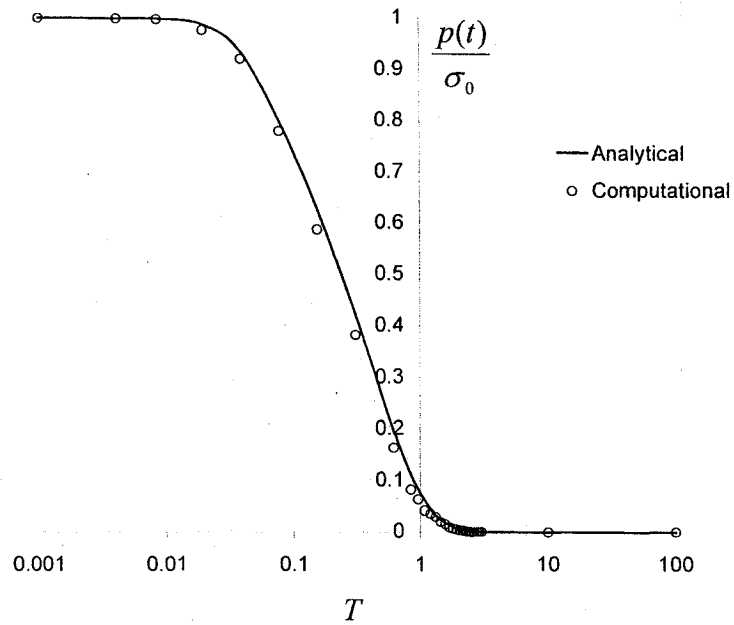


Figure 4.3 A comparison between the computational results obtained by the finite element procedure and analytical results for ideal poroelasticity. (results for both loading and unloading)

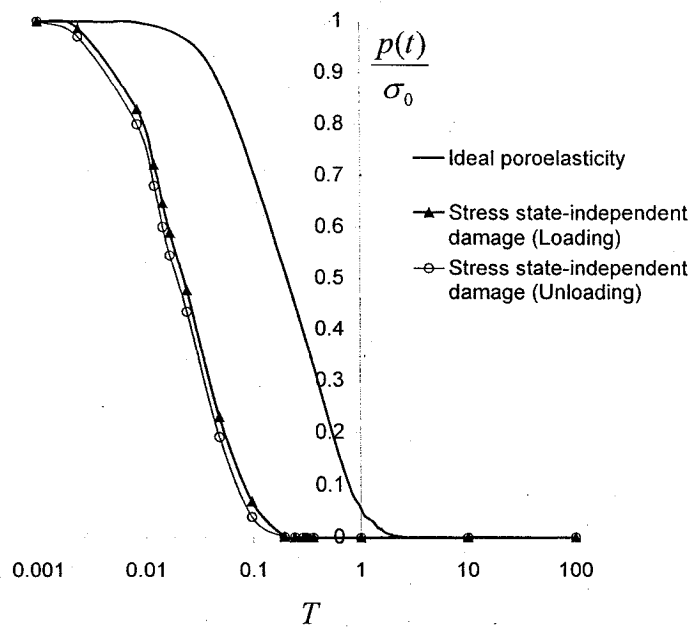


Figure 4.4 Computational results for one-dimensional consolidation (*Stress state-independent evolution of damage*).

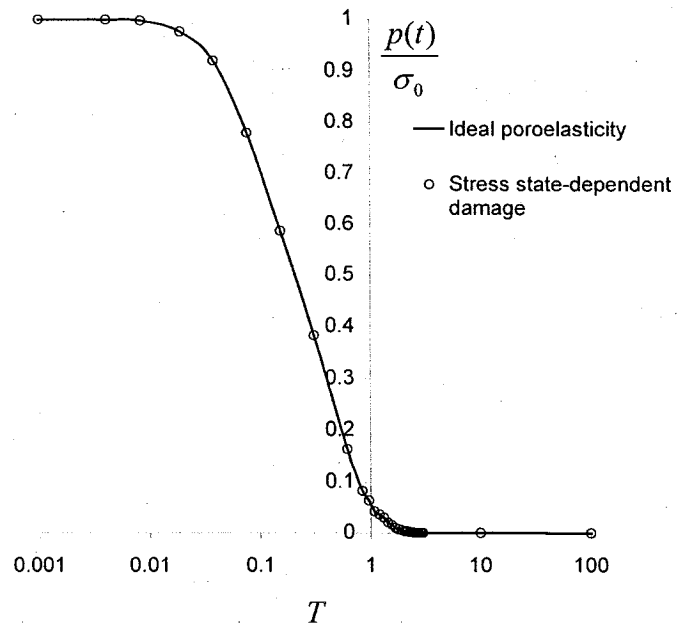


Figure 4.5 Computational results for one-dimensional consolidation (*Stress state-dependent evolution of damage*). (results for both loading and unloading)

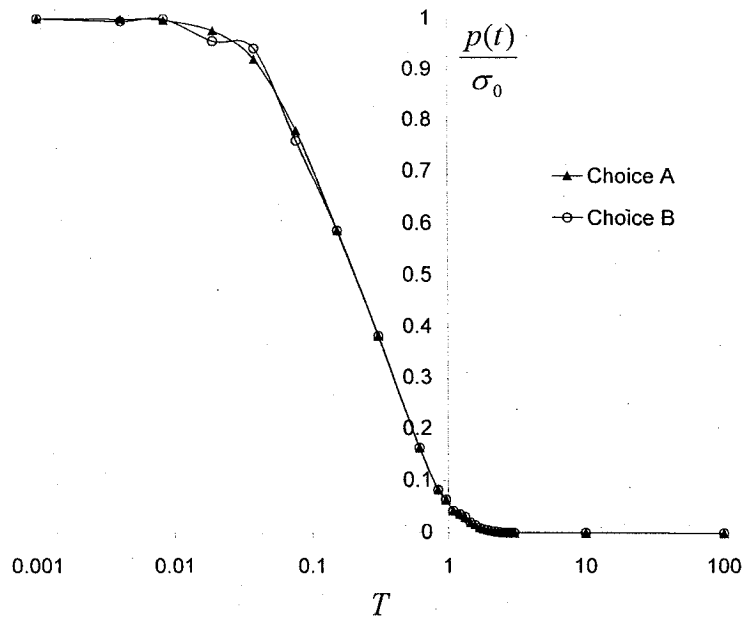


Figure 4.6 Computational results for two choices of computational schemes (A) only edge nodes account for pore pressure effects, (B) all nodes account for pore pressure effects.

### 4.3 The Consolidation of a Poroelastic Sphere

The problem of the consolidation of a poroelastic sphere has been investigated analytically by Mandel (1953) and Cryer (1963). Both these investigations demonstrated that the analytical solutions for pore pressure development at the centre of sphere (Figure 4.7), obtained from Terzaghi's theory and Biot's theory can be considerably different. The application of Biot's theory to the poroelastic sphere predicts an increase in the pore pressure, at an early time, following by a decay, which Terzaghi's theory cannot account for due to the absence of an appropriate form of coupling between mechanical deformations and deformations of the pore fluid. This effect was first observed by Mandel (1953) and confirmed by Cryer (1963) and is generally referred to as the Mandel-Cryer effect. In the following section, the Mandel-Cryer effect in a poroelastic sphere will be discussed.

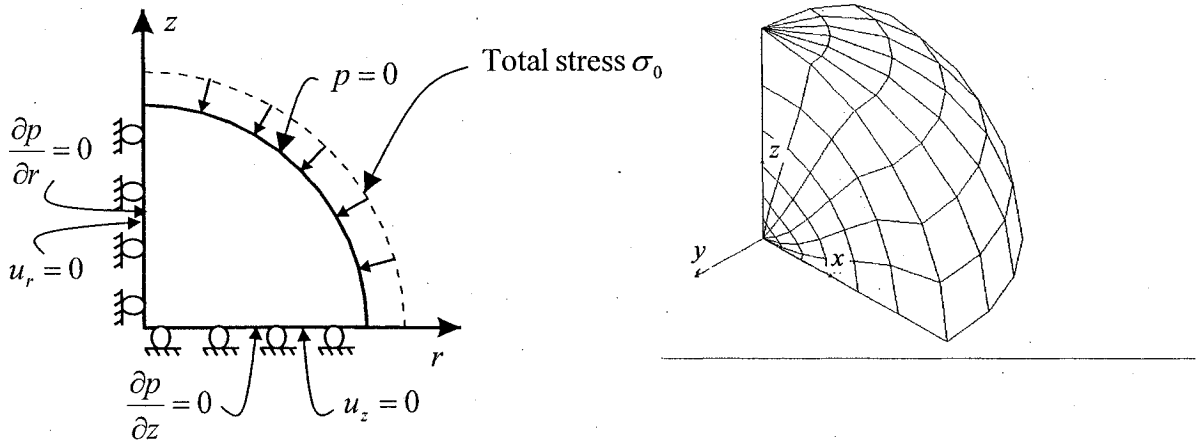


Figure 4.7 The problem of the consolidation of a poroelastic sphere.



### 4.3.1 Analytical Solution for Consolidation of a Poroelastic Sphere Based on Terzaghi's Theory

The partial differential equation governing pore pressure decay in a fluid-saturated poroelastic sphere where constitutive response is defined through Terzaghi's theory is given by,

$$C_v \nabla^2 p = \frac{\partial p}{\partial t} \quad (4.11)$$

The boundary and initial conditions prescribed to a poroelastic sphere are:

$$p(R, t) = \sigma_0 \quad \text{at} \quad t = 0 \quad (4.12a)$$

$$p(a, t) = 0 \quad \text{at} \quad t > 0 \quad (4.12b)$$

where  $a$  is the radius of the sphere. This problem can be solved using Laplace transform techniques and the solution for the pore pressure at the centre of the sphere can be represented (see Cryer, 1963) in the form;

$$\frac{p(0, T)}{\sigma_0} = 1 + O(T^{3/2}) \quad (4.13)$$

where,  $\sigma_0$  is the total radial stress applied at the outer boundary of the poroelastic sphere and  $T$  is a dimensionless factor of time given by,

$$T = \frac{C_v t}{a^2} \quad (4.14)$$

The slope of the time variation of the generated pore pressure against the time factor at the early consolidation times ( $t \rightarrow 0$ ) is given by,

$$\text{Slope} = \frac{\frac{p(0,T) - p(0,0)}{\sigma_0}}{\frac{p(0,0)}{\sigma_0}} = 0 + O(T^{3/2}) \quad (4.15)$$

Therefore, Terzaghi's theory gives a diffusive pattern of the generated pore pressure with time.

#### 4.3.2 Analytical Solution for Consolidation of a Poroelectric Sphere Based on Biot's Theory

Cryer (1963) determined the time-dependent pore pressure development at the centre of a poroelectric sphere and subjected to the total radial stress  $\sigma_0$  at the outer boundary (Figure 4.7), using the theory of poroelasticity, developed by Biot (1941).

In the case of a poroelectric medium, saturated with an incompressible pore fluid, the system of partial differential equations governing the radial displacement  $u_r$  and the pore fluid pressure  $p$  are given by,

$$\mu \nabla \cdot \nabla \mathbf{u} + (\mu + \lambda) \nabla \nabla \cdot \mathbf{u} + \alpha \nabla p + \mathbf{f} = \mathbf{0} \quad (4.16a)$$

$$\frac{\partial p}{\partial t} - \frac{k}{\gamma_w} \beta \nabla \cdot \nabla p + \alpha \beta \frac{\partial \varepsilon_v}{\partial t} = 0 \quad (4.16b)$$

where in spherical coordinates  $R, \theta, \phi$  (see e.g. Selvadurai, 2000 a),

$$\nabla = \frac{\partial}{\partial R} \mathbf{e}_R + \frac{1}{R} \frac{\partial}{\partial \theta} \mathbf{e}_\theta + \frac{1}{R \sin \theta} \frac{\partial}{\partial \phi} \mathbf{e}_\phi \quad (4.17a)$$

$$\nabla \cdot \mathbf{A} = \frac{1}{R^2} \frac{\partial}{\partial R} (R^2 A_R) + \frac{1}{R \sin \theta} \frac{\partial}{\partial \theta} (A_\theta \sin \theta) + \frac{1}{R \sin \theta} \frac{\partial A_\phi}{\partial \phi} \quad (4.17b)$$

Using the spherical coordinate system  $R, \theta, \varphi$  in which radial displacement is  $u_R$  and radial strain  $\varepsilon_{RR}$ , defined by  $\varepsilon_{RR} = \frac{\partial u_R}{\partial R}$  and volumetric strain  $\varepsilon_v$  is in the form of  $\varepsilon_v = \frac{1}{R^2} \frac{\partial}{\partial R}(R^2 u_R)$ , the initial condition associated to the system of equations (4.16) that corresponds to zero volumetric strain at  $t = 0$  can be expressed as,

$$\varepsilon_v = \frac{1}{R^2} \frac{\partial}{\partial R}(R^2 u_R) = 0 \quad \text{at} \quad t = 0 \quad (4.18)$$

The boundary condition associated to the system of equations (4.16) that corresponds to zero pore pressure at the outer surface is given by,

$$p(a, t) = 0 \quad \text{at} \quad t > 0 \quad (4.19)$$

The boundary condition associated to the system of equations (4.16) that corresponds to the radial stress at the outer surface takes the form,

$$2\mu \frac{\partial u_R}{\partial R} + \lambda \frac{1}{R^2} \frac{\partial}{\partial R}(R^2 u_R) = -\sigma_0 \quad (4.20)$$

Using a Laplace transform technique, Cryer (1963) has examined the above initial boundary value problem to develop an expression of the pore pressure. At early times, this result can be expressed as (see Cryer, 1963)

$$\frac{p(0, T)}{\sigma_0} = 1 + \frac{8(1+\nu)(1-2\nu)}{\pi(1-\nu)} \sqrt{T} + O(T^{3/2}) \quad (4.21)$$

where  $T$  is the dimensionless time factor defined by Equation (4.14). Considering the slope of the generated pore pressure vs. the time factor we obtain, for early time of the consolidation process ( $t \rightarrow 0$ ),

$$Slope = \frac{\frac{p(0,T) - p(0,0)}{\sigma_0}}{\frac{p(0,0)}{\sigma_0}} = \frac{8(1+\nu)(1-2\nu)}{\pi(1-\nu)} \sqrt{T} + O(T^{3/2}) \quad (4.22)$$

Therefore, Biot's theory gives an initial increase of the pore pressure at the centre of a poroelastic sphere except for the case when  $\nu = 0.50$ . This increase is referred to as Mandel-Cryer effect. The results of experiments conducted by Gibson *et al.* (1963) and Verruijt (1965) also support the existence of the Mandel-Cryer effect (Figure 4.8).

The result (4.22) shows that the Mandel-Cryer effect is influenced by the mechanical properties of the poroelastic medium and hence damage-induced alterations in poroelastic parameters are expected to influence the Mandel-Cryer effect.

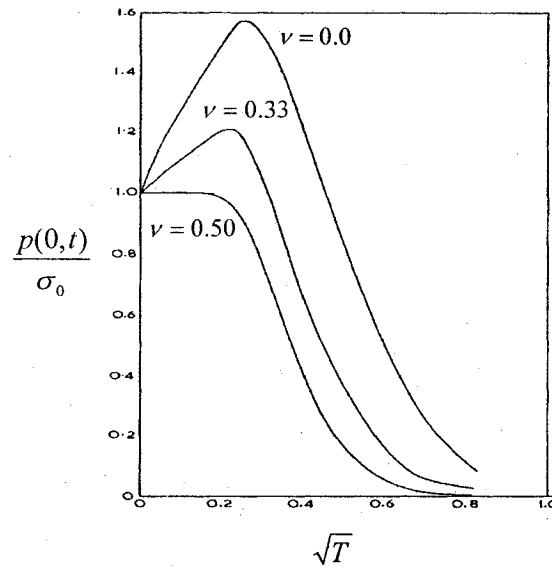


Figure 4.8. The Mandel-Cryer effect, obtained from the experimental observations (After Gibson *et al.*, 1963).

#### 4.4 Numerical Results for Consolidation of A Poroelastic Sphere

The problem of consolidation of a poroelastic sphere (Figure 4.7) is examined to validate the finite element procedure developed for this research. The analytical solution given by

Cryer (1963) is used to compare with the numerical results determined through the finite element procedure.

Cryer (1963) used Laplace transform technique to determine analytically the time-dependent pore pressure development at the centre of a poroelastic sphere, which can be expressed as;

$$\frac{p(T)}{\sigma_0} = \sum_{n=1}^{\infty} \frac{-8\Psi + 2(4\Psi - s_n)/\cos\sqrt{s_n}}{s_n - 12\Psi + 16\Psi^2} \exp(-s_n T) \quad (4.23)$$

where  $\Psi = \mu/(2\mu + \lambda)$ ,  $T$  is defined by (4.14) and  $s_n$  are the roots of the characteristic equation,

$$(s + 4\mu) \sinh \sqrt{s} - 4\mu \sqrt{s} \cosh \sqrt{s} = 0 \quad (4.24)$$

and  $s$  is the Laplace transform parameter.

Figure 4.7 shows the finite element discretization and boundary conditions for the problem of consolidation of a poroelastic sphere. The material parameters used for the computational modelling are those for sandstone given by Cheng and Dusseault (1993) and Shiping *et al.* (1994); i.e.

Elasticity parameters:  $E = 8300 \text{ MPa}$  ;  $\nu = 0.0, 0.33, 0.50$  ;  $\nu_u = 0.4999$

Fluid transport parameter:  $k^0 = 10^{-6} \text{ m/s}$

The radius of the poroelastic sphere is assumed to be  $10(m)$  and the external radial stress applied is  $100\text{kPa}$ .

Figure 4.9 presents a comparison of computational results, obtained from the finite element procedure discussed previously and results of the analytical developments by

Cryer (1963). Figure 4.9 shows a good agreement between the results obtained by the finite element procedure and analytical results.

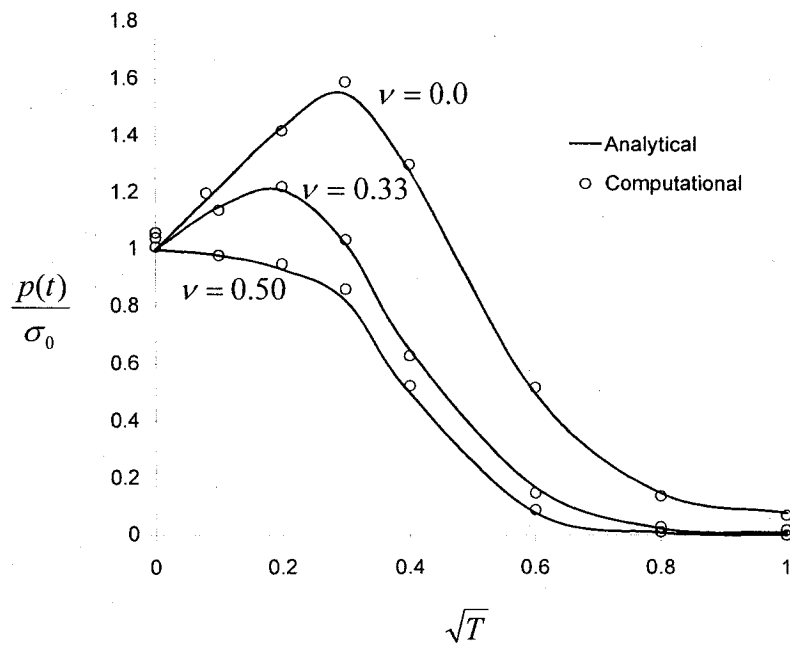


Figure 4.9 Pore pressure development at the centre of a poroelastic sphere

## CHAPTER 5

### THE SPHEROIDAL FLUID-FILLED INCLUSION IN A DAMAGE-SUSCEPTIBLE GEOMATERIAL

#### 5.1 Introduction

The spheroidal fluid inclusion, located in an extended poroelastic medium is an idealized form of the defects in geomaterials. In reality, the sedimentation and glacial tills can result in development of the fluid inclusions. The fluid inclusions can have an arbitrary shape resulting from the in-situ stress states and the preferred orientation of the existing defects. It is therefore convenient to consider a fluid inclusion of an idealized shape. Spheroidal fluid inclusions, including oblate, prolate and spherical inclusions can be treated as an idealized shape of the defects in geomaterials. The fluid inclusions are of interest of different fields of engineering, including engineering geology, petroleum engineering and geotechnical engineering.

Fluid-filled inclusions also belong to a class of problems where the pore pressures increase at early stages of the consolidation process due to the compatible interaction between incompressible pore fluid and the deformations of the porous solid skeleton. As discussed in Chapter 4, the existence of Mandel-Cryer is a result of the formulation of poroelasticity problems in terms of Biot's theory of poroelasticity. The consolidation theories of Terzaghi (1923) and Rendulic (1936) are void of the excess pore pressure effect. Experimental observations of the Mandel-Cryer effect are also given by Gibson *et al.* (1963) and Verruijt (1965).

A physical explanation for the Mandel-Cryer effect is related to the observations that at the early stages of pore pressure development, the changes in volume associated with consolidation will invariably occur at regions close to surfaces that allow the free drainage. The reduction in volume in these exterior regions induces a compression of the interior regions and such stressing action will lead to the development of additional fluid pressures within the interior regions. Therefore, the Mandel-Cryer effect results from these additional fluid pressures. A list of references related to this area is documented by Cryer (1963), Schiffman (1984), Detournay and Cheng (1993) and by Wong *et al.* (1998) in connection with the study of unsaturated soils.

Cryer (1963) also suggested that the amplification and subsequent decay in pore pressure is related to the elastic stiffness and hydraulic conductivity of the poroelastic medium. It is therefore expected that any alterations in poroelastic parameters as a result of the development of damage in the porous skeleton will also influence the amplification and decay in pore pressure within the brittle poroelastic solid. This influence of damage-induced alterations in poroelastic parameters on Mandel-Cryer effect has not been addressed in the literature.

Although not directly related to a fluid inclusion, the work of de Josselin de Jong (1953) examined the time-dependent response of a spherical cavity subjected to an axial loading and located in an extended poroelastic medium. Rice *et al.* (1978) determined an analytical solution for the deformation around a spherical inclusion filled with highly permeable soft material, surrounded by a poroelastic medium and subjected to shear stress. Kanji *et al.* (2003) examined analytically the time-dependent pore pressures and stresses developed within a pressurized hollow cylinder of transversely isotropic poroelastic material. Li (2003) developed an analytical solution to the problem of consolidation around a pressurized borehole located in a poroelastic medium with double porosity, resulting from stressing, in presence of non-isotropic in-situ state of stresses. Li (2003) also indicated that the pore pressure decay in the borehole is influenced by non-isotropy in the in-situ stress state.



The complex geometry and the time-dependency of the fluid pressure within the fluid inclusion can be a significant restriction in using the analytical approach to model the fluid pressure development within the spheroidal fluid inclusion located in an extended poroelastic medium. Therefore the attention is focused on the application of the computational procedures for the study of the spheroidal fluid inclusion problem.

This Chapter deals with computational modelling of fluid pressure development within spheroidal inclusions located at an extended brittle poroelastic medium susceptible to damage. The pore pressure development is due to a far-field tri-axial stress state where the components have a time-dependency as in the form of Heaviside step function. The tri-axial stress state can reflect the in-situ stress state in the geological material resulting from geostatic stresses or the geo-tectonics of the region. Depending upon the geometric aspect ratio, spheroidal fluid inclusions can be grouped into either oblate or prolate inclusions. The influence of damage-induced alterations in the poroelasticity parameters and stress state-dependency of the evolution of damage, on the development of fluid pressure development within the spheroidal fluid inclusion is examined through the computational scheme presented in the previous chapters.

## **5.2 Computational Modelling and Results**

The problems dealing with both oblate and prolate spheroidal fluid inclusions are examined separately. The inclusions are located at an extended damage susceptible poroelastic medium and subjected to a tri-axial state of stress defined by a far-field axial stress  $\sigma_A$  and a far field radial stress  $\sigma_R$  both of which have a time-dependency in the form of a Heaviside step function. The excess pore fluid pressures in the far field are maintained at zero and the development of the fluid pressure within the spheroidal inclusion is investigated for the following cases, (i) damage-induced alterations in both the elasticity and hydraulic conductivity characteristics, (ii) the influence of the anisotropy in the far-field stress state, (iii) The influence of stress state-dependency of the evolution of damage and (iv) the geometric aspect ratio of the spheroidal fluid inclusion. For the purposes of computational modelling, sandstone is selected as a poroelastic

material susceptible to damage. The following parameters are used for sandstone, which have been given by Cheng and Dusseault (1993) and Shiping *et al.* (1994).

Elasticity parameters:  $E = 8300 \text{ MPa}$  ;  $\nu = 0.195$  ;  $\nu_u = 0.4999$

Fluid transport parameter:  $k^0 = 10^{-6} \text{ m/s}$

Failure parameters:  $\sigma_c = 30 \text{ MPa}$  (compressive);  $\sigma_t = 3 \text{ MPa}$  (tensile)

Damage parameters:  $\gamma = \eta = 130$  ;  $D_c = 0.75$  ,  $\beta = 3.0 \times 10^5$

Ideally, the computational modelling of the fluid inclusion should be represented as a fluid element with incompressible behaviour. This entails the re-formation of the computational procedure to account for the fluid response. The procedures for the implementation of the fluid element are discussed by Zienkiewicz and Taylor (2000). In this research, however, the spheroidal fluid inclusion is modelled by considering an alteration in the poroelastic parameters applicable to the inclusion region. This is considered sufficient for purposes of illustrating the overall response of the fluid inclusion. Accordingly, the inclusion is modeled as a non-damage-susceptible poroelastic medium with a relatively low shear modulus (low in relation to the surrounding poroelastic medium) and a relatively high hydraulic conductivity. The specific values of the poroelastic parameters chosen to model the fluid inclusion are as follows:

Elasticity parameters:  $G = 1 \text{ MPa}$  ;  $\nu_f = 0.4999$

Fluid transport parameters:  $k^0 = 10^{-3} \text{ m/s}$

These values give a nearly uniform time-dependent fluid pressure variation within the inclusion region, to within an accuracy of 2% in the spatial variation. These fluid pressures are determined using the pore pressures calculated at the specific locations of the element, which are applicable to the poroelastic element. A reduction of  $G$  by an order of magnitude and the increase in  $k^0$  by an order of magnitude does not result in a noticeable change in the computed fluid pressures. The computational results are verified

at each stage to ensure that all points within the inclusion have the same fluid pressure at any given time.

### 5.2.1 The Oblate Spheroidal Fluid Inclusion

First is considered the problem of an extended poroelastic medium susceptible to damage, which is bounded internally by an oblate spheroidal fluid inclusion (Figure 5.1). The poroelastic medium is subjected to a far-field tri-axial stress state defined by an axial stress  $\sigma_A$  and radial stress  $\sigma_R$  that have a Heaviside step function form. Figure 5.2 shows a typical finite element discretization and the associated boundary conditions used in the computational modelling of the oblate fluid inclusion problem. Figures 5.3 to 5.5 illustrate the range of responses for the time-dependent development of the pressure in the oblate fluid inclusion for the cases where the extended medium exhibits (i) the elastic response without any evolution of damage, (ii) the alterations in elastic stiffness due to evolution of damage with or without alterations in hydraulic conductivity to assess the influence of increase in hydraulic conductivity in time-dependent response and (iii) the geometry of the oblate spheroidal fluid inclusion. The results illustrate the significant influence of the hydraulic conductivity evolution in the poroelastic medium susceptible to damage on both the rise and decay of the pressure in the fluid inclusion. The results indicate that the geometry of the fluid inclusion also has an influence on both the rise and decay of the pressure in the fluid inclusion. As the oblate spheroid flattens or as  $n = b/a$  becomes small, the alterations in the elastic stiffness and hydraulic conductivity of the damage-susceptible poroelastic medium induced by stress amplification in regions of high boundary curvature of the inclusion results in both a more rapid generation of the peak fluid pressure and its decay. Figure 5.6 shows comparisons for the pressure decay in a flattened oblate spheroidal fluid inclusion corresponding to poroelastic materials that exhibit stress state-dependent and stress state-independent evolution of damage for a range of values of the parameter  $R$  that accounts for the non-isotropy of the far-field stress state. It is evident that for the fluid inclusion with an oblate spheroidal shape, the influence of the non-isotropy in the far-field stress state on the pressure decay response increases as  $R$  decreases.

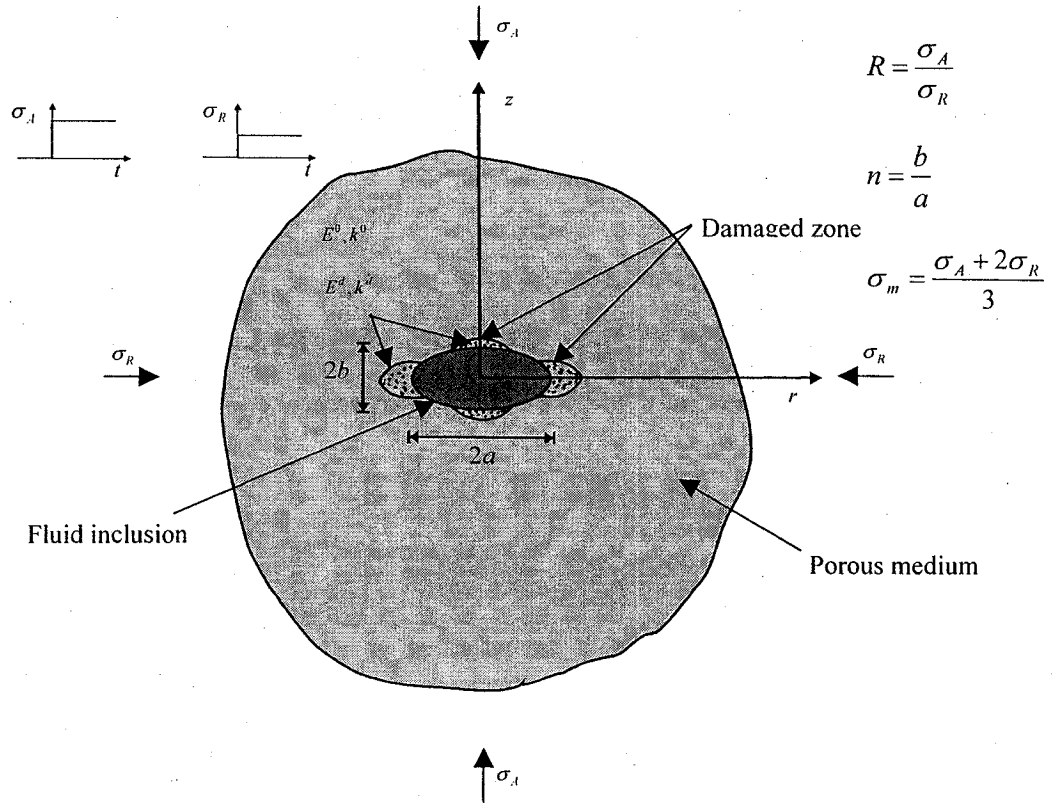


Figure 5.1. Oblate spheroidal fluid inclusion in an extended poroelastic medium.

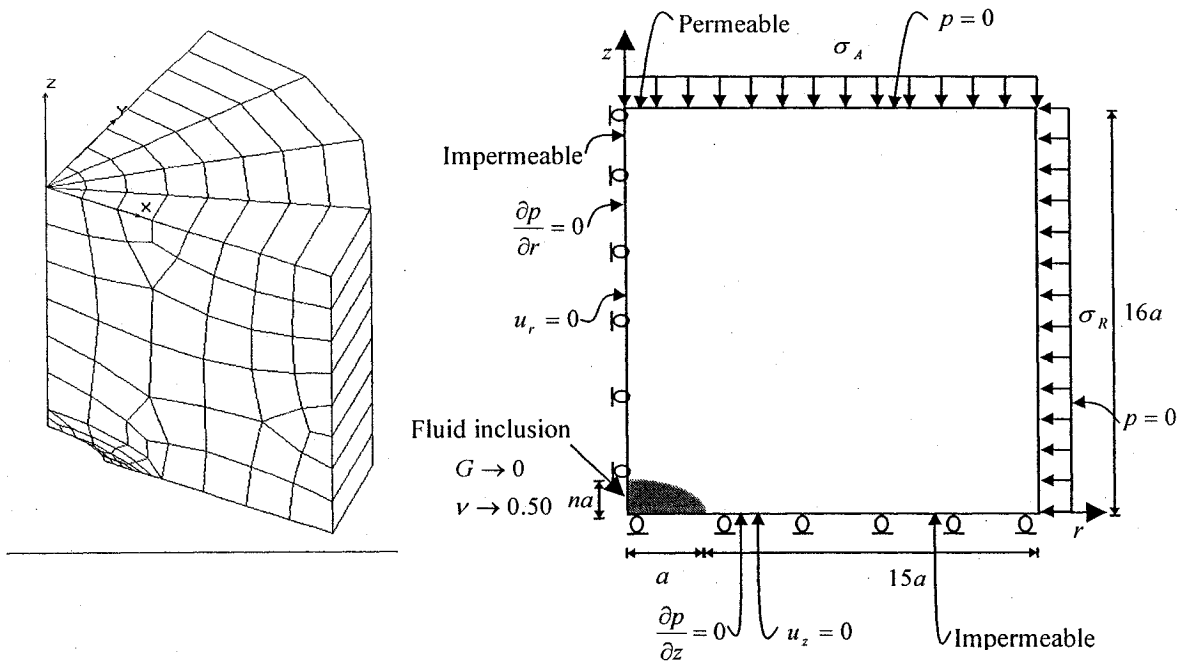


Figure 5.2. Finite element discretization of the damage susceptible poroelastic medium bounded internally by an oblate spheroidal fluid inclusion: geometry and boundary conditions.

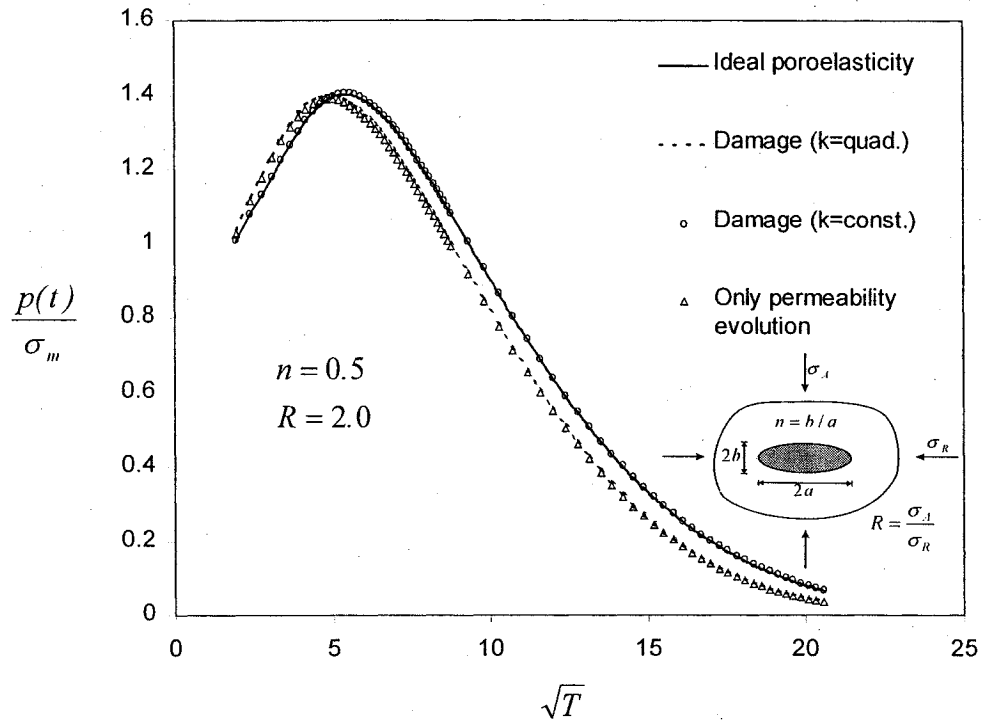


Figure 5.3. Evolution of fluid pressure in the oblate spheroidal fluid inclusion in a non-isotropic far field stress field: Comparison of results for the damaged and ideal poroelasticity material responses ( $n = 0.5$ ). (*Stress state-independent damage evolution*)

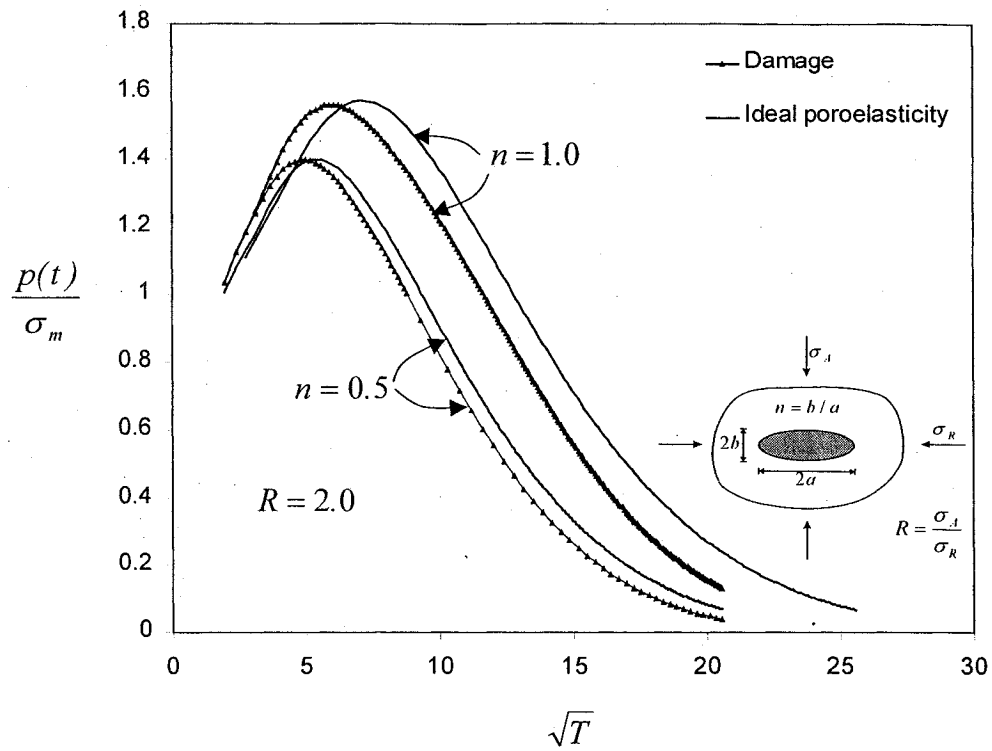


Figure 5.4. Evolution of fluid pressure in the oblate spheroidal fluid inclusion in a non-isotropic far field stress field: Comparison of results of the damaged and ideal poroelasticity material responses ( $n = 0.5; 1.0$ ). (*Stress state-independent damage evolution*)

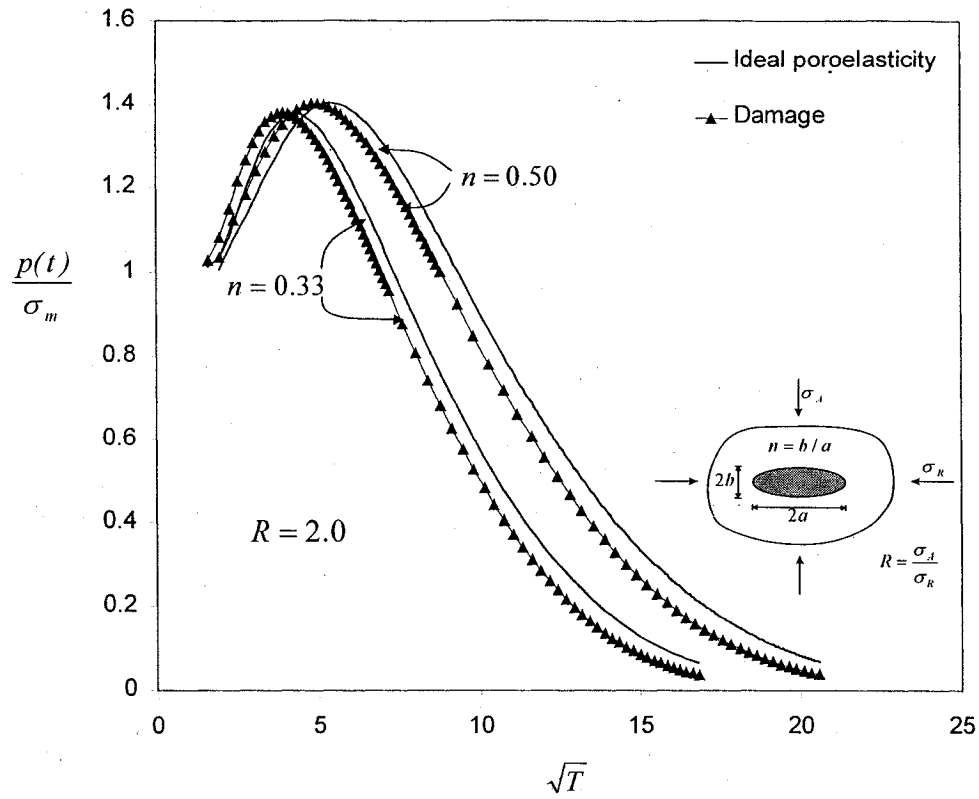


Figure 5.5. Evolution of fluid pressure in the oblate spheroidal fluid inclusion:  
Influence of the geometry of the oblate spheroidal inclusion in a non-isotropic far field  
stress field. (*Stress state-independent damage evolution*)

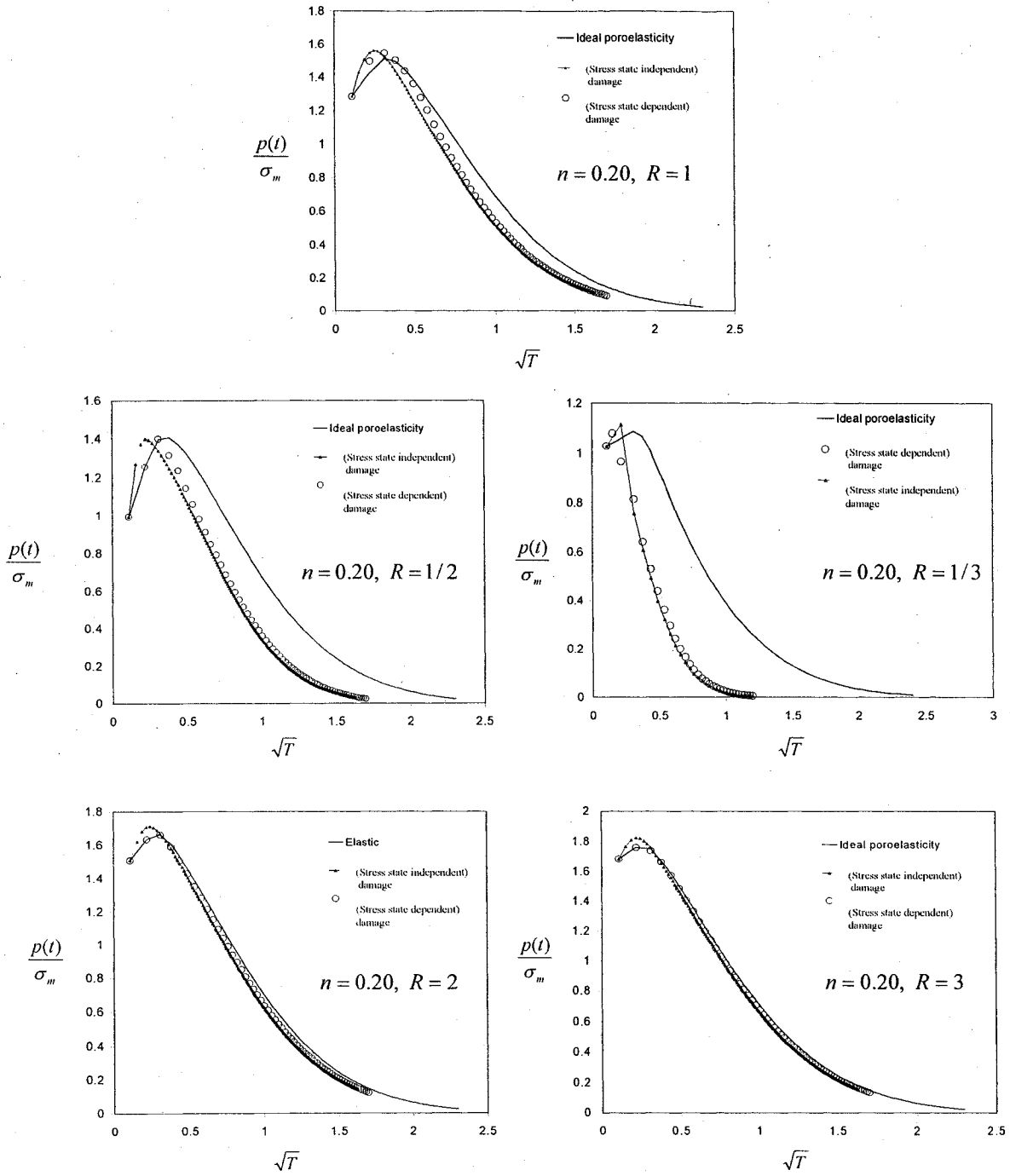


Figure 5.6. Evolution of fluid pressure in the oblate spheroidal fluid inclusion in a non-isotropic far field stress with different deviatoric stress ratios. ( *Stress state-dependent damage evolution.* [  $R = \sigma_A / \sigma_R$  ;  $n = b/a$  ;  $\sigma_m = (\sigma_A + 2\sigma_R)/3$  ] )



### 5.2.2 The Prolate Spheroidal Fluid Inclusion

The computational modelling is now applied to examine the problem of an extended damage-susceptible poroelastic medium, which is bounded internally by a prolate or an elongated fluid inclusion (Figure 5.7). A typical finite element discretization of the poroelastic domain used in the computational modelling of the prolate fluid inclusion and the associated boundary conditions are shown in Figure 5.8. Figures 5.9 to 5.11 demonstrate time-dependent development of fluid pressure in the prolate fluid inclusion for the cases where the poroelastic medium exhibits (i) the elastic response without any evolution of damage, (ii) the alterations in elastic stiffness due to evolution of damage either with or without alterations in hydraulic conductivity and (iii) the geometry of the prolate spheroidal fluid inclusion. Similar to the oblate fluid inclusion problem, the results indicate the relative influence of the alterations in hydraulic conductivity in the damage-susceptible poroelastic medium on both rise and decay in fluid pressure. The variation in the geometry of the elongated spheroid also has an influence on fluid pressure in the elongated fluid inclusion. As the prolate fluid inclusion approaches a needle-shape, both the time to attain the peak fluid pressure and the time for the dissipation of the generated fluid pressure, are reduced. Figure 5.12 illustrates the results that demonstrate the influence of the non-isotropy of the far-field stress state on the rise and decay of the pressure within the fluid inclusion. As the far-field axial stress  $\sigma_A$  increases with respect to the far-field radial stress  $\sigma_R$ , the time for attainment of the peak fluid pressure and the time for decay of this fluid pressure in the fluid inclusion located in the damage-susceptible poroelastic medium are both considerably reduced. In contrast to the results obtained for the oblate or flattened spheroid, the influence of the non-isotropy of the far-field stress state is dominant when  $R$  that accounts for the non-isotropy, increases. Again, the stress amplification as a result of both the shape of the inclusion and the axial stress state contributes to an increase in the damage in the regions that highly stressed thereby altering the amplification and decay processes of the pressure within the fluid inclusion.



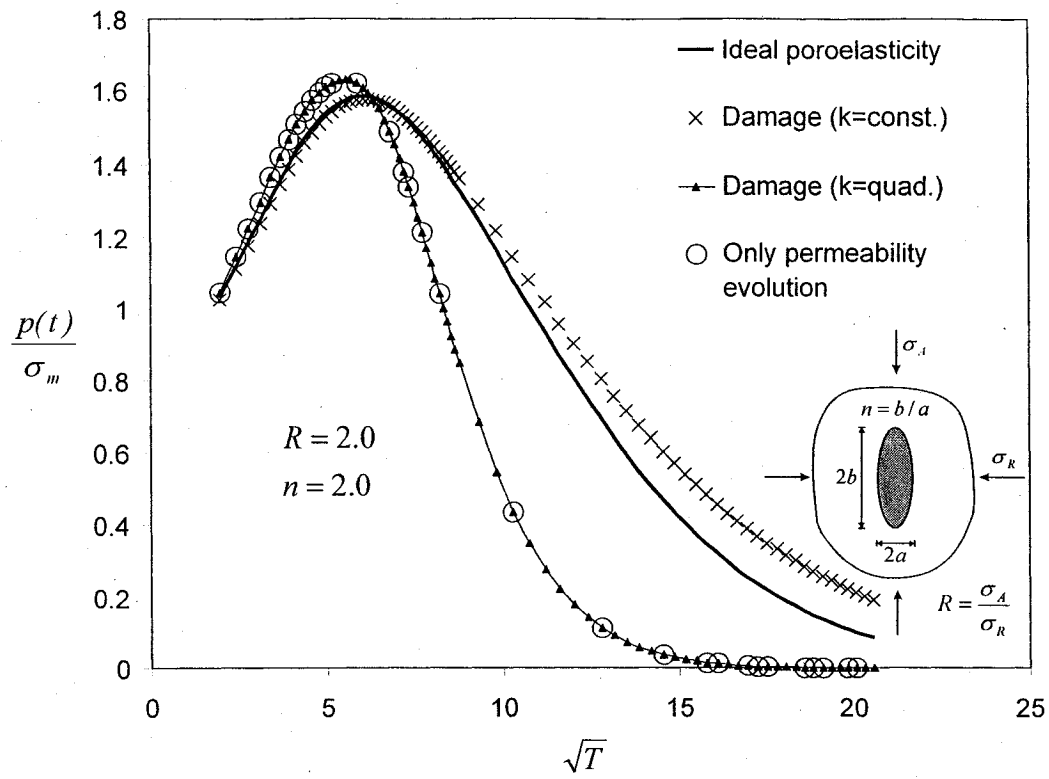


Figure 5.9. Fluid pressure for prolate fluid inclusion in a non-isotropic stress field ( $n = 2.0$ ). (Stress state-independent damage evolution)

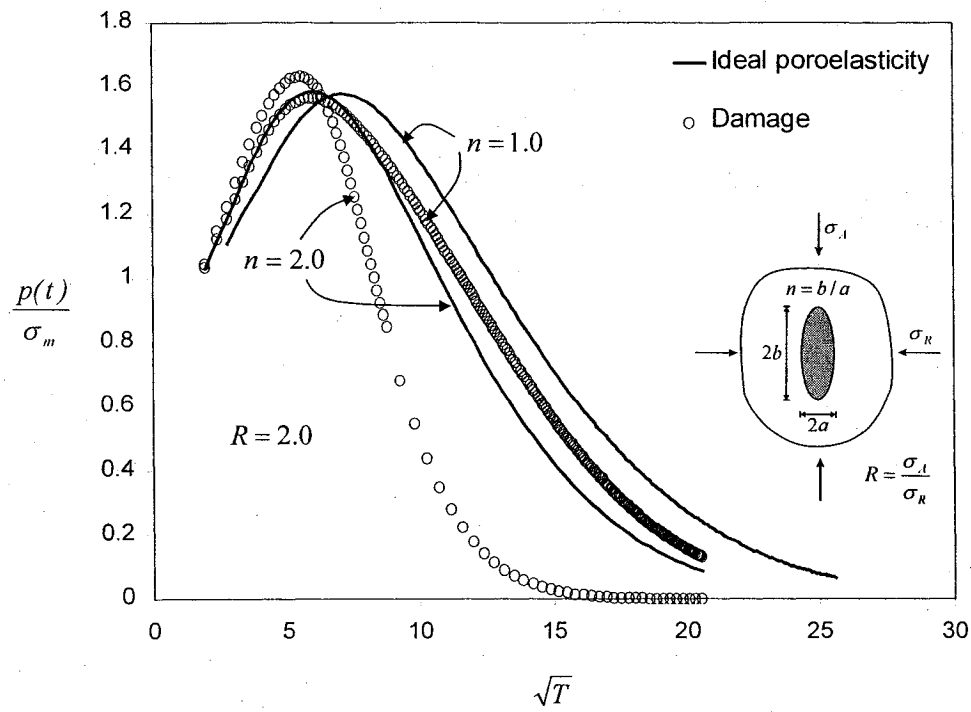


Figure 5.10. Evolution of fluid pressure in the prolate spheroidal fluid inclusion:  
Influence of the geometry of the prolate spheroidal inclusion in a non-isotropic far field  
stress field. (*Stress state-independent damage evolution*)

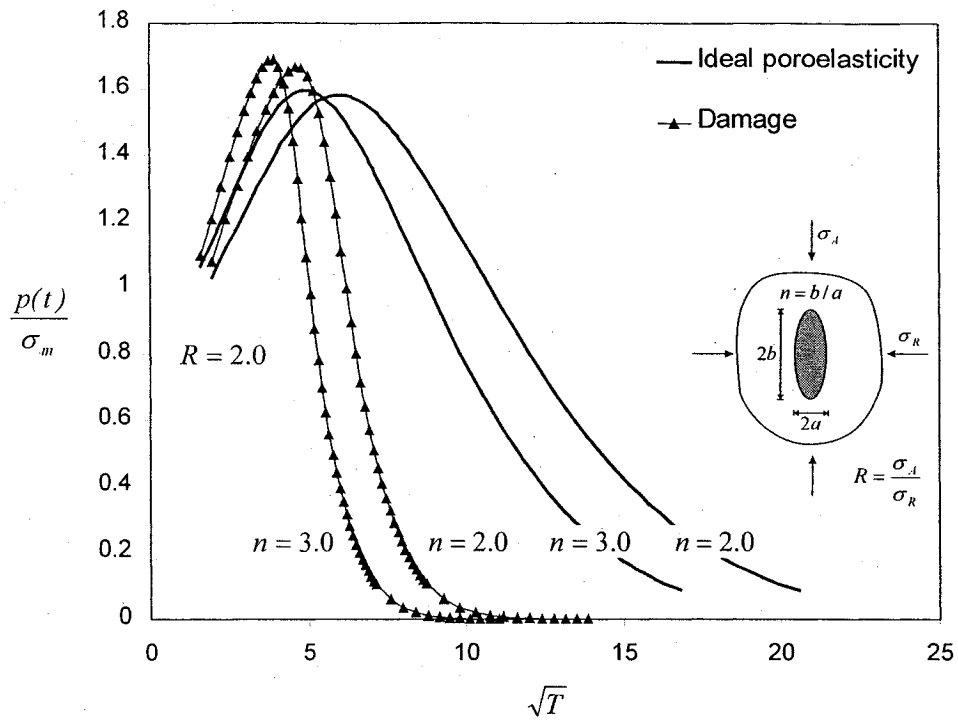


Figure 5.11. Evolution of fluid pressure in the prolate spheroidal fluid inclusion:  
Influence of the geometry of the prolate spheroidal inclusion in a non-isotropic far field  
stress field. (*Stress state-independent damage evolution*)

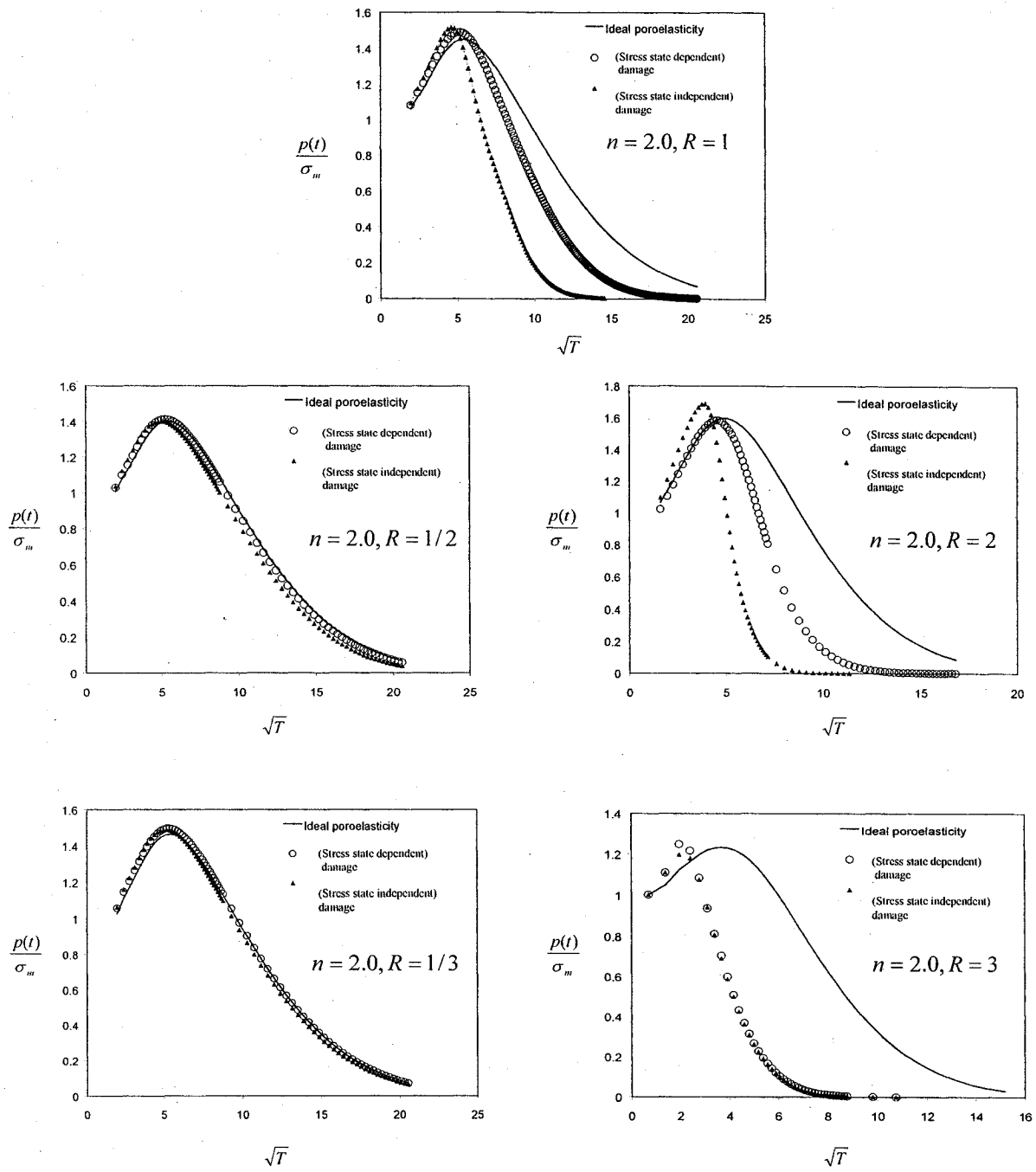


Figure 5.12. Evolution of fluid pressure in the prolate spheroidal fluid inclusion in a non-isotropic far field stress with different deviatoric stress ratios. (*Stress state-dependent damage evolution*) [ $R = \sigma_A / \sigma_R$  ;  $n = b / a$  ;  $\sigma_m = (\sigma_A + 2\sigma_R) / 3$ ]

## CHAPTER 6

### LATERAL LOADING OF A ROCK SOCKET EMBEDDED IN A DAMAGE-SUSCEPTIBLE GEOLOGICAL MEDIUM

#### 6.1 Introduction

Structural elements such as piles, piers or rock sockets have applications in geotechnical engineering. They are used frequently to transmit axial, lateral and torsional loads to the interior of the supporting geological medium. An early investigation of related interest is the work of Reese and Matlock (1956). They investigated the problem dealing with the calculation of the ultimate lateral resistance of a pile derived from process at a pile-sand interface. Broms (1965) also investigated the ultimate lateral load of a pile embedded in sands or clays. Poulos and Davis (1980) presented a set of elastic solutions for flexible piles subjected to both axial and lateral loading. Xu and Poulos (2000) investigated the elastic response of a group of piles embedded in an elastic half-space and subjected to a lateral load. Short anchor piles and rock sockets are used quite frequently in rock mechanics applications where foundations resting on rock formations need to be anchored against uplift and lateral loads. Parkin and Donald (1975) investigated the different aspects related to the design and performance of rock sockets embedded in Melbourne mudstone. Pells and Turner (1979) determined an elastic solution applicable to rock sockets located in a half-space region and subjected to an axial load. Rowe and Pells (1980) studied analytically, the axial deformation of a rock socket embedded in mudstone. This problem was also investigated by Donald *et al.* (1980) who used the finite element methods to model the interaction problem. Williams and Pells (1981) also investigated the skin resistance of rock sockets located in soft rocks, using full scale load tests. Glos and Briggs (1983) conducted a full scale test on rock sockets embedded in a

soft rock to determine the elastic deformation of the rock sockets at the low stress levels associated with the working loads. Rowe and Armitage (1987) studied analytically the behaviour of drilled piers in soft rock, to determine in particular the influence of the disturbance of the rock region due to shaft drilling on the bearing capacity of the rock piers. Whitworth and Turner (1989) conducted a full scale tests on the rock socket piles in the Sherwood Sandstone of Central Birmingham, UK. Douglas and Williams (1993) presented a documentation of the design of West Gate Freeway Project in Sydney, Australia as a study case for the design of rock sockets embedded in soft rocks including mudstone and sandstone. Leong and Randolph (1994) examined the deformation and failure of rock socket piles using finite element methods. These authors modelled the response of the rock sockets by appeal to the theory of plasticity.

A parameter that defines the flexible or rigid nature of a rock socket embedded in a geologic medium is its relative flexibility. The relative flexibility of the pile is determined through a combination of parameters including the rock socket dimensions (e.g. length ( $L$ ) and diameter ( $d$ )) and the elastic stiffness ratio between pile material and geomaterial ( $E_p / E_s$ ). These parameters can be combined to develop a non-dimensional parameter usually referred to as the relative stiffness. The relative stiffness parameter usually evolves in an analysis and formulation of a soil-pile or geologic medium-rock socket or soil-structure interaction problem (see Selvadurai, 1979a). An example of such a non-dimensional relative stiffness parameter is,

$$R = \frac{\pi}{64} \frac{E_p}{E_s} \left(\frac{d}{L}\right)^4 \quad (6.1)$$

As indicated by Poulos and Davis (1980), as the relative stiffness  $R$  becomes large ( $R > 100$ ) the flexibility of the pile in bending becomes small and the pile can be considered as a rigid element. The idealization of a pile as a rigid element is a useful limiting case for determining the pile-geomaterial interaction behaviour for anchor piles and rock sockets that are normally associated with many civil engineering applications. Furthermore, when the effects of flexibility of the pile can be eliminated, the resulting



analysis is considerably simpler than the equivalent analysis that takes into consideration the influence of flexibility. The focus of this research is to investigate the time-dependent behaviour of a rigid anchor pile, which is embedded near the surface of a saturated geomaterial half-space region. The classical theory of poroelasticity developed by Biot (1941) can be used to examine the mechanics of fluid saturated geologic materials such as fluid saturated sandstone, mudstone, shale and other soft rocks, which usually require the use of anchor piles and rock sockets to sustain uplift and lateral loads. The consideration of fluid saturation effects in the supporting geomaterial introduces time-dependent effects into the modelling of the interaction problem. Bjerrum *et al.* (1958) were the first to present a review of available evidence related to the time-dependent response of the piles embedded in saturated geomaterials. The evidence was also discussed in detail by Bjerrum and Flodin (1960). The studies discussed by Bjerrum *et al.* (1958) dealt mainly with piles embedded in soft clays where effects of both primary consolidation and secondary creep were present in the material behaviour. Soderberg (1962) used the classical theory of poroelasticity and an approximate procedure to examine the time-dependent response of the rigid piles embedded in cohesive soils. Poulos and Davis (1968) developed an analytical solution for the problem of a single rigid pile surrounded by a poroelastic region with either an incompressible or a compressible pore fluid. The results were also presented for the response of the single rigid pile embedded either in a poroelastic half-space region or a poroelastic region of a finite depth. The poroelasticity solutions are only for the case of the single rigid pile embedded in a poroelastic medium and subjected to an axial load and do not account for the time-dependent response of a laterally loaded rigid pile. In order to investigate time-dependency in the embedded pile or rock socket problem it is necessary to use the computational procedures that take into account the coupled aspects present in the theory of poroelasticity.

In this chapter we examine the problem of the lateral translational behaviour of a rigid pier or rock socket that is embedded at the surface region of a damage susceptible fluid saturated poroelastic medium. The evolution of damage in the supporting brittle poroelastic medium can influence the transient time-dependent response of the short rigid

pile, resulting primarily from the alterations in poroelastic properties. The damage-induced reduction in elastic parameters can result in a larger lateral displacement of the rock socket at the end of the consolidation process and the damage-induced increase in the hydraulic conductivity is expected to accelerate the consolidation process in the surrounding poroelastic medium. Furthermore, the lateral loading of the rock socket can introduce the development of damage that is stress state-dependent due to the development of both compressive and tensile stress states in the supporting brittle geomaterial. This stress state-dependency of the evolution of damage can also have an influence on the time-dependent behaviour of the rigid short pile.

In the analysis of the laterally loaded rigid pile considered here the exposed end of the pile is subjected to a lateral load in the form of a Heaviside step time function (Figure 6.1). The computational modelling accounts for the evolution of damage in porous skeleton with alterations in both elasticity and hydraulic conductivity characteristics. The stress state-dependency in the evolution of damage is also taken into consideration. In the treatment of the isolated rigid pile, the supporting geomaterial is generally regarded as a semi-infinite domain. The finite modelling of a semi-infinite domain as a finite region does place restrictions on the extensive applicability of the results. One possibility is to incorporate infinite elements for the computational modelling of the domain (see e.g. Bettess and Zienkiewicz, 1977, Selvadurai and Gopal, 1986 and Schrefler and Simoni, 1987, etc.). The alternative approach is to calibrate the modelling of the domain by comparing the results for the computational modelling with equivalent results, mostly analytical, applicable to the problem of a laterally loaded rigid pile embedded in an elastic medium. Once the adequacy of the computational representation of the semi-infinite domain is established, the computational modelling can be extended to the consideration of the poroelasticity problem that incorporates both effects of classical poroelasticity and damage phenomena.

## 6.2 Elastic Solutions for a Rigid Pile Embedded in an Elastic Half-space

In this section, we examine the computational modelling of the problem of the axial loading of a rigid pile embedded in an isotropic elastic half-space and compare the results of the elastic stiffness derived from the computational modelling with equivalent results available in the literature.

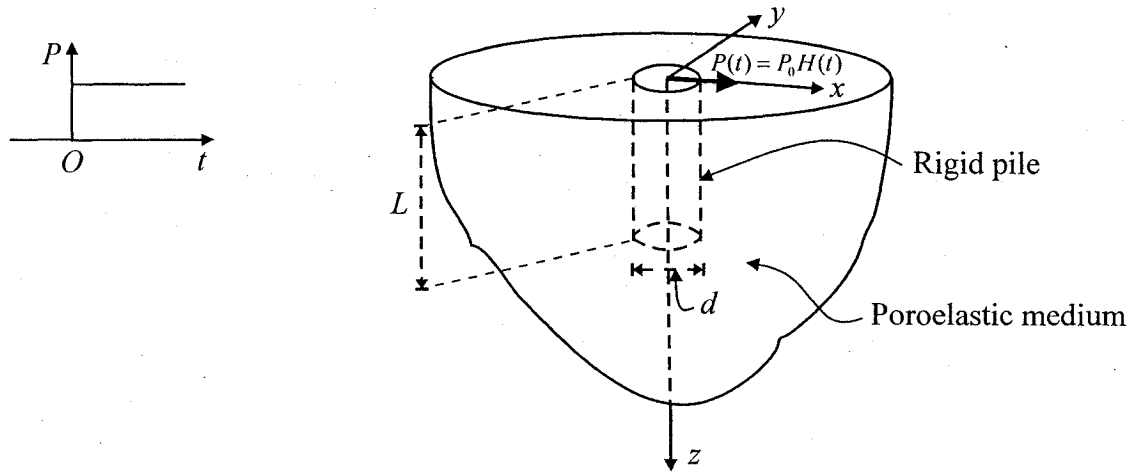


Figure 6.1. A laterally loaded rigid pile embedded in a poroelastic geomaterial

The problem of the axial loading of a cylindrical elastic inclusion embedded in an elastic half-space was examined by Muki and Sternberg (1969). These authors used the results developed by Mindlin (1936) for the internal loading of a half-space to formulate the integral equations and proceeded to solve these numerically. The problem of rigid spheroidal anchor region embedded in an isotropic elastic half-space and subjected to an axial load was developed by Selvadurai (1976). Luk and Keer (1979) developed an analytical solution for a cylindrical elastic inclusion embedded in an elastic half-space and subjected to the axial loading and compared the results for the axial stiffness with the exact closed form solution given by Selvadurai (1976). This problem has also been

extended to cover the problem of the lateral loading (see e.g. Apirathvorakij and Karasudhi, 1980 and Poulos and Davis, 1980). The problem of the rigid pile embedded in an elastic medium also provides solutions that are applicable to the poroelasticity modelling of the analogous problem. The elasticity solution applicable to the case where  $\nu = 0.50$  corresponds to the poroelastic behaviour at the start of the consolidation process and  $\nu = \nu'$  corresponds to the poroelastic result corresponding to  $t \rightarrow \infty$ . The elasticity solutions are incapable of providing information of the rate of consolidation experienced by the pile. An analytical treatment of a hollow rigid pile embedded in an isotropic elastic half-space region is developed by Selvadurai and Rajapakse (1985). In this study the fundamental solutions associated with the interior loading of a half-space region were used to generate the integral equations for unknown interface tractions. These authors were able to determine the results for the stiffness of the hollow pile under generalized displacements and rotation. For the purposes of calibration of the computational procedures developed in this thesis, we present the results for the translational elastic stiffness for the case of a rigid cylindrical pile that is embedded in a half-space region and subjected to a lateral load. The alternative analytical results were developed by Poulos and Davis (1980) and Apirathvorakij and Karasudhi (1980) and Selvadurai and Rajapakse (1985). The Table 6.1 presents the results of these analytical solutions for the case of a rigid pile embedded in an elastic half-space for a Poisson's ratio  $\nu = 0.195$ . In Table 6.1,  $P_0$  is the lateral force;  $\mu$  is the shear modulus;  $d$  is the pile diameter and  $\Delta_h$  is translational displacement of the head of the rigid pile along the line of application of the lateral force. Table 6.1 indicates that the analytical solution given by Selvadurai and Rajapakse (1985) provides estimates for the stiffness for a larger range of pile dimensions. For this research the elastic solutions given by Selvadurai and Rajapakse (1985) are employed as the basic solutions for the purposes of validating the accuracy of the computational methodologies for the purely elastic problem.

Table 6.1 Comparison of translational stiffness of a laterally loaded rigid pile embedded in elastic half-space for different given analytical solutions. ( $\nu = 0.195$ )

Method of Analysis	$2P_0 / \mu d \Delta_h$		
	$L/d = 1.0$	$L/d = 2.0$	$L/d = 4.0$
Apirathvorakij and Karasudhi (1980)	—	8.13	9.54
Poulos and Davis (1980)	6.25	8.93	10.84
Selvadurai and Rajapakse (1985)	7.03	9.80	11.44

### 6.3 Computational Modelling of the Laterally Loaded Rock Socket

In this section we examine the problem of a rigid rock socket pile (length ( $L$ ) and diameter ( $d$ )), embedded in bonded contact with a damage-susceptible poroelastic half-space and subjected to a lateral load (Figure 6.1). Rock sockets are generally regarded as short rigid piles. As an example, the maximum  $L/d$  ratio investigated by Rowe and Armitage (1987) is 4.0; Leong and Randolph (1994) modelled  $L/d$  ratios that ranged from 1 to 5 and Whitworth and Turner (1989) examined values of  $L/d$  that ranged from 1 to 5. At the interface between the rock socket and the poroelastic medium, several types of pore pressure boundary conditions exist. Since complete bonding conditions are assumed, no separation is allowed to develop at the rock socket-poroelastic medium interface. Therefore, the displacements and pore fluid pressures are the only prescribed boundary conditions at the rock socket-poroelastic medium interface. It is also assumed that the displacements are continuous at the rock socket-poroelastic medium interface. The pore pressure boundary condition at the interface can depend on the method of installation of the rock socket and the hydraulic conductivity characteristics of the rock socket in relation to the poroelastic medium. Therefore, the boundary conditions corresponding to pore fluid pressure at the interface of rock socket-poroelastic medium

cannot be determined with certainty. In the computational modelling, it is assumed that at the interface, the pore pressure can exhibit boundary conditions that correspond to either completely pervious (i.e. fully draining) or completely impervious (i.e. undrained) conditions. In order to model the rock socket as a rigid cylindrical element, the elastic modulus of the rock socket region is considered to be  $10^3$  times greater than the elastic modulus of the undamaged supporting poroelastic region. This enables the modelling of a nearly rigid rock socket (with  $L/d = 4.0$ ) and the relative rotation between the head ( $z = 0$ ) and the toe ( $z = L$ ) of the rock socket along its axis to be less than  $10^{-4}$  radians. In the finite element modelling, the interface between the rock socket and the poroelastic region does not correspond to a precise cylindrical surface, therefore, the adopted domain discretization ensures that the interface corresponds, approximately, to a cylindrical shape. The head of the rock socket is subjected to a lateral load directed along the  $x$ -axis, in the form of a Heaviside step function of time (Figure 6.1).

Since the poroelastic region is homogeneous, the problem exhibits a state of symmetry about the plane containing the line of action of the horizontal force  $P(t)$ . In the computational modelling therefore, attention is restricted to a region with the following dimensions:  $-15d \leq x \leq 15d$ ;  $0 \leq y \leq 20d$ ;  $0 \leq z \leq 20d$ , where  $d$  is the diameter of the rigid rock socket. The boundary conditions at the outer surfaces of the region correspond to the conventional zero normal displacement and zero shear traction conditions applicable to the porous skeletal response and the pore fluid pressure boundary conditions are prescribed to be zero. The finite element discretization and the associated boundary conditions applicable to the two classes of interface conditions (pervious/impervious) are shown in Figures 6.2 and 6.3. We consider the problem related to a rigid cylindrical rock socket that is embedded in a poroelastic medium susceptible to damage for the following categories (i) ideal poroelastic response of the medium without any damage evolution; (ii) the poroelastic response of the medium with evolution of damage but no alterations in hydraulic conductivity characteristics; (iii) the poroelastic response with evolution of damage and alterations in both elasticity and hydraulic conductivity characteristics and (iv) the poroelastic response of the medium with stress state-dependent evolution of damage and alterations in both elasticity and hydraulic conductivity characteristics.

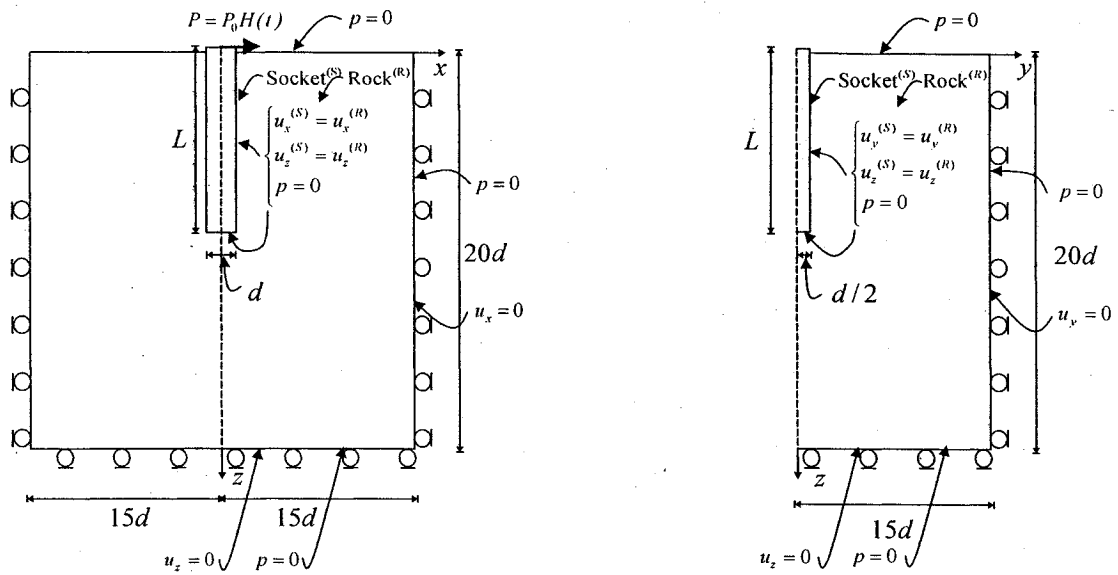


Figure 6.2. Boundary conditions for a pervious interface between rock socket and geomaterial

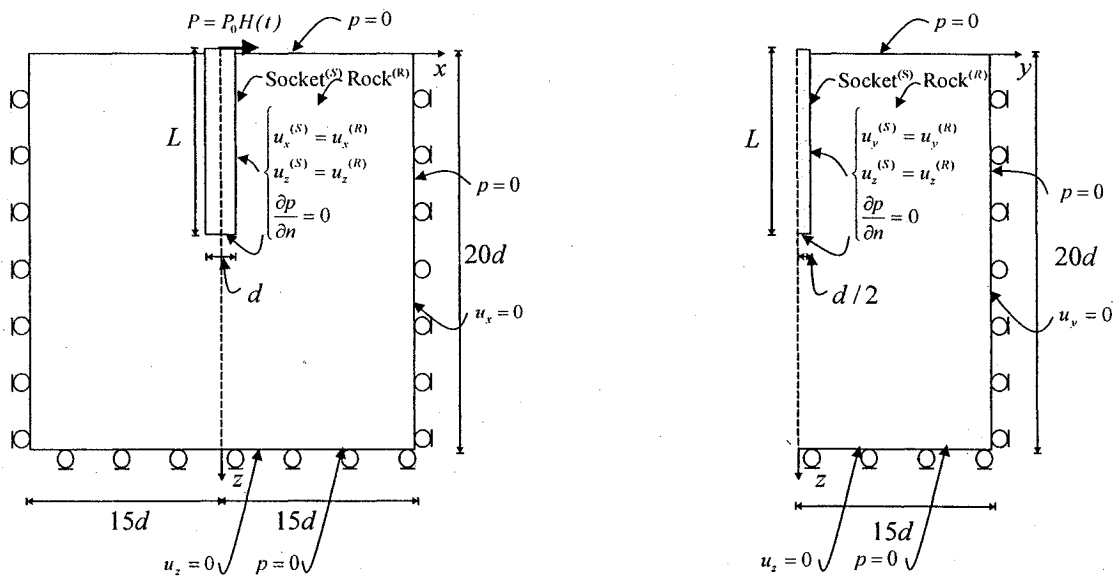


Figure 6.3. Boundary conditions for an impervious interface between rock socket and geomaterial

## 6.4 Computational Results

In the computational modelling, the idealized problem corresponding to a rock socket embedded in a half-space is modelled as a finite domain. It is therefore necessary to evaluate the dimensions of the finite domain that will approximate a half-space region. We first consider the theoretical problem of a rigid pile, embedded in an elastic half-space region. Solutions were presented by Poulos and Davis (1980) and Selvadurai and Rajapakse (1985). The analytical results obtained by these authors for the rigid pile have been compared with equivalent results obtained through the computational modelling where the domain is of finite extent. The validation of the results for the non-dimensional parameter  $2P_0 / \mu d \Delta_h$ , (where  $P_0$  is the lateral load;  $\mu$  is the shear modulus;  $d$  is the pile diameter and  $\Delta_h$  is translational displacement of the head of the pile along the line of action of the lateral load direction), with the pile geometry defined by the parameter  $L/d$  are shown in Table 6.2. The results show good agreement between the analytical results given by Selvadurai and Rajapakse (1985) and the computational estimates for values of  $L/d > 1$ . The results of Poulos and Davis (1980) correlate well with the computational results when  $L/d \approx 1$ .

Table 6.2. Comparison of translational stiffness of a rigid pile subjected to a lateral load and elastic behaviour of the medium ( $\nu = 0.195$ )

	$2P_0 / \mu d \Delta_h$		
Method of Analysis	$L/d = 1.0$	$L/d = 2.0$	$L/d = 4.0$
Present study	6.28	9.71	11.26
Poulos and Davis (1980)	6.25	8.93	10.84
Selvadurai and Rajapakse (1985)	7.03	9.80	11.44



These results indicate that the computational methodologies can be successfully adopted to model the problem of the elastic behaviour of the laterally loaded rigid pile embedded in an isotropic elastic half-space. We now extend the computational modelling to include the problem of laterally load of a rock socket that is embedded in a damage-susceptible poroelastic medium. We consider all aspects of damage-induced alterations in the poroelastic properties and stress state-dependency in the modelling. The material parameters are those that are provided for sandstone by Cheng and Dusseault (1993) and Shiping *et al.* (1994):

Elasticity parameters:  $E = 8300 \text{ MPa}$  ;  $\nu = 0.195$  ;  $\nu_u = 0.4999$

Fluid transport parameter:  $k^0 = 10^{-6} \text{ m/s}$

Failure parameters:  $\sigma_C = 30 \text{ MPa}$  (compressive);  $\sigma_T = 3 \text{ MPa}$  (tensile)

Damage parameters:  $\gamma = \eta = 130$  ;  $D_C = 0.75$  ,  $\beta = 3.0 \times 10^5$

The finite element discretization of the three-dimensional region containing the laterally loaded rock socket is shown in Figure 6.4. The computational modelling is performed for different values of the length to diameter ( $L/d$ ) ratio of the rock socket. The non-dimensional parameter, which is used to represent the time-dependent translational response of the rigid pile is the same as that used by Selvadurai and Rajapakse (1985) (i.e.  $2P_0 / \mu d \Delta_h$ , where  $P_0$  is the magnitude of the lateral load which is constant with time and  $\Delta_h$  is now time-dependent). The time factor used to simplify the normalized time is defined by;

$$T = \frac{8\mu(1-\nu)k^0 t}{(1-2\nu)d^2} \quad (6.2)$$

where  $\mu$ ,  $\nu$  are shear modulus and Poisson's ratio of the porous skeleton, respectively and  $k^0$  is the hydraulic conductivity of the undamaged poroelastic material. The degree of consolidation of the pile as estimated from the pile head translational displacement is defined by:

$$U = \frac{\Delta_h(t) - \Delta_h(0)}{\Delta_h(\infty) - \Delta_h(0)} \quad (6.3)$$

where  $\Delta_h(t)$  is the translational displacement at the center of pile in the direction of applied load, at time  $t$ .

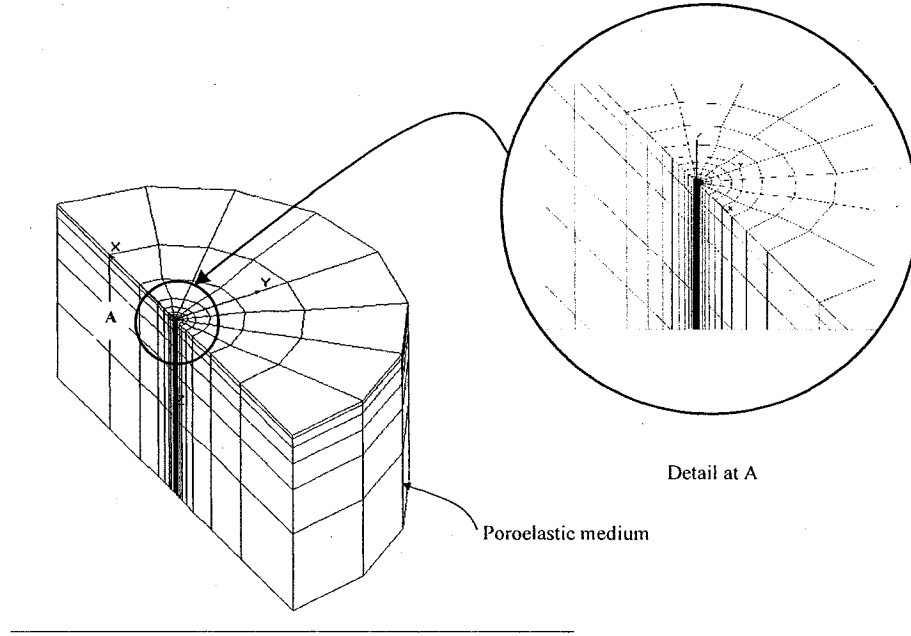


Figure 6.4. Finite element discretization of the rock socket-poroelastic medium system.

Figure 6.5 illustrates the time-dependent translational displacement at the head of a rock socket with aspect ratio  $L/d = 1.0$ , for the case where the interface between the rock socket and the poroelastic medium is assumed to be completely pervious (i.e. fully drained). The excess pore water pressures at this interface are therefore zero. The results presented in Figure 6.5 are related to the four categories of poroelastic response of (i) ideal poroelasticity that does not account for any evolution of damage in porous skeleton, (ii) poroelastic damage with only reduction in elastic stiffness, (iii) stress state-independent evolution of damage with both alterations in elasticity and hydraulic characteristics and (iv) stress state-dependent evolution of damage with both alterations in elasticity and hydraulic conductivity characteristics. The results show that damage-induced alterations in hydraulic conductivity of

the brittle poroelastic medium have a greater influence on the transient response of the rock socket than the situation where there is only evolution of damage with reduction in elastic stiffness and without any alteration in the hydraulic conductivity. Computational results for the stress state-dependent modelling of damage evolution shows less of a difference between the ideal poroelastic situation than that for the analysis involving damage-induced alterations in both elasticity and hydraulic conductivity characteristics. This is likely due to development of compressive stress within the damage-susceptible poroelastic medium, which is restricted mainly to one side of the laterally loaded rock socket and that the evolution of damage is restricted in view of the stress state-dependent criteria for damage evolution. Figure 6.6 illustrates the time-dependent lateral displacement at the head of a rock socket with  $L/d = 1.0$ , for the case where the interface between the rock socket and the poroelastic medium is impervious (fully undrained). The results show the same trend as for the analysis involving the impervious interface. Figure 6.7 illustrates a comparison between the two cases for pervious and impervious interfaces for the case where  $L/d = 1.0$ . The influence of damage-induced alterations in the case of the impervious interface is greater, but the differences are marginal. The change is due to slower rate of pore water pressure dissipation for the case of an impervious interface and that any alterations in the hydraulic conductivity of the brittle poroelastic medium can influence the time-dependent response in a greater rate. Figures 6.8 and 6.9 illustrate the results for the degree of consolidation of the laterally loaded rock socket derived, respectively, for interfaces with pervious and impervious pore fluid pressure boundary conditions. These results indicate that the rate of consolidation increases for situations where damage-induced alterations in the hydraulic conductivity characteristics are taken into account. Furthermore, for poroelastic behaviour that accounts for stress state-dependent damage evolution, the change is less significant. Figures 6.10 to 6.19 illustrate similar results applicable to the problems where the rock socket dimensions correspond to  $L/d = 2.0$  and  $4.0$ .

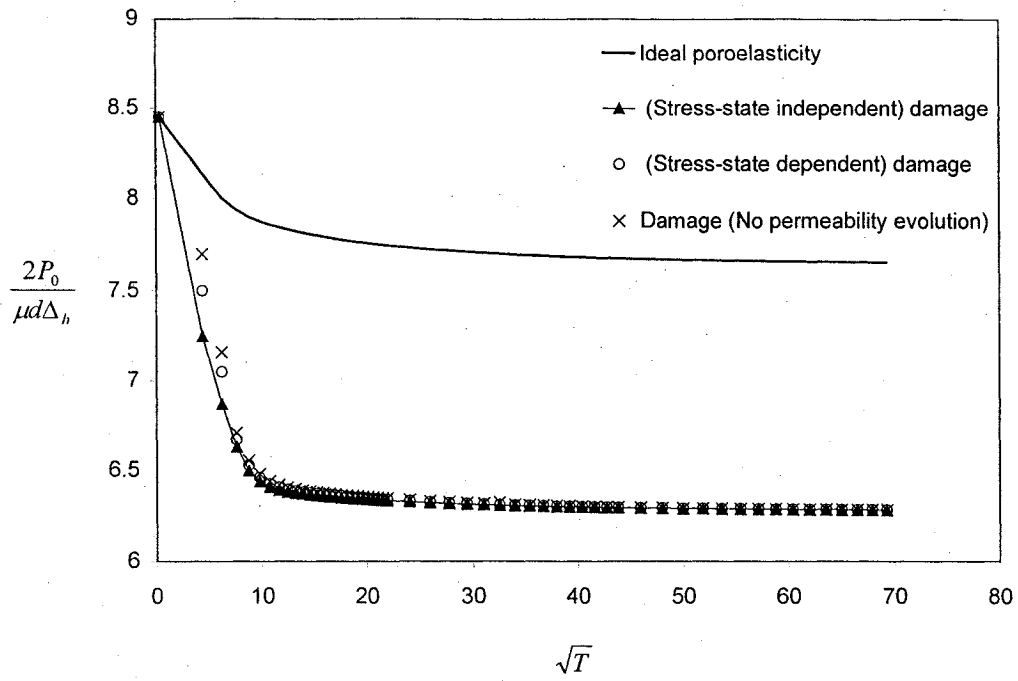


Figure 6.5. Numerical results for the time-dependent translational displacement of a rock socket ( $L/d = 1.0$ ) embedded in a brittle poroelastic half-space (pervious interface).

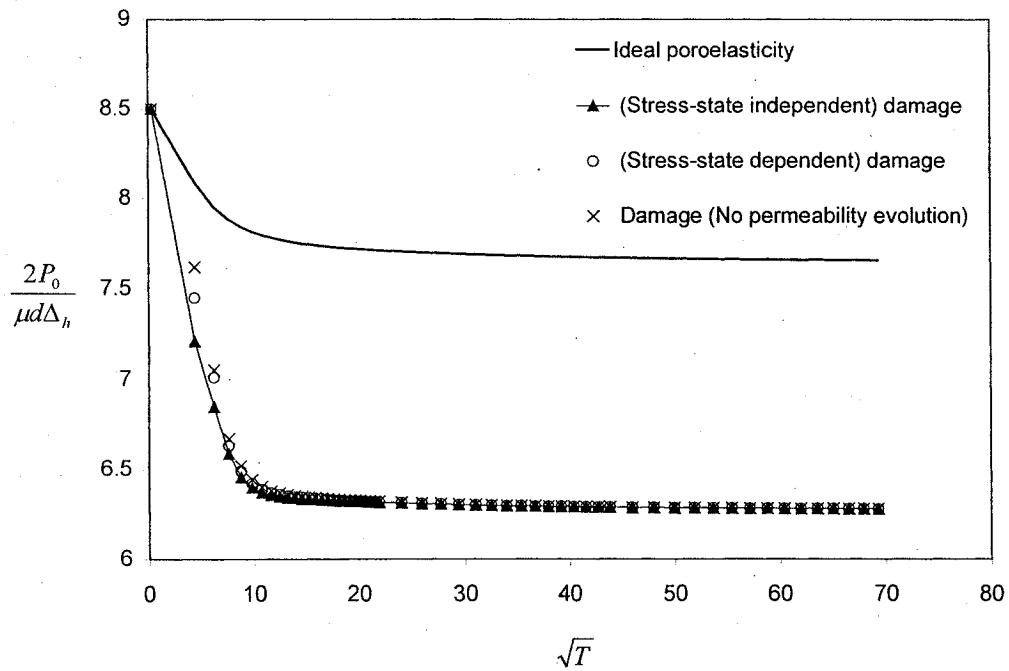


Figure 6.6. Numerical results for the time-dependent translational displacement of a rock socket ( $L/d = 1.0$ ) embedded in a brittle poroelastic half-space (impervious interface).

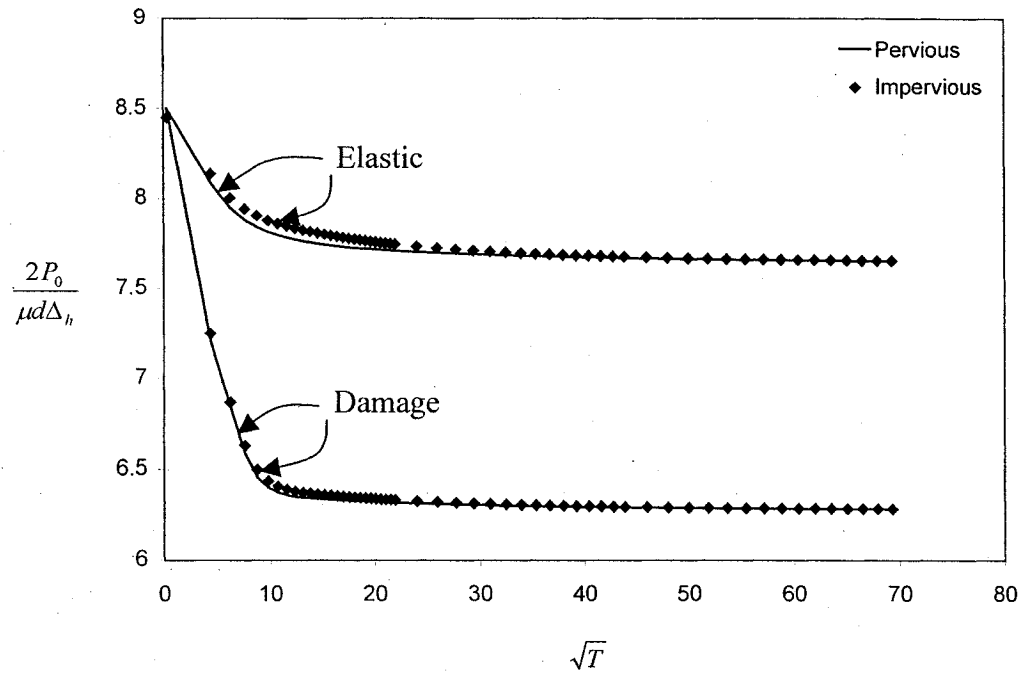


Figure 6.7. Comparison of results for the rock socket with ( $L/d = 1.0$ ) with either a pervious or an impervious interface between the rock socket and poroelastic half-space.

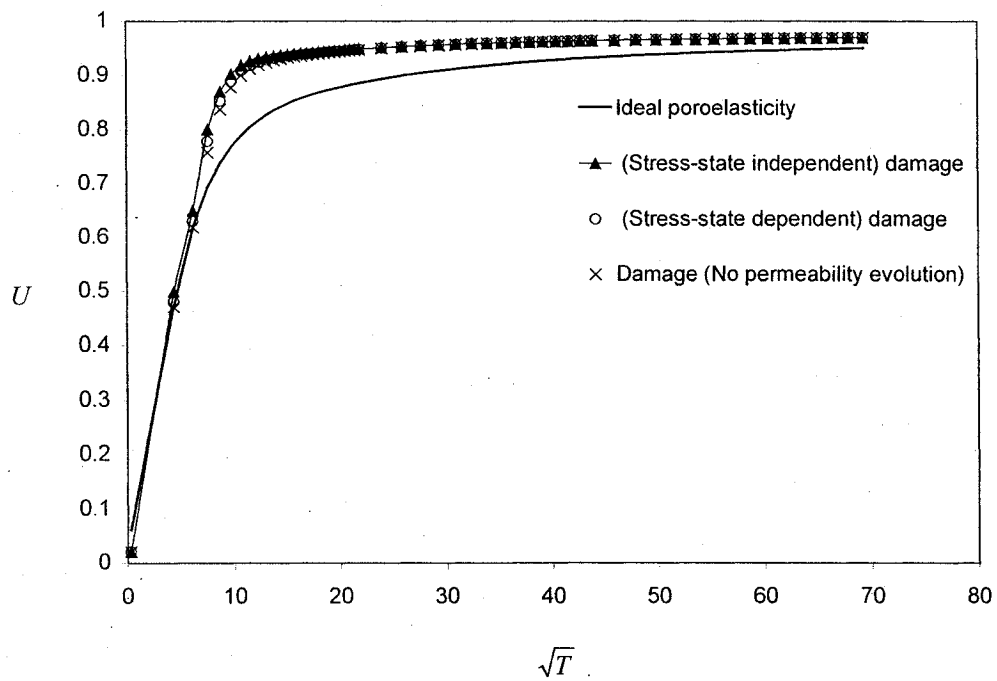


Figure 6.8. Numerical results for the degree of consolidation of a laterally loaded a rock socket ( $L/d = 1.0$ ) embedded in a brittle poroelastic half-space (pervious interface).

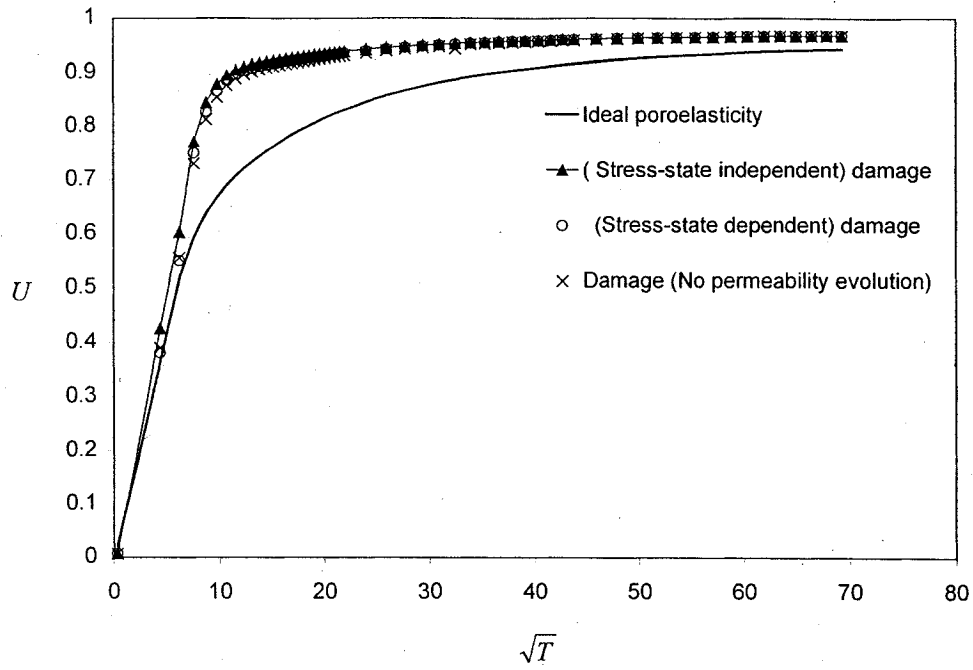


Figure 6.9. Numerical results for the degree of consolidation of a laterally loaded rock socket ( $L/d = 1.0$ ) embedded in a brittle poroelastic half-space (impervious interface).

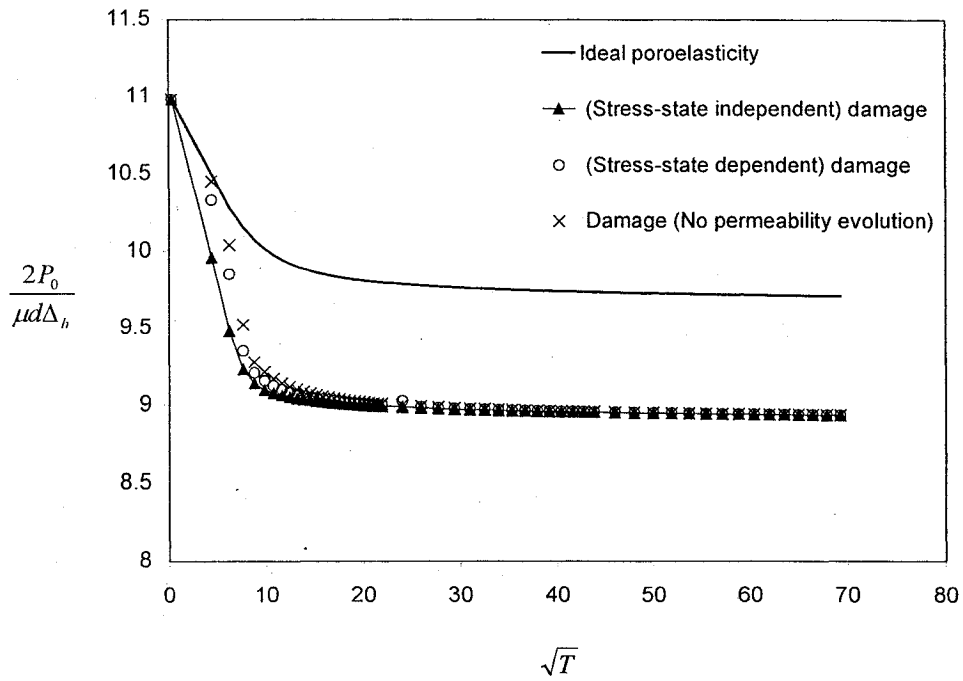


Figure 6.10. Numerical results for the time-dependent translational displacement of a rock socket ( $L/d = 2.0$ ) embedded in a brittle poroelastic half-space (pervious interface).

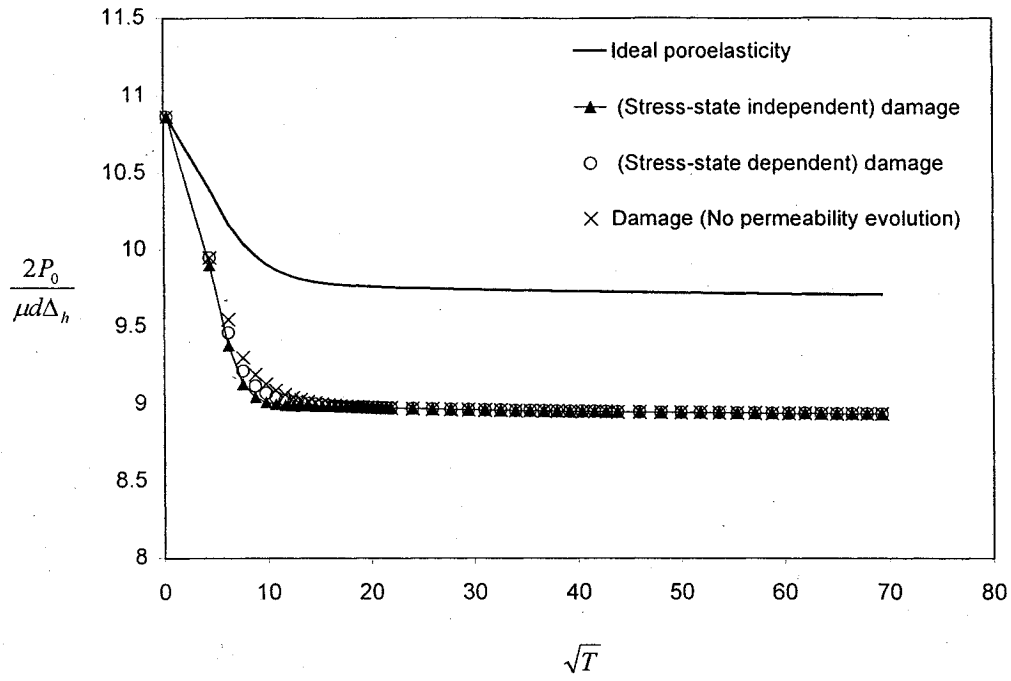


Figure 6.11. Numerical results for the time-dependent translational displacement of a rock socket ( $L/d = 2.0$ ) embedded in a brittle poroelastic half-space (impervious interface).

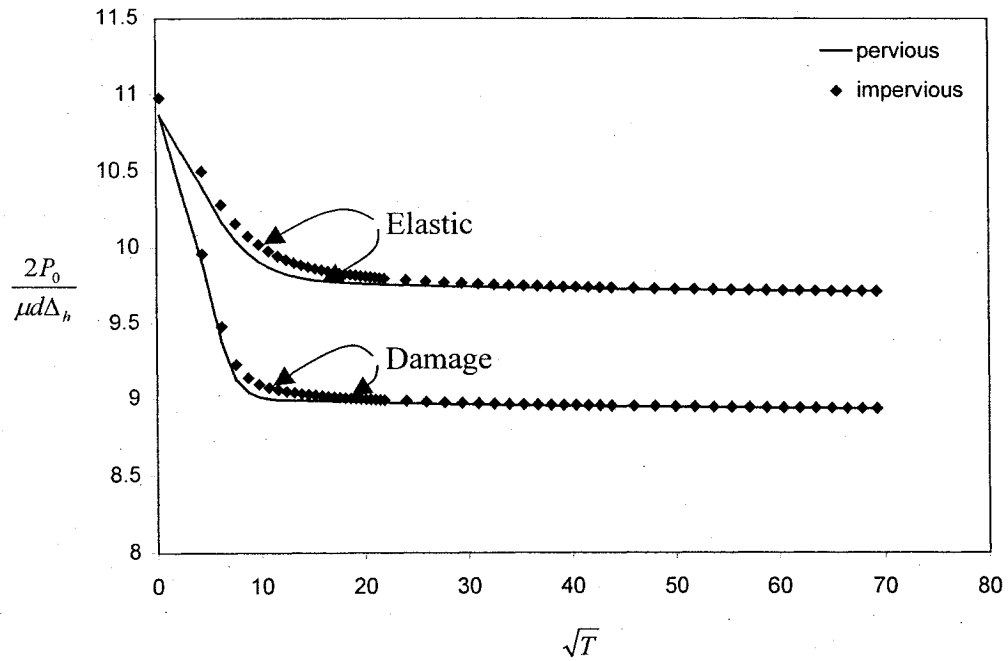


Figure 6.12. Comparison of results for the rock socket with ( $L/d = 2.0$ ) with either a pervious or an impervious interface between the rock socket and poroelastic half-space.

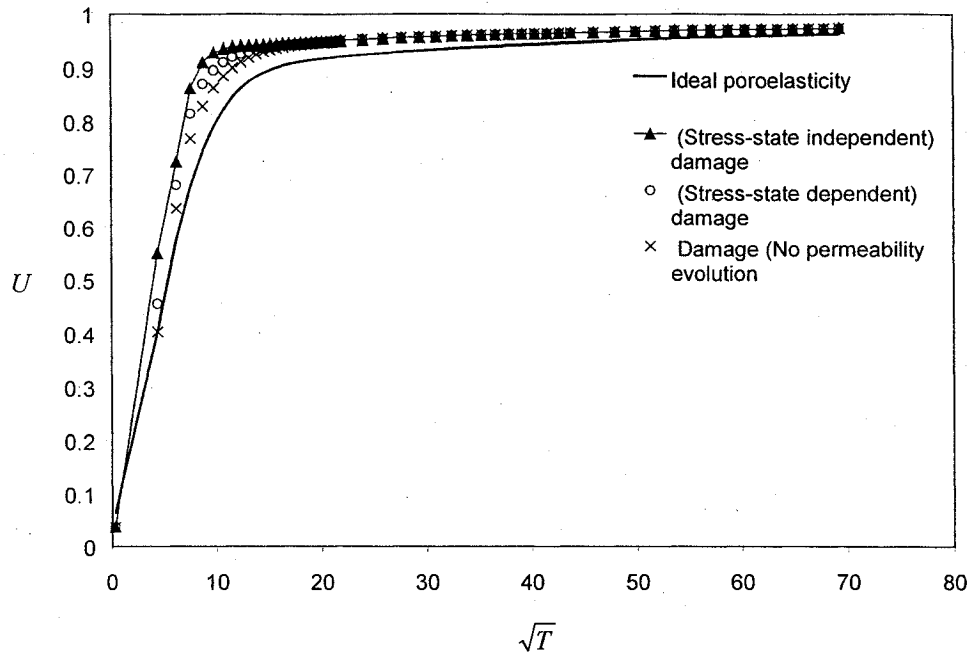


Figure 6.13. Numerical results for the degree of consolidation of a laterally loaded rock socket ( $L/d = 2.0$ ) embedded in a brittle poroelastic half-space (pervious interface).

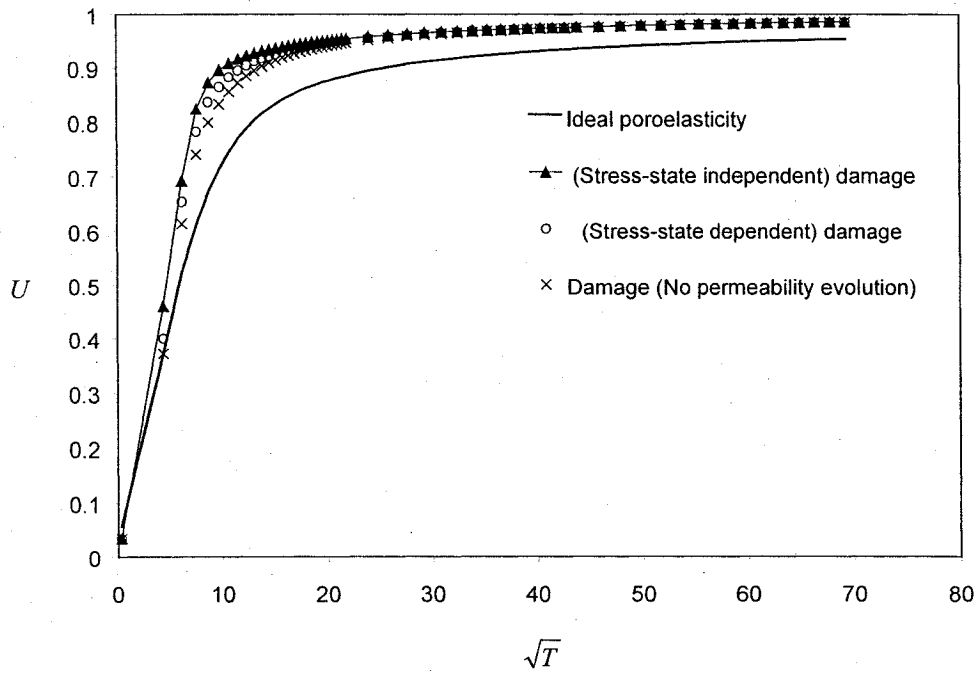


Figure 6.14. Numerical results for the degree of consolidation of a laterally loaded rock socket ( $L/d = 2.0$ ) embedded in a brittle poroelastic half-space (impervious interface).



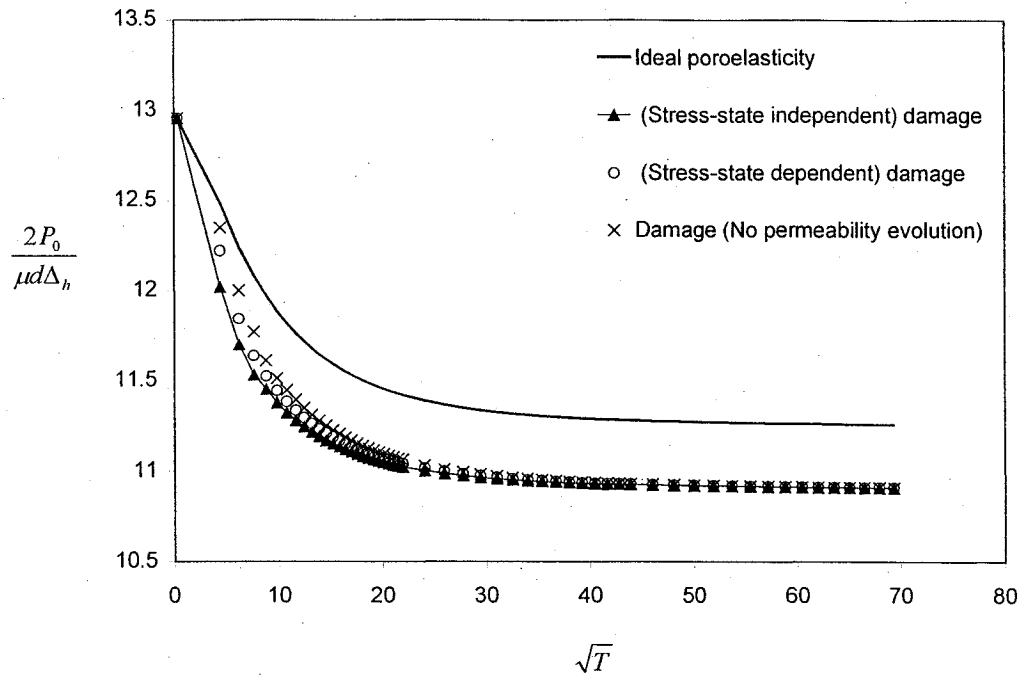


Figure 6.15. Numerical results for the time-dependent translational displacement of a rock socket ( $L/d = 4.0$ ) embedded in a brittle poroelastic half-space (pervious interface).

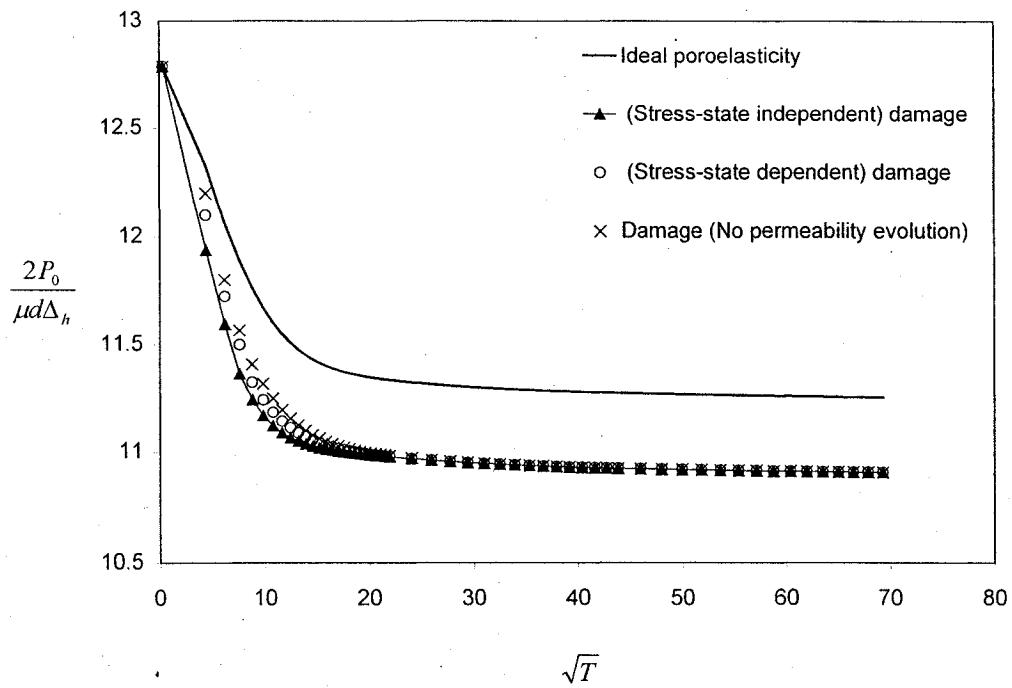


Figure 6.16. Numerical results for the time-dependent translational displacement of a rock socket ( $L/d = 4.0$ ) embedded in a brittle poroelastic half-space (impervious interface).

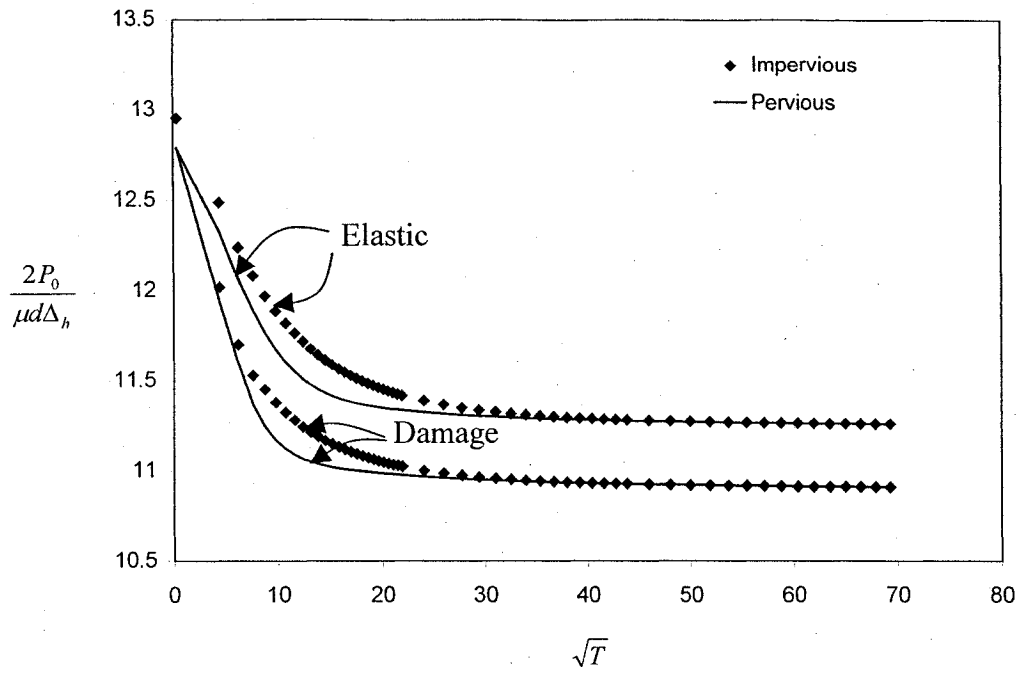


Figure 6.17. Comparison of results for the rock socket with  $(L/d = 4.0)$  with either a pervious or an impervious interface between the rock socket and poroelastic half-space.

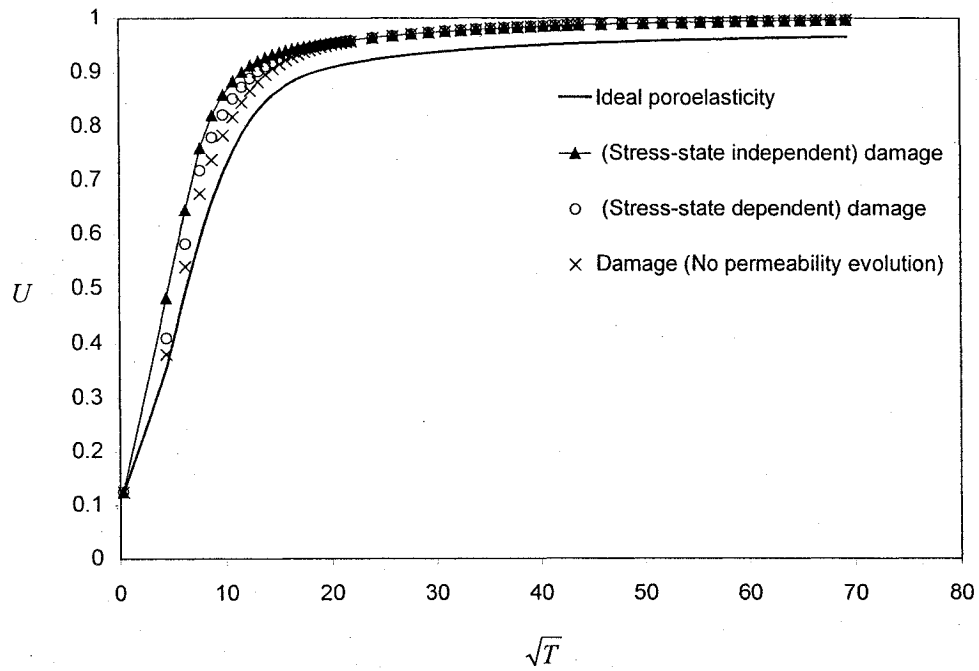


Figure 6.18. Numerical results for the degree of consolidation of a laterally loaded rock socket  $(L/d = 4.0)$  embedded in a brittle poroelastic half-space (pervious interface).

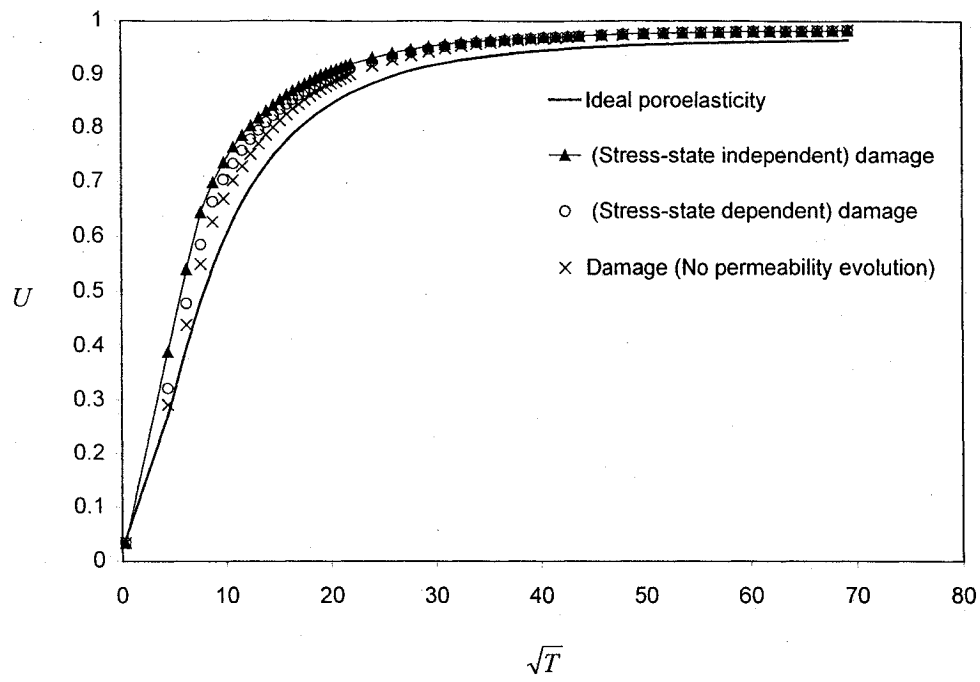


Figure 6.19. Numerical results for the degree of consolidation of a laterally loaded rock socket ( $L/d = 4.0$ ) embedded in a brittle poroelastic half-space (impervious interface).

## **CHAPTER 7**

# **MECHANICS OF AN IN-PLANE LOADED RIGID ANCHORAGE EMBEDDED IN A DAMAGE-SUSCEPTIBLE POROELASTIC REGION**

### **7.1 Introduction**

Anchorage are used quite extensively in geotechnical engineering practice to provide restraint against tensile and uplift loads. The applications of anchorages include earth retaining structures, slope stabilization procedures, structures such as guyed towers in power transmission, restraints for pipelines subjected to uplift and earth movement.

The geotechnical study of anchors requires the estimation of both their ultimate load carrying capacity and the estimation of their time-independent and time-dependent displacements under sustained loads in the working range. With prestressed anchors, the time-dependent loss of anchorage loads also becomes an important consideration in their geotechnical design. The mechanical behaviour of anchors is largely determined by (i) their geometry, (ii) the method of installation of the anchorage and (iii) the geomaterial in which the anchor is installed. The technology aspects of these considerations is given in articles by Girault (1969) and Hanna (1972, 1982) and Adams and Klym (1972), who also give detailed accounts for different types of anchorages, their installation and the procedures for the estimation of the ultimate and working load responses. The study of anchor behaviour is best approached by considering (i) the types of anchors (i.e.) general shapes or specialized configurations, (ii) types of geomaterials in which the anchor is installed and (iii) the method of installation of the anchorages. The study of the

mechanical behaviour of anchors installed in granular media requires approaches that are quite distinct of those required for the study of anchorages that are located in cohesive-fluid saturated geomaterials. The former category of anchors has been extensively studied, starting from the work of Balla (1961) and others including the studies Meyerhof and Adams (1968), Vesic (1971, 1972) and Ladanyi and Johnston (1974). These studies include the modelling of plate and cylindrical anchors, which are either with shallow embedment or deeply located in granular soil media. Developments in this area include both experimental and computational procedures (Davie and Sutherland, 1977), Rowe and Davis, 1982) that have been used to estimate both their ultimate load capacity and the load-deformation behaviour.

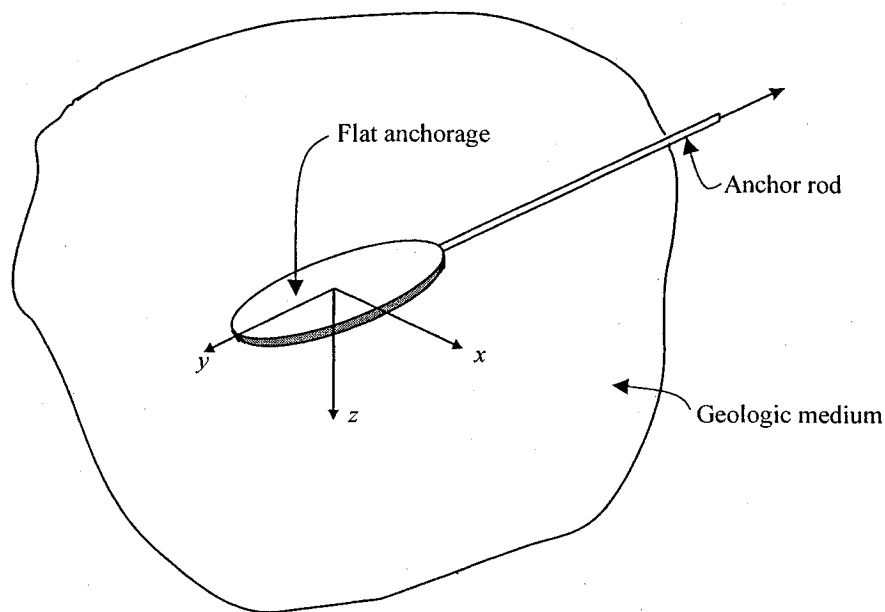


Figure 7.1 A flat anchorage located in a geologic medium

In this Chapter, we are primarily concerned with the study of the mechanics of flat anchors, which are embedded in fluid saturated poroelastic media that are susceptible to damage evolution during their loading in a sustained manner. A flat anchor is an idealized concept of an anchorage that can be created by the pressurization of a geologic medium by a cementitious fluid. The pressurization results in the development of a hydraulic fracture zone, which allows for migration of the cementitious fluid, when hardened, serves as the anchorage. The orientation of the anchorage zone can be arbitrary and will depend on the in-situ geostatic state of stress (and the fracture characteristics of

the geomaterial). The desirable flat anchorage is one where the flat anchorage is oriented along the line of application of the anchor rod force (Figure 7.1).

The flat anchor problem has been examined quite extensively in connection with the study of their time-independent elasto-static behaviour. Although these elastic solutions are not directly related to the topic of poroelastic geomaterials susceptible to micro-mechanical damage analysis of such anchorages, they represent an extensively studied topic in geomechanics, which can be used to examine the accuracy of computational schemes that are used to examine the purely poroelastic behaviour of the anchor region. It should be noted that in a generalized elastic solution for an anchor problem, the case involving  $\nu = 0.50$  corresponds to the consolidation response as  $t \rightarrow 0$  and the elastic solution with  $\nu \rightarrow \nu'$  corresponds to the poroelastic response as  $t \rightarrow \infty$ . The earliest study of the flat plate anchor problem is due to Collins (1962), who presented an exact closed form solution to the problem of the axial loading of a circular anchor plate located in an isotropic elastic infinite medium. Keer (1965) examined the problem related to the in-plane loading of a circular anchor plate located in an isotropic elastic infinite medium. The study by Kassir and Sih (1968) dealt with the problem of a rigid anchor plate embedded in an isotropic elastic medium and subjected to a generalized force resultants at centroid. More general approaches to the study of disc shaped anchor problems were presented by Kanwal and Sharma (1976) and Selvadurai (1976), who examined problems related to spheroidal anchor region, embedded in elastic media, using singularity methods and spheroidal function techniques, respectively. From these solutions, the results for disc anchor problems and elongated needle shaped anchor problems can be recovered as special cases. These studies have also been extended by Zurieck (1988) to include the problem of a spheroidal anchor region located in a transversely isotropic region. An extensive series of studies of the disc anchor problem related to an elastic medium of infinite extent was conducted by Selvadurai and coworkers who extended these studies to include transversely isotropic behaviour of the elastic medium, the influence of bi-material regions, elliptic geometry of the disc and the influence of boundary surfaces, etc. (Selvadurai, 1978, 1979b, 1980, 1993, 1994, 1999, 2000c and 2003, Selvadurai and Singh, 1984a,b and Selvadurai and Au, 1986).

Related investigations dealing with flat anchor problems were also given by Gladwell (1999), who examined the axial loading of a disc inclusion located at a bi-material region and confirmed the applicability of the bounding technique first developed by Selvadurai (1984) for the evaluation of the axial stiffness of inclusions located at a bi-material interface region. Selvadurai (2003) has also extended the application of the bounding technique for the study of the in-plane loading of circular plate anchor located at the interface of two dissimilar elastic half-space regions.

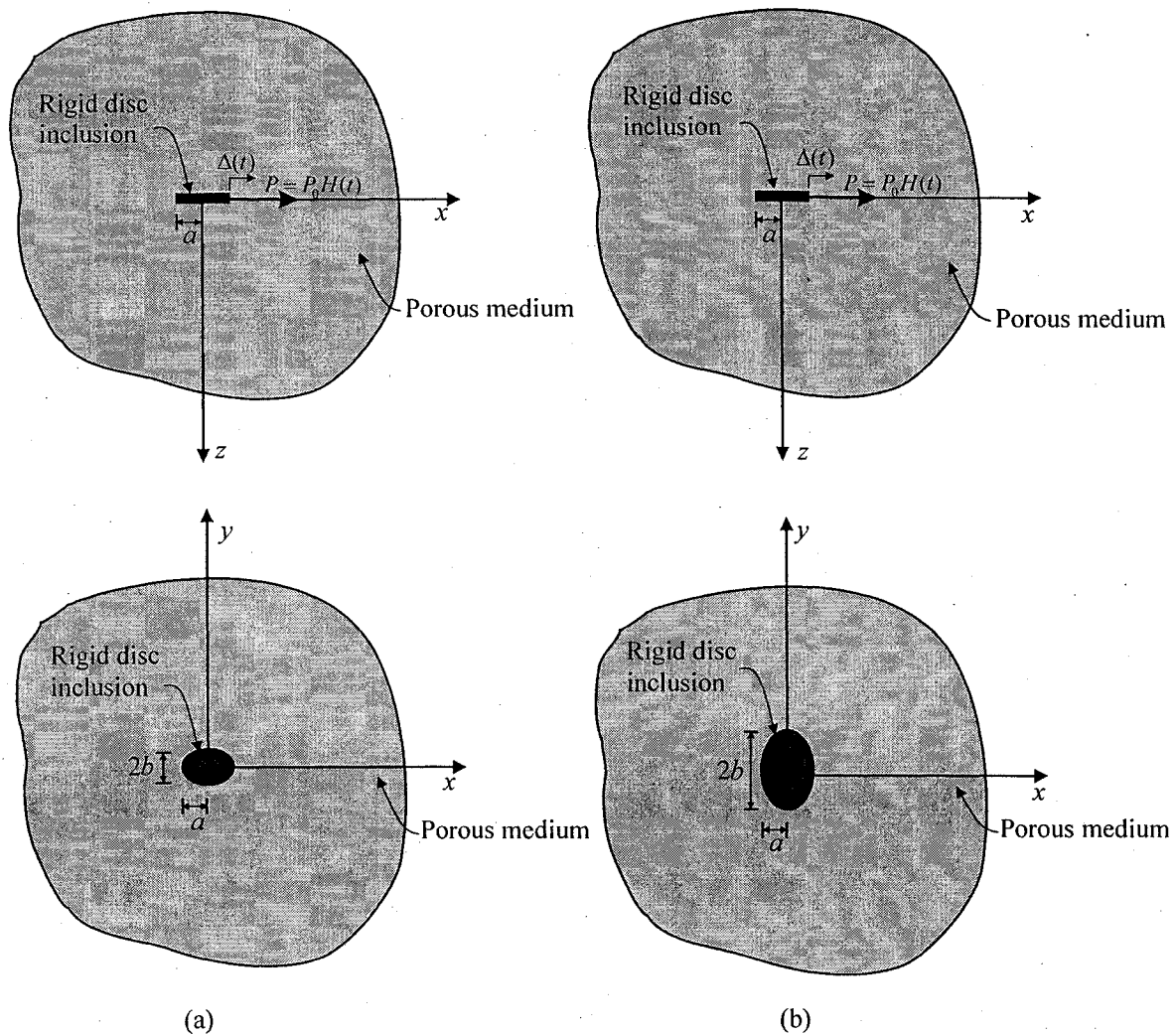


Figure 7.2 Rigid disc inclusion surrounded with a brittle poroelastic medium (a)  $b/a < 1$ ,  
(b)  $b/a > 1$

The studies of anchor problems in general, dealing with poroelastic media are relatively scarce. Selvadurai and Gopal (1986) presented a solution to the problem of a disc embedded at the base of a borehole in a poroelastic medium in connection with their modelling of the screw plate test. The translation of a rigid spheroidal anchor located in a poroelastic medium was examined by Rajapakse and Senjuntichai (1995), who used a boundary element approach. The modelling of the Biot consolidation problem for a disc inclusion located at an indenter of an infinite space region and subjected to generalized force resultants was given by Yue and Selvadurai (1995). These authors presented the complete sets of integral equations, governing the problems in the half-space domain and the solution of the resulting Fredholm integral equations and Laplace transform inversion was performed numerically. This investigation represents the only comprehensive study of the problem of a disc anchor related to a poroelastic medium of infinite extent, which also provided the time-dependent consolidation response. Of related interest are the studies by Selvadurai (1978, 1981) which examine the time-dependent response of anchors that are embedded in viscoelastic media. The analytical study of the flat anchor problem related to a poroelastic medium can be attempted only when the geometry of the flat anchor region corresponds to a regular simple shape, such as either a circular or elliptical shape. The analytical study of the flat anchor problem can also be made intractable when other process such as damage-induced alterations in the deformability properties and the fluid transport properties of the poroelastic medium changes with time. In this Chapter, we apply the computational methodologies developed in the previous chapters to the study of the in-plane loading of a flat anchor region that is embedded in a damage susceptible poroelastic medium of infinite extent. Although the computational procedure can be applied to plate or flat anchor region of arbitrary shape and arbitrary loading, to keep the changes in the parameters influencing the poroelastic behaviour to a minimum and to allow consideration of comparison with available analytical results, we restrict attention to the consideration of the in-plane loaded disc anchor problem examined in this section. The variables investigated in the computational modelling includes (i) the geometry of the elliptical plate or flat anchor in relation to the direction of loading, (ii) the evolution of elasticity and hydraulic conductivity parameters in relation



to damage development and (iii) the stress state-dependency of the evolution of damage and its influence of the time-dependent translation of the anchor.

## 7.2 Elastic Solution for the In-Plane Loading of a Flat Anchor Region

In this section, we examine the problem of a rigid elliptical flat anchor, which is embedded in bonded contact with an isotropic elastic medium. The analytical solution to the problem where the surrounding geomaterial exhibits isotropic perfectly elastic characteristics was first presented by Kassir and Sih (1968). An analytical solution for the in-plane translation of an elliptical anchor located at a bi-material elastic interface was given by Selvadurai and Au (1986). These authors determined the in-plane translation of an elliptical anchorage located at a bi-material elastic interface in the following form;

$$P_0 = \frac{8\pi a \Delta \mu_1 e_0^2}{\{(3 - 4\nu_1)e_0^2 + 1\}K(e_0) - E(e_0)} \{(1 - \nu_1) + R(1 - \nu_2)\chi\} \quad (7.1)$$

where

$$\chi = \left[ \frac{\{(3 - 4\nu_1)e_0^2 + 1\}K(e_0) - E(e_0)}{\{(3 - 4\nu_2)e_0^2 + 1\}K(e_0) - E(e_0)} \right]; e_0^2 = (a^2 - b^2)/a^2; R = \mu_1 / \mu_2 \quad (7.2)$$

where  $P_0$  is the in-plane load and  $a, b$  are the dimensions of the elliptic anchorage;  $\Delta$  is the horizontal displacement of the anchor and  $\mu_1, \nu_1, \mu_2, \nu_2$  are the shear modulus and Poisson's ratio for the materials and  $K(e_0)$  and  $E(e_0)$  are the complete elliptic integrals (see e.g. Byrd and Friedman, 1971).

Selvadurai (2003) gave a set of bounds for the in-plane translation of a circular disc anchor located at a bi-material elastic interface, which takes the form;

$$\frac{(\varpi_1 + \Gamma \varpi_2)}{2\varpi_1\{2 + \beta_2 + 3\varpi_2\alpha_2\} + 2\varpi_2\Gamma\{2 + \beta_1 + 3\varpi_1\alpha_1\}} \leq \frac{P_0}{32a\Delta(\mu_1 + \mu_2)} \leq \frac{(7 - 8\nu_1)(1 - \nu_2) + \Gamma(7 - 8\nu_2)(1 - \nu_1)}{(1 + \Gamma)(7 - 8\nu_1)(7 - 8\nu_2)} \quad (7.3)$$

where

$$\alpha_i = \frac{1}{2\pi} \ln(3 - 4\nu_i); \quad \beta_i = \frac{(1 - 2\nu_i)}{\pi\alpha_i}; \quad \varpi_i = \frac{\alpha_i\beta_i}{(1 + \alpha_i^2)}; \quad \Gamma = \mu_1 / \mu_2 \quad (7.4)$$

where  $P_0$  is the in-plane load and  $a$  is the radius of the circular anchorage;  $\Delta$  is the horizontal displacement of the anchor and  $\mu_1, \nu_1, \mu_2, \nu_2$  are the shear modulus and Poisson's ratio for the materials. Table 7.1 presents the elastic solution for the circular and elliptical anchors using the analytical results given by Selvadurai and Au (1986) and Selvadurai (2003). The results in Table 7.1 is for the rigid anchorage located in an elastic region, therefore we substitute  $\mu_1 = \mu_2$  and  $\nu_1 = \nu_2$  in (7.1) and (7.3). The average of the upper and lower bound, obtained by equation (7.3) is used in Table 7.1. The elastic parameters used in (7.1) and (7.3) follow as;

Elasticity parameters:  $E = 8300 \text{ MPa}$  ;  $\nu = 0.195$

Failure parameters:  $\sigma_C = 30 \text{ MPa}$  (compressive);  $\sigma_T = 3 \text{ MPa}$  (tensile)

The anchor dimension  $a$  is assumed to be 1.0(m) and the applied load  $P_0$  to the anchorage is 314 kN .

Table 7.1 illustrates the analytical results for elliptical and disc anchors in the form of a dimensionless parameter proposed by Selvadurai (2003) as  $P_0 / 64a\Delta\mu$  where  $P_0$  is the in-plane load and  $a$  is either radius of disc for the case of circular anchorage or the dimension of the elliptical anchor along the direction of application of the load,  $\Delta$  is the horizontal displacement of the anchorage and  $\mu$  is the shear modulus of the surrounding

elastic region. It should be noted that the analytical result for the in-plane elastic stiffness of the rigid disc anchorage can be approximated as the average of the upper and lower bounds given by Selvadurai (2003). Alternatively, the exact result is given by (see e.g. Kassir and Sih, 1968 and Selvadurai, 1980b) in the following form;

$$\frac{P_0}{64\mu a\Delta} = \frac{(1-\nu)}{(7-8\nu)} \quad (7.5)$$

Table 7.1. Comparison of results for ideal elastic analysis ( $\nu = 0.195$ )

Disc shape	$P_0 / 64a\Delta\mu$			
	Circular	Ellipse (1/2)	Ellipse (1/3)	Ellipse (1/5)
Present study	0.141	0.0485	0.0290	0.0104
Analytical solution	0.139 Selvadurai (2003)	0.0480 Selvadurai and Au (1986)	0.0283 Selvadurai and Au (1986)	0.0100 Selvadurai and Au (1986)

### 7.3 Computational Modelling

The problem of a rigid anchorage embedded in bonded contact with a damage-susceptible poroelastic region and subjected to an in-plane load in the form of a Heaviside step function of time is examined through the computational scheme developed in the course of this research (Figure 7.2). The prescribed boundary conditions for pore fluid pressure and displacements are shown in Figure 7.3.

Since the poroelastic region is homogeneous, the problem exhibits a state of symmetry about the plane containing the line of action of the horizontal force  $P(t)$ . Therefore, the attention is restricted to a model of the region;  $-30a \leq x \leq 30a$ ;  $0 \leq y \leq 30a$ ;  $0 \leq z \leq 30a$ , where  $a$  is either radius of disc for the case of circular anchorage or the anchor dimension along the direction of the applied load, for the case of elliptical anchorage. The boundary conditions at the outer surfaces of the region correspond to the

conventional zero normal displacement and zero shear traction conditions applicable to the porous skeleton and the pore fluid pressure boundary conditions are prescribed to be zero. We consider the problem of a rigid flat anchor embedded in a damage-susceptible poroelastic region for the following categories of poroelastic responses (i) ideal poroelastic response of the medium without any evolution of damage; (ii) the poroelastic response of the medium with the evolution of damage but no alterations in hydraulic conductivity characteristics; (iii) the poroelastic response with the evolution of damage and alterations in both elasticity and hydraulic conductivity characteristics; (iv) the poroelastic response of the medium with stress state-dependent evolution of damage and alterations in both elasticity and hydraulic conductivity characteristics.

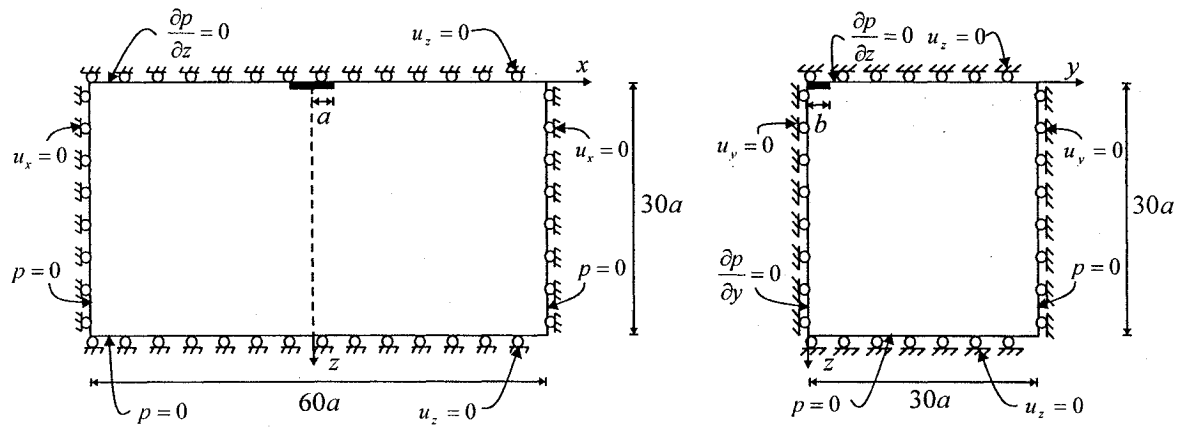


Figure 7.3. Boundary conditions for a rigid flat anchorage surrounded with a poroelastic medium.

#### 7.4 Computational Results and Discussion

In the computational modelling, the idealized problem that corresponds to a rigid anchorage embedded in an infinite region is modelled as an anchorage in a finite domain. Therefore, it is necessary to evaluate the influence of the dimensions of the computational domain used in the finite element modelling. To evaluate this, we first examine the problem of a rigid anchorage, which is embedded in an extended elastic region. As noted previously, the problem has been investigated by a number of the researchers and we use here the analytical solution given by Kassir and Sih (1968) and Selvadurai and Au (1986)

for the problem of rigid elliptical anchorage and the results given by Selvadurai (2003) for the case of rigid circular disc anchorage. The computational results have been compared with equivalent analytical results given above. Table 7.1 provides a comparison of the results obtained from analytical and computational approaches for  $P_0 / 64a\Delta\mu$ , (where  $P_0$  is the in-plane load and  $a$  is either radius of disc for the case of circular anchorage or the radius along the direction of applied load for the case of elliptical anchorage and  $\Delta$  is the horizontal displacement of the anchor and  $\mu$  is the shear modulus of the surrounding elastic region). For a range of anchor shapes, the results show reasonable agreement between the analytical and the computational estimates.

For the purposes of the computational modelling, we select sandstone as the damage-susceptible poroelastic material with the following properties given by Cheng and Dusseault (1993) and Shiping *et al.* (1994);

Elasticity parameters:  $E = 8300 \text{ MPa}$  ;  $\nu = 0.195$  ;  $\nu_u = 0.4999$

Fluid transport parameters:  $k^0 = 10^{-6} \text{ m/s}$

Failure parameters:  $\sigma_c = 30 \text{ MPa}$  (compressive);  $\sigma_t = 3 \text{ MPa}$  (tensile)

Damage parameters:  $\gamma = \eta = 130$  ;  $D_c = 0.75$  ,  $\beta = 3.0 \times 10^5$

The anchor dimension  $a$  is assumed to be 1.0(m) and the applied load  $P_0$  to the anchorage is 314 kN .

The finite element discretizations of the three-dimensional domain containing the laterally loaded rigid anchor region are shown in Figure 7.4.

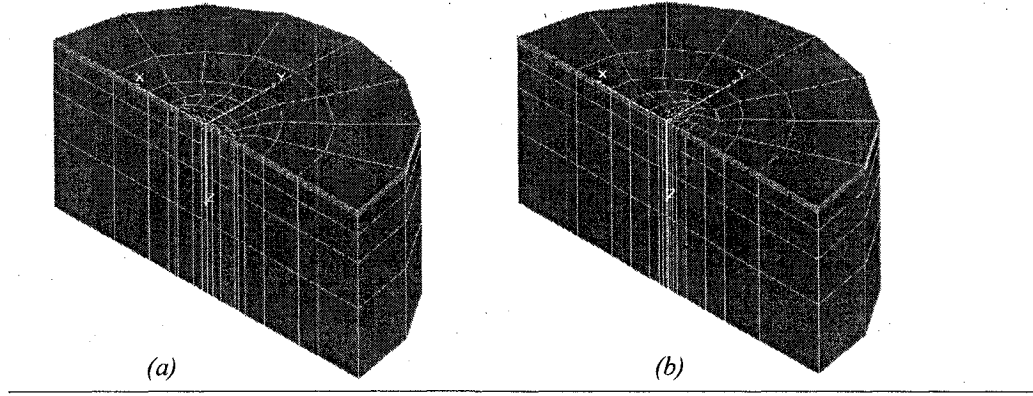


Figure 7.4. Finite element discretization for a flat rigid anchorage for cases (a)  $b/a < 1$   
(b)  $b/a > 1$

The computational modelling is performed for different aspect ratios ( $b/a$ ) (see Figure 7.2). The non-dimensional parameter, which corresponds to the horizontal displacement of the rigid anchor is the same as that used by Selvadurai (2003) and takes the form  $P_0 / 64a\Delta\mu$ , (where  $P_0$  is the lateral load,  $a$  is the anchor dimension,  $\Delta$  is the horizontal displacement of the anchor and  $\mu$  is the shear modulus of the surrounding elastic region). The time factor takes the form;

$$T = \frac{2\mu(1-\nu)k^0 t}{(1-2\nu)a^2} \quad (7.6)$$

where  $\mu$ ,  $\nu$  are shear modulus and Poisson's ratio of the porous skeleton, respectively and  $k^0$  is the hydraulic conductivity for the virgin state,  $a$  is either the radius of the disc for the case of circular anchor or anchor dimension along the direction of the applied load for the case of elliptical anchor and  $t$  is time.

Figure 7.5 presents a comparison between the analytical results presented for the time-dependent displacement of the flat circular anchor in an extended poroelastic medium developed by Yue and Selvadurai (1995) and the analogous computational results derived

from this research. These results illustrate a satisfactory agreement in both the magnitude and time-dependent variation between the analytical and computational results.

Figure 7.6 illustrates the transient time-dependent horizontal displacement of a rigid disc anchor. The results presented in this Figure is related to the four categories of poroelastic responses namely ideal poroelasticity, poroelastic damage with only reduction in elastic stiffness, stress state-independent evolution of damage with both alterations in elasticity and hydraulic conductivity characteristics and the stress state-dependent evolution of damage with both alterations in elasticity and hydraulic conductivity characteristics. The results show that damage-induced alterations in hydraulic conductivity of the brittle poroelastic medium have a greater influence on the time-dependent response of the disc anchor than the case of evolution of damage with only reduction in elastic stiffness and without alterations in hydraulic conductivity. The computational results for stress state-dependent modelling of damage evolution indicate less of a difference between the ideal poroelastic case and that involving damage-induced alterations in elasticity and hydraulic conductivity characteristics. This is most likely due to the development of a compressive state of stress within the damage-susceptible poroelastic medium, located at one region of the rigid disc anchor. According to the stress state-dependent criteria for damage evolution, this region cannot experience damage-induced alterations in poroelastic parameters.

Figure 7.7 illustrates the time-dependent horizontal displacement for the case of an elliptical anchorage subjected to an in-plane load directed along its major axis ( $b/a = 1/2$ ). The results indicate similar trends for the elliptical anchor, however the results show greater of a difference between the modelling involving ideal poroelasticity and the modelling that involves damage-induced alterations in poroelasticity parameters. This is likely due to development of high shear stress zones at the tip of the anchor. Figures 7.8 and 7.9 illustrate identical results applicable to the rigid elliptical anchorage with  $b/a = 1/3$  and  $b/a = 1/5$ . The results show greater influence of damage-induced alterations in the hydraulic conductivity on the time-dependent in-plane displacement of the rigid anchorage, which could be attributed to the elliptical shape of the anchorage.

Figure 7.10 illustrates time-dependent horizontal displacement for an elliptical anchorage subjected to an in-plane load along the direction of minor axis for ( $b/a = 2$ ). The results show the same trend for both the disc anchor and the elliptical anchor subjected to a lateral load directed along the major axis. In comparison to the results for disc anchor, computational results for the case of elliptical anchor subjected to an in-plane load directed along the minor axis shows a greater difference between the ideal poroelastic case and the case that involves damage-induced alterations in poroelastic parameters again, this is likely due to development of the zones of high stress at the tip of the anchor. Figure 7.11 and 7.12 illustrate similar results applicable to the rigid elliptical anchor dimensions defined by  $b/a = 3$  and  $b/a = 5$ .

In general, the computational results presented in this Chapter indicate that the geometric shape of the anchoring can increase the damage-induced alterations in the hydraulic conductivity and consequently influence the transient behaviour of the anchorage. The elongated anchorage can generate higher shear stresses at the edge of anchorage and this results in the evolution of damage in the zone surrounding the rigid anchor, which again influences the consolidation response.

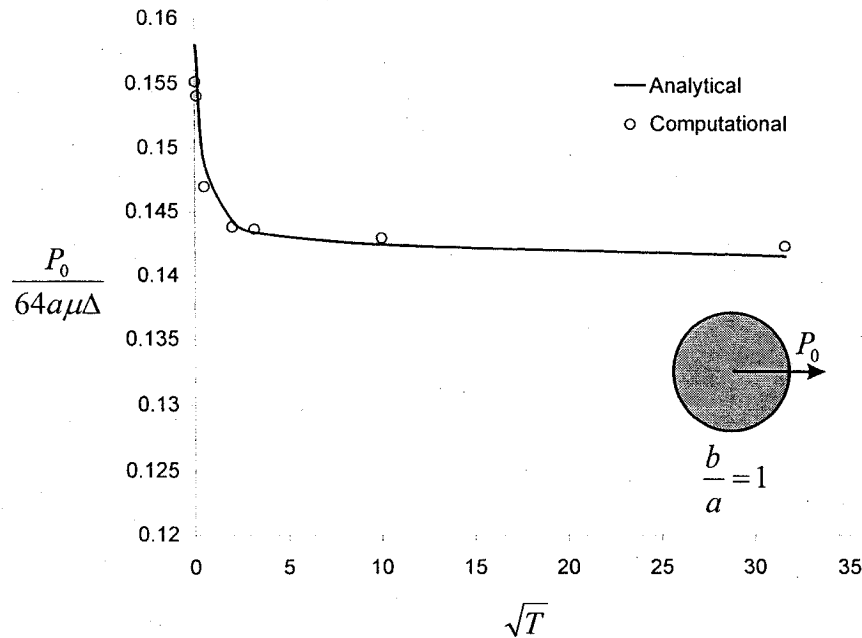


Figure 7.5 A comparison between the analytical results given by Yue and Selvadurai (1995) for an impermeable circular anchorage and the computational results.



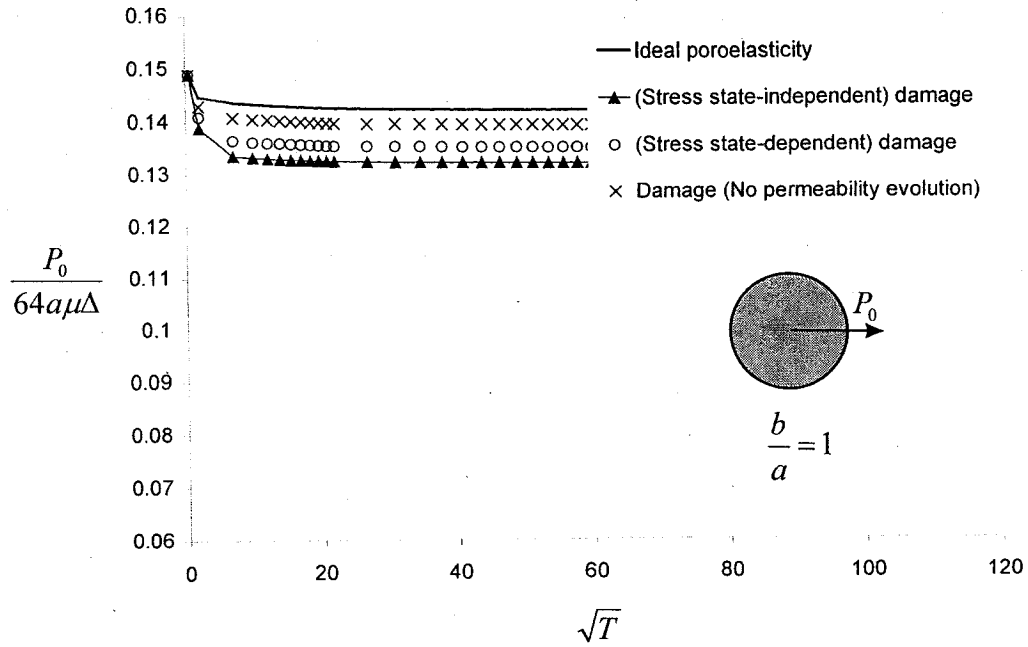


Figure 7.6. Numerical results for the time-dependent in-plane stiffness for a rigid flat anchor embedded in a poroelastic medium susceptible to damage.

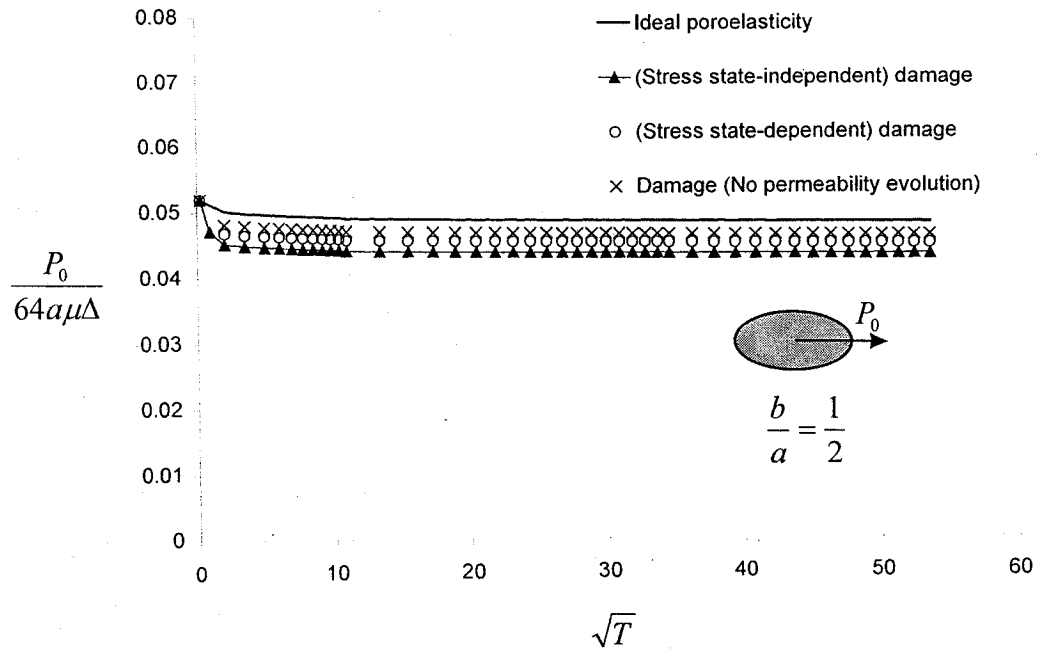


Figure 7.7. Numerical results for the time-dependent in-plane stiffness for a rigid flat anchor ( $b/a = 1/2$ ) embedded in a poroelastic medium susceptible to damage.

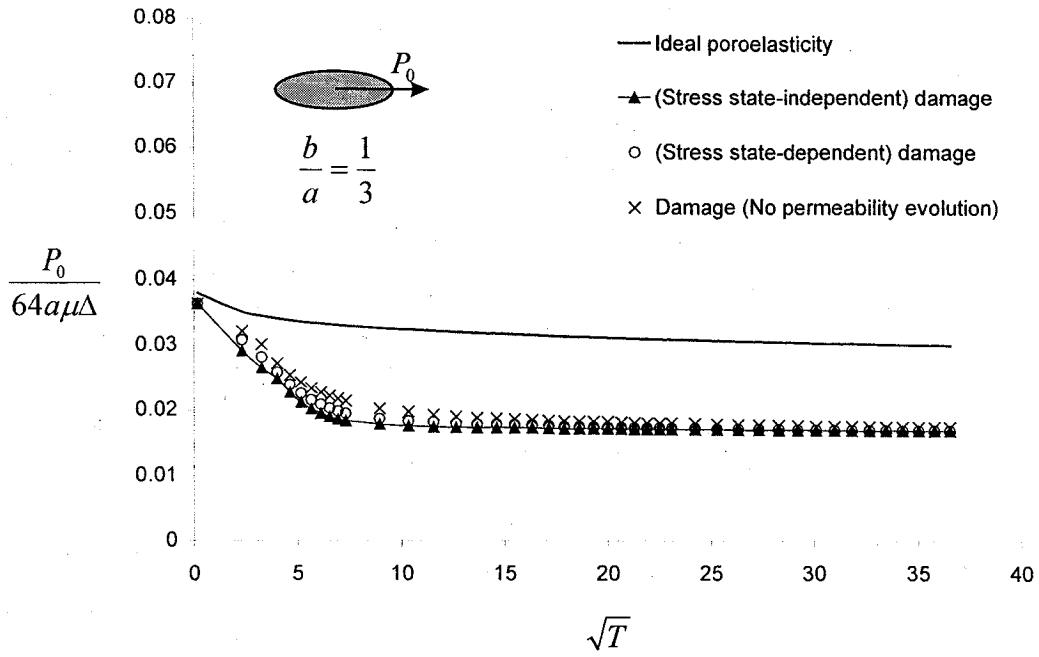


Figure 7.8. Numerical results for the time-dependent in-plane stiffness for a rigid flat anchor ( $b/a = 1/3$ ) embedded in a poroelastic medium susceptible to damage.

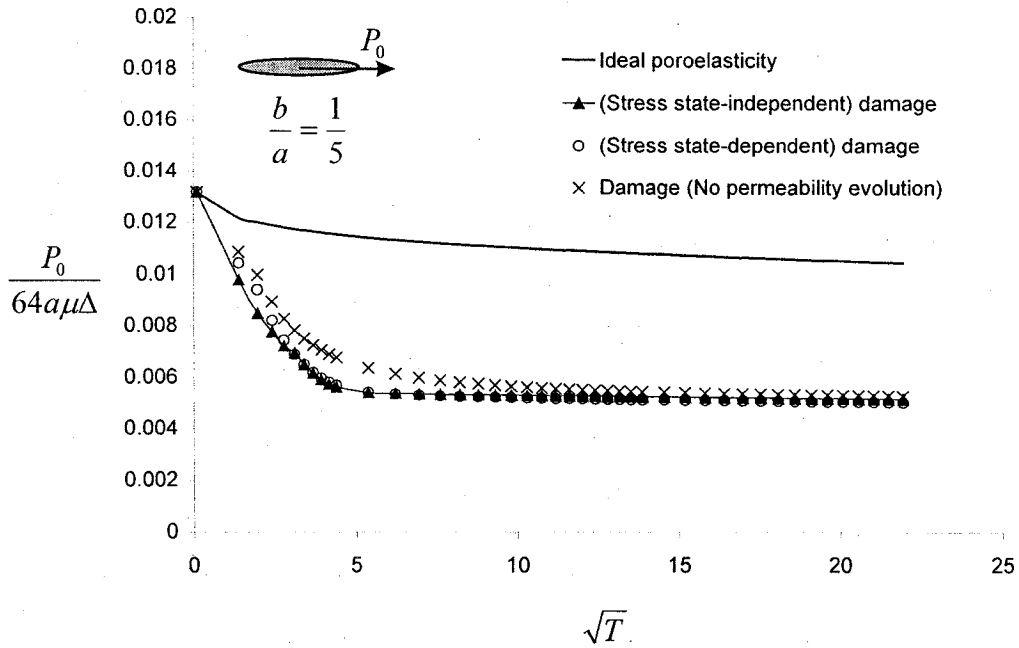


Figure 7.9. Numerical results for the time-dependent in-plane stiffness for a rigid flat anchor ( $b/a = 1/5$ ) embedded in a poroelastic medium susceptible to damage.

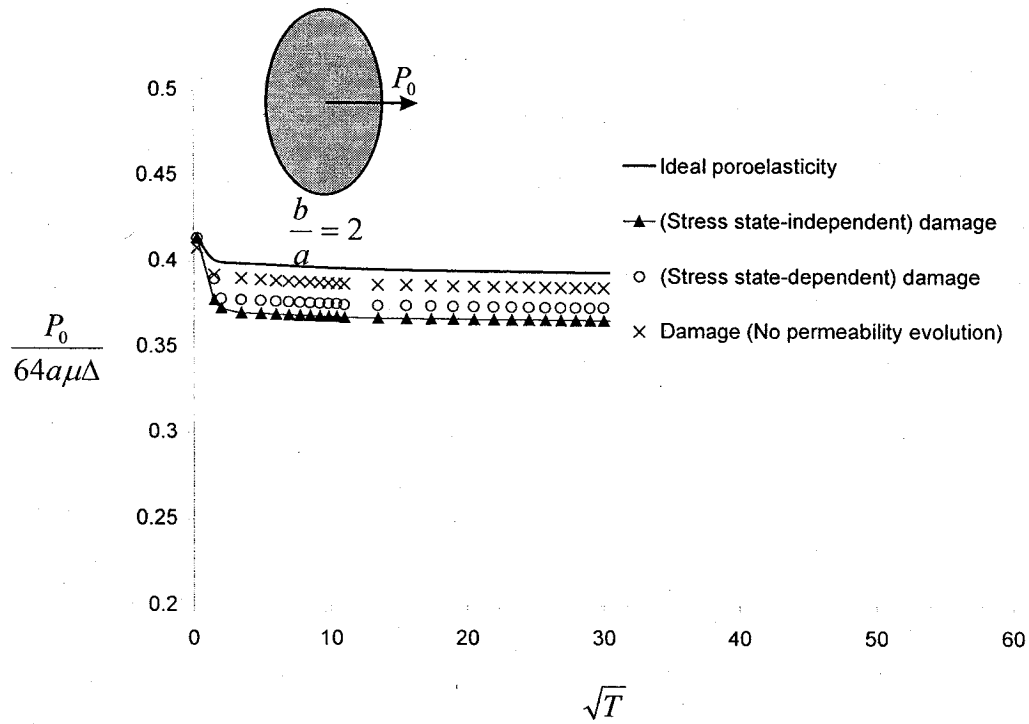


Figure 7.10. Numerical results for the time-dependent in-plane stiffness for a rigid flat anchor ( $b/a = 2$ ) embedded in a poroelastic medium susceptible to damage.

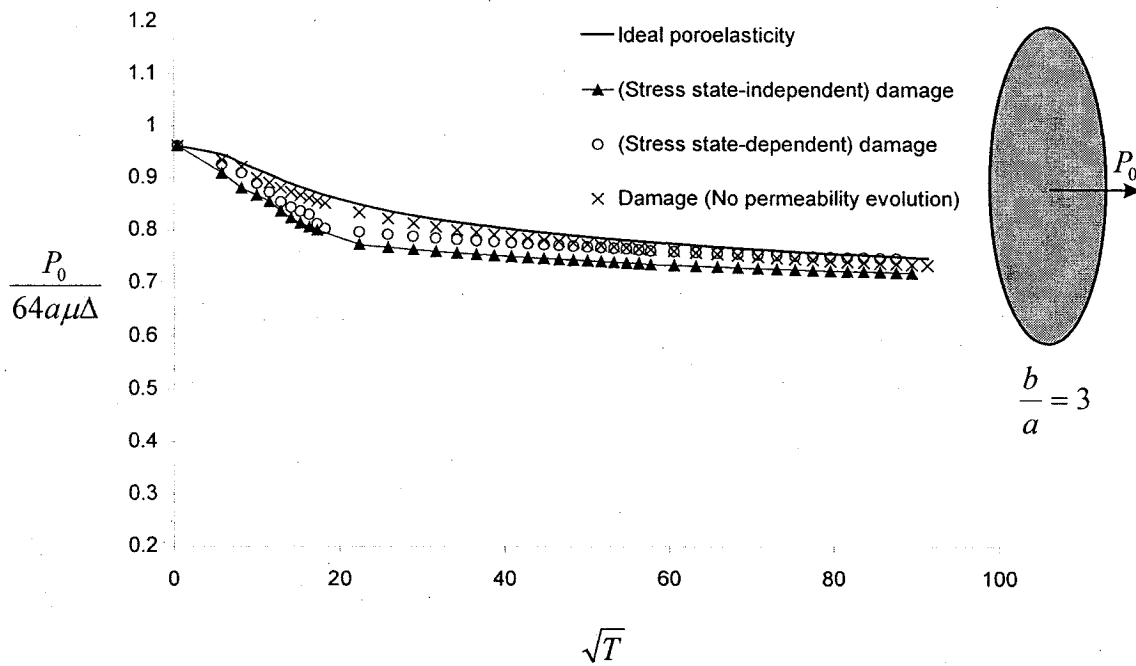


Figure 7.11. Numerical results for the time-dependent in-plane stiffness for a rigid flat anchor ( $b/a = 3$ ) embedded in a poroelastic medium susceptible to damage.

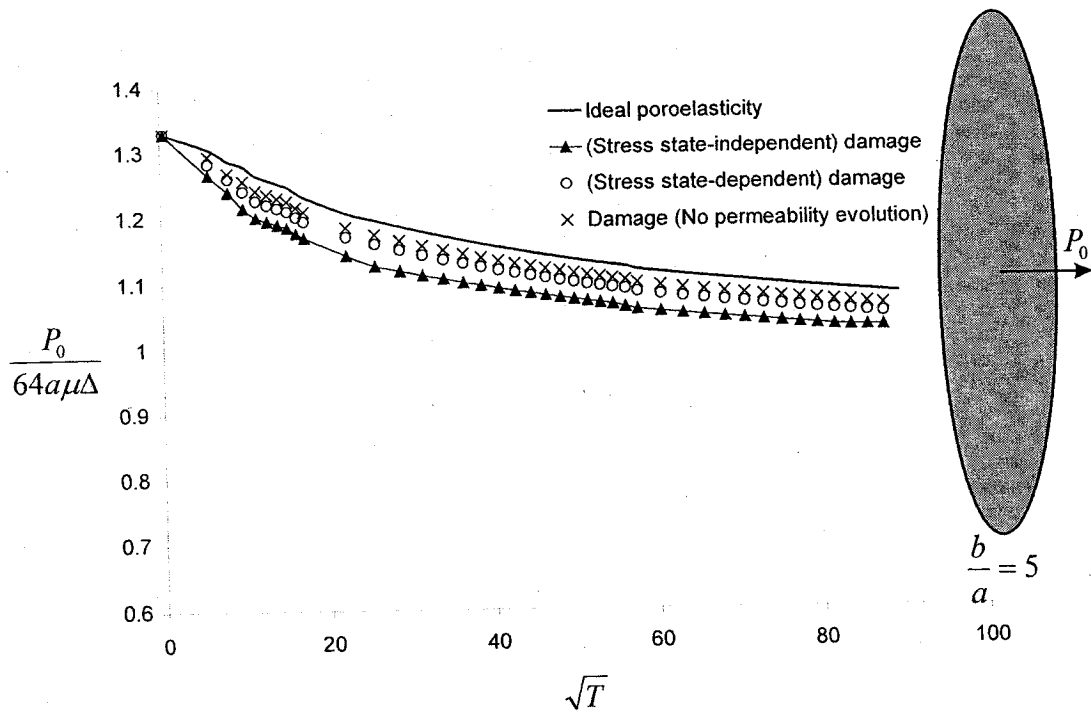


Figure 7.12. Numerical results for the time-dependent in-plane stiffness for a rigid flat anchor ( $b/a = 5$ ) embedded in a poroelastic medium susceptible to damage.

## **CHAPTER 8**

### **CONCLUSIONS AND RECOMMENDATIONS**

#### **8.1 General**

In the preceding chapters, an iterative finite element procedure was presented to study the evolution of micro-mechanical damage in a poroelastic medium susceptible to damage. The computational procedure developed has also been used to examine problems of interest in geomechanics and to examine the influence of the damage-induced alterations in poroelastic parameters on the time-dependent response of a damage-susceptible poroelastic medium. In this final Chapter, we shall summarize the main achievements of this research and suggest recommendations for future work.

#### **8.2 Summary and Concluding Remarks**

Fluid-saturated poroelastic materials such as soft rocks and heavily over consolidated saturated clays can exhibit non-linear responses, which could result from the development of micro-mechanical damage in porous fabric. The damage-susceptible poroelastic material can experience such non-linear responses even at stress levels well below the peak. The development of micro-defects can alter both the deformability and the hydraulic conductivity characteristics of porous media and consequently can influence the time-dependent behaviour of damage-susceptible poroelastic materials. One of the objectives of the research is to examine the influence of the evolution of damage in porous skeleton on the time-dependent behaviour of a damage-susceptible poroelastic medium. The classical theory of poroelasticity developed by Biot (1941) has been

extended to examine the influence of the damage-induced alterations in both elasticity and hydraulic conductivity characteristics of poroelastic materials. An iterative finite element procedure has been developed to account for the evolution of damage-induced alterations in poroelastic properties. The evolution of damage in the brittle poroelastic media can exhibit dependency on the state of stress. The consolidation behaviour of a poroelastic medium is influenced by the state of stresses within the medium. One of the objectives of the research is also to extend the computational procedures to account for the stress state-dependency on the evolution of damage in damage-susceptible poroelastic media.

The review of the literature on computational modelling of poroelastic media indicates that the computational modelling of damage-susceptible brittle poroelastic media that accounts for the stress state-dependent damage-evolution in both elasticity and hydraulic conductivity characteristics received limited attention. The research has developed procedures to examine these phenomena applicable to three-dimensional problems. In order to achieve the objectives of the research, the following steps of the research program have been completed.

1. A finite element procedure has been developed, which is applicable to the study of problems related to the theory of poroelasticity with three-dimensional geometries. In this step, the poroelastic medium is modelled as a deformable elastic porous fabric filled with an incompressible fluid. A twenty-node isoparametric element is used to model the intact geomaterial. The polynomial shape functions that correspond to the variation of the pore pressure field are one order lower than those that correspond to the displacement fields. This results in the minimized spatial oscillations in pore pressure obtained by the computational modelling. The computational scheme is also verified by appeal to available analytical solutions in the literature for the consolidation of poroelastic media, including the classical solution for the consolidation in one-dimension developed by Terzaghi (1923), and the consolidation of a poroelastic sphere developed by Cryer (1963).

2. The computational modelling of classical theory of poroelasticity is extended to examine the behaviour of the damage-susceptible poroelastic media. The iterative finite element procedure accounts for the damage-induced alterations in both elasticity and hydraulic conductivity characteristics of the poroelastic media. Furthermore, the stress state-dependency of the evolution of damage in the brittle poroelastic media is taken into account. In order to model the evolution of damage in damage-susceptible poroelastic materials, the concept of *Continuum Damage Mechanics* is incorporated into the classical theory of poroelasticity to model the porous skeletal behaviour. The main features of the iterative finite element procedure developed in connection with this research for the study of damage-susceptible media can be summarized as follows:

- The elasticity and hydraulic conductivity characteristics of the porous medium are represented as functions of the state of isotropic damage in the brittle geomaterial. The deterioration in elastic stiffness as a reduction in the linear elastic modulus is governed by the isotropic damage evolution function for soft rocks proposed by Cheng and Dusseault (1993). This damage evolution function is characterized by the dependency of the damage parameter on the distortional strain invariant. The alterations in hydraulic conductivity of the brittle porous fabric are governed by a damage evolution function, postulated based on the available experimental observations conducted on brittle saturated sandstone by (Shiping *et al.*, 1994).
- At each time increment, the elasticity and hydraulic conductivity characteristics are updated at each integration point within an element composing the discretized domain. The coupling between the state of strains and the state of damage at each time step is achieved by an iterative approach in a time-dependent analysis. The standard Newton-Raphson technique is used in the iterative algorithm. The adopted convergence criterion is based on the norm of the evolution of damage variable, related to a specified tolerance. The initial state of damage either uniform or non-uniform can also be prescribed in the computational modelling.
- The dependency of the evolution of damage on the stress state is modelled by considering the state of volumetric strain in an element of the fluid saturated

geomaterial. Experimental observations by Schulze *et al.* (2001) show no significant damage evolution when the state of stresses applied to an element of a brittle geomaterial results in volume reduction of the porous skeleton. The iterative finite element procedure has been extended to include the stress state-dependency on the damage evolution. In the modelling, the possibility of the evolution of damage is characterized as the state of stresses that results in expansion in the brittle geomaterials. In order to model stress state-dependent damage, the volumetric strain is determined for each element and damage within can be initiated only when, the volumetric strain is positive. It should be mentioned that convention sign rule is implemented in the computational scheme developed in this research.

3. The computational scheme is used to examine a number of problems of interest to geomechanics. The problems follow as; (i) the fluid pressure development and decay within a spheroidal fluid inclusion surrounded by a damage-susceptible fluid saturated geomaterial; (ii) the time-dependent translational displacement at the head of a rock socket embedded in a damage-susceptible fluid-saturated soft rock and (iii) the time-dependent in-plane displacement of a flat rigid anchorage located in a damage-susceptible fluid saturated geomaterial. Due to the coupled nature of the poroelasticity problem, the effects of damage evolution, and the influence of complex geometries associated with these problems, solutions can be obtained only through computational procedure. The computational results presented in the thesis to examine the influence of evolution of damage on the time-dependent behaviour of the above problems are considered to be original and relevant to geomechanics. The problems are modelled according to four categories (i) ideal poroelasticity with no damage evolution, (ii) damage evolution with only alteration in elasticity properties and no change in the hydraulic conductivity properties during the damage process, (iii) stress state-independent evolution of damage with alterations in both elasticity and hydraulic conductivity properties and (iv) stress state-dependent evolution of damage with alterations in both elasticity and hydraulic conductivity properties. The main features of the computational



modelling of the problems discussed in this thesis and related computational results can be summarized as;

- The problem of a spheroidal fluid inclusion located in a damage-susceptible geomaterial and subjected to a far field triaxial stress state (in the form of a Heaviside step function of time) has been examined through the computational procedure developed. The fluid pressure development and decay is influenced by the damage-induced alterations in poroelastic parameters. The influence of damage evolution on the time-dependent behaviour of a damage-susceptible saturated geomaterials results mainly from the alterations in the hydraulic conductivity characteristics. This influence is greater when the spheroidal fluid inclusion is elongated or the spheroidal fluid inclusion is subjected to a triaxial far field stress state with the radial stress larger than the axial stress. Furthermore, the influence of damage-induced alterations in poroelastic properties on fluid pressure development and decay within the spheroidal fluid inclusion is greater when damage evolution is stress state-independent. For stress state-dependent evolution of damage, the development of the compaction zones results in no evolution of damage within damage-susceptible geomaterial.
- The time-dependent displacement of a rigid rock socket embedded in a damage-susceptible saturated geomaterial and subjected to a lateral load (in the form of a Heaviside step function of time) has been examined for a range of aspect ratios  $L/d$ . The consolidation of the medium is enhanced for rock sockets when the damage-induced alterations in poroelastic parameters are taken into account. The evolution of damage on the time-dependent behaviour of a rock socket is also influenced by the length to diameter ratio ( $L/d$ ) for the rigid rock socket. The damage evolution has a greater influence on the time-dependent translational displacement of a rigid rock socket with a larger ratio of ( $L/d$ ). Furthermore, the stress state-dependency of the damage evolution can enhance the time-dependent translational displacement of the rigid rock socket.

- The time-dependent displacement of a flat rigid anchorage located in a damage-susceptible geomaterial subjected to an in-plane load (in the form of a Heaviside step function of time) has been examined for a range of elliptical anchorage shapes using computational schemes developed. The time-dependent in-plane displacement of the flat rigid anchorage is influenced by the damage-induced alterations in the poroelasticity parameters. This influence varies with the different geometries of anchors. The circular disc anchor exhibits the least alterations in the time-dependent response due to the evolution of damage. The difference between the ideal poroelastic geomaterials and the damage susceptible geomaterial is increased for the elliptical anchorages as a result of stress concentration that can occur at the tip of the anchorage. The damage-induced alteration in poroelastic parameters has a greater influence on the time-dependent response of the elliptical anchorage with a greater ratio of dimensions. The influence of damage evolution on the time-dependent behaviour of damage-susceptible saturated geomaterials is again attributed mainly to the alterations in the hydraulic conductivity characteristics. Furthermore, the stress state-dependency of evolution of damage and stress levels can influence the time-dependent response of a flat rigid anchorage.

### **8.3 Recommendations for Future Work**

In the preceding sections, the main achievements of this research have been summarized. The research has extended the classical theory of poroelasticity for damage-susceptible geomaterials through an iterative finite element procedure to account for the evolution of damage with alterations in both elasticity and hydraulic conductivity characteristics. The computational scheme is verified by comparison with the analytical solutions available in the literature for problems in the classical theory of poroelasticity. The computational scheme has been successfully applied to the problems of interest in geomechanics, applied mechanics and civil engineering. In the ensuing, possible extensions to the research are suggested.

- As discussed previously in the literature review of this research, there is only a limited number of experimental observations dealing with the damage-induced evolution of hydraulic conductivity in geomaterials. Furthermore, in most of the available observations, the stress state-dependency of the evolution of damage has not been addressed due to the fact that the experimentation involved uniaxial testing of samples of geomaterial. The research can be extended to the experimental evaluation of the damage-induced alterations in hydraulic conductivity of geomaterials where the stress state can be of a general triaxial state. Results derived from such experimentation can be used to develop better representations of the damage-induced evolution of, notably the hydraulic parameters.
- The damage-induced alterations in hydraulic conductivity characteristics of geomaterials, investigated in this research is in the form of an increase in hydraulic conductivity due to the evolution of micro-mechanical damage at the stress levels well below peak damage levels. The computational scheme can be extended to account for any arbitrary damage-induced alteration in the hydraulic conductivity characteristics of geomaterials, including a decrease in hydraulic conductivity characteristics due to the void collapse at high confining stress states associated with geomaterials.
- The scope of the research can also be extended to include anisotropic damage models, which can be used to model directional dependency in the damage phenomena in porous media. The damage evolution criteria governing alterations in both the deformability and hydraulic conductivity characteristics of damage-susceptible porous media should then be formulated in generalized tensorial form.

## References

- Aboustit B.L., S.H. Advani and J.K. Lee, 1985, Variational principles and finite element simulations for thermo-elastic consolidation, *Int. J. Numer. Anal. Meth. Geomech.*, **9**, 49-69.
- Adams J.I. and T.W. Klym, 1972, A study of anchorages for transmission tower foundations, *Can. Geotech. J.*, **9**, 89-104.
- Agbezuge L.K. and H. Deresiewicz, 1975, The consolidation settlement of a circular footing, *Israel J. Tech.*, **13**, 264-269.
- Altay G.A. and M.C. Dokmeci, 1998, A uniqueness theorem in Biot's poroelasticity theory, *J. Appl. Math. Phys. (ZAMP)*, **49**, 838-847.
- Apirathvorakij V. and P. Karasudhi, 1980, Quasi static bending of a cylindrical elastic bar partially embedded in a saturated elastic half space, *Int. J. Solids Struct.*, **16**, 625-644.
- Atkinson C. and R.V. Craster, 1991, Plane strain fracture in poroelastic media, *Proc. Royal Soc., Series A*, **434**, 605-633.
- Aubertin M., L. Li and R. Simon, 2000, A multiaxial stress criterion for short- and long-term strength of isotropic rock media, *Int. J. Rock Mech. Min. Sci.*, **37**, 1169-1193.
- Balla A., 1961, The resistance to breaking out of mushroom foundations for pylons, *Proc. 5<sup>th</sup> Int. Conf. Soil Mech. Fdn. Eng.*, Paris, 569-576.
- Banerjee P.K. and R. Butterfield, 1981, Transient flow through porous elastic media, *Developments in Boundary Element Methods-2*, (P.K. Banerjee and R.P. Shaw, Eds.), Applied Science Publishers, England, Chapter 2.
- Bart M., J.F. Shao and D. Lydzba, 2000, Poroelastic behaviour of saturated brittle rock with anisotropic damage, *Int. J. Numer. Anal. Meth. Geomech.*, **24**, 1139-1154.
- Bary B., J.-P. Bournazel and E. Bourdarot, 2000, Poro-damage approach to hydrofracture analysis of concrete, *J. Engng. Mech.*, ASCE, **126**, 937-943.
- Bathe K.-J., 1996, *Finite Element Procedures*, Englewood Cliffs, Prentice Hall, N.J.
- Bazant Z.P., 1986, Mechanics of distributed cracking, *Appl. Mech. Rev.*, **39**, 675-705.

- Bazant Z.P., 1991, *Stability of Structures: Elastic, Inelastic, Fracture and Damage Theories*, Oxford University Press, New York.
- Bettess P. and O.C. Zienkiewicz, 1977, Diffraction and refraction of surface waves using finite and infinite elements, *Int. J. Numer. Meth. Engng.*, **11**, 1271-1290.
- Bieniawski Z.T., H.G. Denkhaus and U.W. Vogler, 1967, Failure of fractured rock, *Int. J. Rock Mech. Min. Sci. Geomech. Abstr.*, **6**, 323-346.
- Biot M.A., 1941, General theory of three-dimensional consolidation, *J. Appl. Phys.*, **12**, 155-164.
- Biot M.A., 1955, Theory of elasticity and consolidation for a porous anisotropic solid, *J. Appl. Phys.*, **26**, 182-185.
- Biot M.A., 1956, General solution of the equation of elasticity and consolidation for a porous material, *J. Appl. Mech.*, ASME, **23**, 91-95.
- Biot M.A. and D.G. Willis, 1957, The elastic coefficient of the theory of consolidation, *J. Appl. Mech.*, **24**, 594-601.
- Bjerrum L. and N. Flodin, 1960, The development of soil mechanics in Sweden, 1900-1925, *Géotechnique*, **10**, 1-18.
- Bjerrum L., Hansen and Sevaldson, 1958, Geotechnical investigations for a quay structure in Horton, *Nor. Geotech. Publ.*, **28**, p. 12.
- Booker J.R. and C. Savvidou, 1984, Consolidation around a point heat source, *Int. J. Numer. Anal. Meth. Geomech.*, **9**, 173-184.
- Booker J.R. and J.C. Small, 1975, An investigation of the stability of numerical solution of Biot's equations of consolidation, *Int. J. Solids. Struct.*, **11**, 907-917.
- Booker J.R. and J.C. Small, 1984, The time-deflection behaviour of a circular raft of finite flexibility on a deep clay layer, *Int. J. Numer. Anal. Meth. Geomech.*, **8**, 343-357.
- Booker J.R. and J.C. Small, 1986, The behaviour of an impermeable flexible raft on a deep layer of consolidating soil, *Int. J. Numer. Anal. Meth. Geomech.*, **10**, 311-327.
- Brace W.F., J.B. Walsh and W.T. Frangos, 1978, Permeability of granite under high pressure, *J. Geophys. Res.*, **73**, 2225-2236.
- Brebbia C.A., J.C.F. Telles and L.C. Wrobel, 1984, *Boundary Element Techniques*, Springer-Verlag, Berlin.

- Broms B.B., 1965, Design of laterally loaded piles, *Proc. ASCE*, 79-99.
- Brownell Jr D.H., S.K. Grag and J.W. Pritchett, 1977, Governing equations for geothermal reservoir, *Water Res. Res.*, **13**, 929-934.
- Budiansky B. and R.J. O'Connell, 1976, Elastic moduli of a cracked solid, *Int. J. Solids Struct.*, **12**, 81-97.
- Byrd P.F. and M.D. Friedman, 1971, *Handbook of Elliptic Integrals*, Springer-Verlag, Berlin.
- Cernuschi F., S. Ahmaniemi, P. Vuoristo and T. Mantyla, 2004, Modelling of thermal conductivity of porous materials: application to thick thermal barrier coatings, *J. Euro. Ceramic Soc.*, **24**, 2657-2667.
- Cheng A.H.-D., E. Detournay and Y. Abousleiman (Eds.), 1998, Poroelasticity. Maurice A. Biot Memorial Issue, *Int. J. Solids Struct.*, **35**, 4513-5031.
- Cheng A.H.-D. and J.A. Ligget, 1984a, Boundary integral equation method for linear porous elasticity with applications to soil consolidation, *Int. J. Numer. Meth. Engng.*, **20**, 255-278.
- Cheng A.H.-D. and J.A. Ligget, 1984b, Boundary integral equation method for linear porous elasticity with applications to fracture propagation, *Int. J. Numer. Meth. Engng.*, **20**, 279-296.
- Cheng H., 1987, *Study of Complete Force-displacement Curves for Red Sandstone Subjected to Various End-boundary Conditions under Uniaxial Compression*, J.S.W. Jiaotong Univ., **3**, 100-107. (in Chinese)
- Cheng H. and M.B. Dusseault, 1993, Deformation and diffusion behaviour in a solid experiencing damage: A continuous damage model and its numerical implementation, *Int. J. Rock Mech. Min. Sci. and Geomech. Abstr.*, **30**, 1323-1331.
- Chiarella C. and J.R. Booker, 1975, The time-settlement behaviour of a rigid die resting on a deep clay layer, *Quart. J. Mech. Appl. Math.*, **28**, 317-328.
- Chopra M.B. and G.F. Dargush, 1995, Boundary Element Analysis of stresses in an axisymmetric soil mass undergoing consolidation, *Int. J. Numer. Anal. Meth. Geomech.*, **19**, 195-218.
- Chow C.H. and J. Wang, 1987, An anisotropic theory of elasticity for continuum damage mechanics, *Int. J. Fracture*, **33**, 3-16.
- Christian J.T. and J.W. Boehmer, 1970, Plane strain consolidation by finite elements, *J. Soil Mech. Found. Div., ASCE*, **SM 4**, 1435-1457.

- Cleary M.P., 1977, Fundamental solutions for a fluid-saturated porous solid, *Int. J. Solids. Struct.*, **13**, 785-806.
- Collins W.D., 1962, Some axially symmetric stress distributions in elastic solids containing penny-shaped cracks I., Cracks in an infinite solid and a thick plate, *Proc. Royal. Soc. A*, **203**, 359-386.
- Cook N.G.W., 1965, Fracture of rock, *Int. J. Rock Mech. Min. Sci. Geomech. Abstr.*, **2**, 389-403.
- Coste F, A. Bounenni, S. Chanchole and K. Su (2002) A method for measuring mechanical, hydraulic and hydromechanical properties during damaging in materials with low permeability, *Hydromechanical and Thermohydromechanical Behaviour of Deep Argillaceous Rock*, (N. Hoteit, K. Su, M. Tijani and J.-F. Shao (Eds.)), A.A. Balkema, The Netherlands, 109-116.
- Coussy O., 1995, *Mechanics of Porous Media*, John Wiley, New York.
- Cowin S.C., 2001, *Bone Mechanics Handbook*, CRC Press.
- Cryer C.W., 1963, A comparison of the three dimensional consolidation theories of Biot and Terzaghi, *Quart. J. Mech. Appl. Math.*, **16**, 401-412.
- Cui L., A.H.-D. Cheng and V.N. Kaliakin, 1996, Finite element analyses of anisotropic poroelasticity: A generalized Mandel's problem and an inclined borehole problem, *Int. J. Numer. Anal. Meth. Geomech.*, **20**, 381-401.
- Cui L., V.N. Kaliakin, Y. Abousleiman and A.H.-D. Cheng, 1997, Finite element formulation and application of poroelastic generalized plane strain problems, *Int. J. Rock. Mech. Min. Sci.*, **34**, 953-962.
- Darcy H., 1856, *Les fontaines publiques de Dijon*, Victor Dalmont, Paris.
- Dargush G.F. and P.K. Banerjee, 1991, A boundary element method for axisymmetric soil consolidation, *Int. J. Solids. Struc.*, **28**, 897-915.
- Davie J.R. and H.B. Sutherland, 1977, Uplift resistance of cohesive soils, *J. Geotech. Engng. , ASCE*, **103**, 935-952.
- Davis R.O. and A.P.S. Selvadurai, 1996, *Elasticity and Geomechanics*, Cambridge University Press, Cambridge, England.
- Davis R.O. and A.P.S. Selvadurai, 2002, *Plasticity and Geomechanics*, Cambridge University Press, Cambridge, England.

- de Boer R. (Ed.), 1999, *Porous Media: Theory and Experiments*, Kluwer Academic Publications, Dordrecht, The Netherlands.
- de Boer R., 2000, *Theory of Porous Media*, Springer Verlag, Berlin, Germany.
- de Boer R. and W. Ehlers, 1990, Uplift, friction and capillarity: three fundamental effects for liquid-saturated porous solids, *Int. J. Solids. Struct.*, **26**, 43-51.
- de Josselin de Jong G., 1953, Consolidation around pore pressure meters, *J. Appl. Phys.*, **24**, 922-928.
- de Josselin de Jong G., A. Verruijt, 1965, Primary and secondary consolidation of a spherical clay sample, *Proc. the Sixth Int. Con. Soil Mech. Fdn. Engng.*, **1**, 254-258.
- Deresiewicz H., 1977, On the indentation of a consolidating half-space, II. Effect of Poisson's ratio, *Israel J. Tech.*, **15**, 89-97.
- Desai C.S. and J.T. Christian (Eds.), 1977, *Numerical Methods in Geotechnical Engineering*, John Wiley & Sons, N.Y.
- Desai C.S. and H.J. Siriwardane, 1984, *Constitutive Laws for Engineering Materials with Emphasis on Geologic Materials*, Prentice-Hall Inc., Englewood Cliffs, N.J.
- Detournay E. and A.H.-D. Cheng, 1991, Plane strain analysis of a stationary hydraulic fracture in a poroelastic medium, *Int. J. Solids. Struct.*, **27**, 1645-1662.
- Detournay E. and A.H.-D. Cheng, 1993, Fundamentals of poroelasticity, *Comprehensive Rock Engineering*, Pergamon Press, **II**, 113-171.
- de Wiest R.M.J. (Ed.), 1969, *Flow Through Porous Media*, Academic Press, New York.
- Dominguez J., 1992, Boundary element approach for dynamics poroelastic problems, *Int. J. Numer. Meth. Engng.*, **35**, 307-324.
- Donald I.B., S.W. Sloan and H.K. Chiu, Theoretical analyses of rock socketed piles, *Proc. Int. Conf. On Struct. Founds. On Rock*, **1**, 303-316.
- Douglas D.J. and A.F. Williams, 1993, Large piles in weak rock West Gate Freeway project, *Comprehensive Rock Engineering*, (Edited by J. A. Hudson), **5**, 727-757.
- Eskandari H. and J. Nemes, 1999, An isotropic damage model based on a tensorial representation of damage, *Int. J. Damage Mech.*, **8**, 254-272.



- Farhat C. and N. Sobh, 1990, A consistency analysis of a class of concurrent transient implicit/explicit algorithms, *Comput. Meth. Appl. Mech. Engng.*, **84**, 147-162.
- Fillunger P., 1913, Der auftrieb in talsperren, *Osterr. Wochenschrift fur den Offentl. Baudienst*, **19**, 532, 556, 567-570.
- Fourier J., 1822, *Théorie Analytique de la Chaleur*, Chez Firmin Didot, Pere et Fils, Paris, France.
- Fung Y.C., 1965, *Foundations of Solid Mechanics*, Prentice Hall, Englewood Cliffs, N.J.
- Galerkin B.G., 1915, Series solution of some problems of elastic equilibrium of rods and plates, *Vestn. Inzh. Tech.*, **19**, 897-908. (in Russian)
- Gangi A.F., 1978, 'Variation of whole and fractured porous rock permeability with confining pressure', *Int. J. Rock Mech. Min. Sci. Geomech. Abstr.*, **15**, 249-257.
- Gaszynski J. and G. Szefer, 1978, Axisymmetric problem of the indenter for the consolidating semi-space with mixed boundary conditions, *Arch. Mech. Stos.*, **30**, 17-26.
- Gatelier N., F. Pellet and B. Loret, 2002, Mechanical damage of an anisotropic porous rock in cyclic triaxial tests, *Int. J. Rock Mech. Min. Sci.*, **39**, 335-354.
- Gawin D., F. Pesavento and B.A. Schrefler, 2002, Simulation of damage-permeability coupling in hydro-thermo-mechanical analysis of concrete at high temperature, *Commun. Numer. Meth. Engng.*, **18**, 113-119.
- Ghaboussi J. and E.L. Wilson, 1973, Flow of compressible fluid in porous elastic media, *Int. J. Numer. Meth. Engng.*, **5**, 419-442.
- Gibson R.E., A. Gobert and R.L. Schiffman, 1989, On Cryer's problem with large displacements, *Int. J. Numer. Anal. Meth. Geomech.*, **13**, 251-262.
- Gibson R.E., K. Knight and P.W. Taylor, 1963, A critical experiment to examine theories of three dimensional consolidation, *Proc. Euro. Con. Soil Mech. Fdn. Engng.*, Wiesbaden, **1**, 69-76.
- Gibson R.E., R.L. Schiffman and S.L. Pu, 1970, Plane strain and axially symmetric consolidation of a clay layer on a smooth impervious base, *Quart. J. Mech. Appl. Math.*, **23**, 505-520.
- Giraud A. and G. Rousset, 1996, Time-dependent behaviour of deep clays, *Engng. Geol.*, **41**, 181-195.

- Girault P., 1969, Discussion on anchorages especially in soft ground, *Proc. Seventh Int. Con. Soil Mech. Fdn. Engng*, Mexico City, 214-215.
- Gladwell G.M.L., 1999, On inclusions at a bi-material elastic interface, *J. Elasticity*, **54**, 27-41.
- Glos G.H. and O.H. Briggs, 1983, Rock sockets in soft rock, *J. Geotech. Engng. , ASCE*, **109**, 525-535.
- Griffith A.A., 1921, The phenomena of rupture and flaw in solids, *Phil. Trans. Roy. Soc.*, **A221**, 163-198.
- Gurtin M., 1964, Variational principles for linear elastodynamics, *Arch. Rat. Mech. Anal.* , **16**, 34-50.
- Hanna T.H., 1972, Studies on anchors and anchor-supported retaining walls in sand. In stress-strain behaviour of soils, *Proc. Roscoe Mem. Symp*, Cambridge, 450-458
- Hanna T.H., 1982, *Foundations in Tension*, Clausthal-Zellerfeld, Federal Republic of Germany: Trans. Tech. Pub., McGraw Hill, N.Y.
- Harr M.E., 1966, *Foundations of Theoretical Soil Mechanics*, McGraw Hill, N.Y.
- Hunsche U. and A. Hampel, 1999, Rock salt-the mechanical properties of the host rock material for a radioactive waste repository, *Engng. Geol.*, **52**, 271-291.
- Jana R.N., 1963, Deformation in an infinite poroelastic medium with a long circular cylindrical hole, *Quart. J. Mech. Appl. Math.*, **16**, 137-148.
- Ju J.W., 1990, Isotropic and anisotropic damage variables in continuum damage mechanics, *J of Engng. Mech.*, ASCE, **116**(12), 2764-2769.
- Kachanov L.M., 1958, Time of rupture process under creep conditions, *Isv. Akad. Nauk SSR Otd. Tekh.*, **8**, 26-31.
- Kanji M., Y. Abousleiman and R. Ghanem, 2003, Poromechanics of anisotropic hollow cylinders, *J. Engng. Mech.*, ASCE, **129**, 1277-1287.
- Kanwal R.P. and D.L. Sharma, 1976, Singularity methods for elastostatics, *J. Elasticity*, **6**, 405-418.
- Kassir M.K. and G.C. Sih, 1968, Some three-dimensional inclusions problems in elasticity theory, *Int. J. Solids. Struct.*, **4**, 225-241.

- Kassir M.K. and J. Xu, 1988, Interaction functions of a rigid strip bonded to saturated elastic half-space, *Int. J. Solids Struct.*, **24**, 915-936.
- Keer L.M., 1965, A note on the solution of two asymmetric boundary value problems, *Int. J. Solids. Struct.*, **1**, 257-264.
- Khalili N. and A.P.S. Selvadurai, 2003, A fully coupled constitutive model for thermo-hydro-mechanical analysis in elastic media with double porosity, *Geophys. Res. Lett.*, **30**, 2268, doi: 10.1029/2003GL018838.
- Kiyama T., H. Kita, Y. Ishijima, T. Yanagidani, K. Akoi and T. Sato, 1996, Permeability in anisotropic granite under hydrostatic compression and tri-axial compression including post-failure region, *Proc. 2<sup>nd</sup> North Amer. Rock Mech. Symp.*, 1643-1650.
- Krajcinovic D., 1984, Continuum damage mechanics, *Appl. Mech. Rev.*, **37**, 1-6.
- Krajcinovic D., 1996, *Damage Mechanics*, North-Holland, Amsterdam, The Netherlands.
- Krajcinovic D. and G.U. Fonseka, 1981, The continuous damage theory of brittle materials, *J. Appl. Mech.*, **48**, 809-815.
- Ladanyi B. and G.H. Johnston, 1974, Behaviour of circular footing and plate anchors embedded in permafrost, *Can. Geotech. J.*, **11**, 531-553.
- Lambe T.W. and R.V. Whitman, 1969, *Soil Mechanics*, John Wiley & Sons, N.Y.
- Lan Q. and A.P.S. Selvadurai, 1996, Interacting indentors on a poroelastic half-space, *J. Appl. Math. Phys.*, **47**, 695-716.
- Lee H.-J., J.S. Daniel and Y.R. Kim, 2000, Continuum damage mechanics-based fatigue model of asphalt concrete, *J. Mater. Civil. Engng., ASCE*, **12**, 105-112.
- Lemaitre J., 1984, How to use damage mechanics, *Nucl. Engng. Des.*, **80**, 233-245.
- Lemaitre J. and J.L. Chaboche, 1990, *Mechanics of Solid Materials*, Cambridge University Press, Cambridge, England.
- Leong E.C. and M.F. Randolph, 1994, Finite element modelling of rock-socketed piles, *Int. J. Numer. Anal. Meth. Geomech.*, **18**, 25-47.
- Lewis R.W. and B.A. Schrefler, 1998, *The Finite Element Method in the Static and Dynamic Deformation and Consolidation of Porous Media*, John Wiley, New York.

- Li X., 2003, Consolidation around a borehole embedded in media with double porosity under release of geostatic stresses, *Mech. Res. Commun.*, **30**, 95-100.
- Luk V.K. and M. Keer, 1979, Stress analysis for an elastic half-space containing an axially loaded rigid cylindrical rod, *Int. J. Solids. Struct.*, **15**, 805-827.
- Mahyari A.T., 1997, *Computational Modelling of Fracture and Damage in Poroelastic Media*, Ph.D. Thesis, McGill University.
- Mahyari A.T. and A.P.S. Selvadurai, 1998, Enhanced consolidation in brittle geomaterials susceptible to damage, *Mech. Cohes.-Fric. Mater.*, **3**, 291-303.
- Mandel J., 1950, Etude mathématique de la consolidation des sols, actes du colloque international de mécanique, Poitier, France, **4**, 9-19.
- Mandel J., 1953, Consolidation des sols (étude mathématique), *Geotechnique*, **3**, 287-299.
- Mazars J., 1982, Mechanical damage and fracture of concrete structures, *Adv. Fract. Res.*, **4**, Pergamon Press, Oxford, 1499-1506.
- Mazars J. and Z.P. Bazant (Eds.), 1989, *Cracking and Damage. Strain Localization and Size Effect*, Elsevier Appl. Sci., N.Y.
- Mazars J. and G. Pijaudier-Cabot, 1989a, Continuum damage theory-applications to concrete, *J. Engng. Mech. Div.*, ASCE, **115**, 345-365.
- Mazars J. and G. Pijaudier-Cabot, 1989b, Damage fracture and size effect in concrete, *Geomaterials: Constitutive Equations and Modelling*, (F. Darve, Ed.), Elsevier Applied Science, London.
- McNamee J. and R.E. Gibson, 1960a, Displacement functions and linear transforms applied to diffusion through porous elastic media, *Quart. J. Mech. Appl. Math.*, **13**, 98-111.
- McNamee J. and R.E. Gibson, 1960b, Plane strain and axially symmetric problems of the consolidation of a semi-infinite clay stratum, *Quart. J. Mech. Appl. Math.*, **13**, 210-227.
- McTigue D.E., 1986, Thermoelastic response of fluid saturated porous rock, *J. Geophys. Res.*, **91**, 9533-9542.
- Meyerhof G.G. and J.I. Adams, 1968, The ultimate uplift capacity of foundations, *Can. Geotech. J.*, **5**, 225-244.
- Mindlin R.D., 1936, Force at a point in the interior of a semi-infinite solid, *Physics*, **7**, 195-202.

- Muki R. and E. Sternberg, 1969, On the diffusion of an axial load from an infinite cylindrical bar embedded in an elastic medium, *Int. J. Solids. Struct.*, **5**, 587-605.
- Nemes J.A. and E. Speciel, 1996, Use of a rate-dependent continuum damage model to describe strain-softening in laminated composites, *Comput. Struct.*, **58**, 1083-1092.
- Nguyen T.S., 1995, *Computational Modelling of Thermal-Hydrological-Mechanical Processes in Geological Media*, Ph.D. Thesis, McGill University.
- Noorishad J., C.F. Tsang and P.A. Witherspoon, 1984, Coupled thermal-hydraulic-mechanical phenomena in saturated fractured porous rock: numerical approach, *J. Geophys. Res.*, **89**, 365-373.
- Pao W.K.S., R.W. Lewis and I. Masters, 2001, A fully coupled hydro-thermo-poro-mechanical model for black oil reservoir simulation, *Int. J. Numer. Anal. Meth. Geomech.*, **25**, 1229-1256.
- Parkin A.K. and L.B. Donald, 1975, Investigations for rock socketed piles in Melbourne mudstone, *Proc. 2<sup>nd</sup> Australia-New Zealand Conf. Geomech.*, Institute of Engineers, Brisbane, Australia.
- Patsouls G. and J.C. Gripps, 1982, An investigation of the permeability of Yorkshire Chalk under differing pore water and confining pressure conditions, *Energy Sources*, **6**, 321-334.
- Pells P.J.N. and R.M. Turner, 1979, Elastic solutions for the design and analysis of rock-socketed piles, *Can. Geotech. J.*, **16**, 481-487.
- Planas J. and M. Elices, 2003, Modeling Cracking and Damage of Concrete during Cooling to Very Low Temperatures, *Key Engng. Mater.*, **251-252**, 437-446.
- Poulos H.G. and E.H. Davis, 1968, The settlement behaviour of single axially loaded incompressible piles and piers *Geotechnique*, **18**, 351-371.
- Poulos H.G. and E.H. Davis, 1980, *Pile Foundation Analysis and Design*, John Wiley and Sons, NY.
- Rajapakse R.K.N.D. and T. Senjuntichai, 1995, An indirect boundary integral equation method for poroelasticity, *Int. J. Numer. Anal. Meth. Geomech.*, **19**, 587-614.
- Randolph M.F. and C.P. Wroth, 1979, An analytical solution for the consolidation around a driven pile, *Int. J. Numer. Anal. Meth. Geomech.*, **3**, 217-229.

- Reese L.C. and H.S. Matlock, 1956, Non-dimensional solutions for laterally loaded piles with soil modulus proportional to depth, *Proc. 8<sup>th</sup> Texas Conf. On Soil Mech. and Fdn. Engng.*, 1-41.
- Rendulic L., 1936, Porenziffer und Poren Wasserdruk in Tonen, *Bauingenieur*, **17**, 559-564.
- Rice J.R. and M.P. Cleary, 1976, Some basic stress diffusion solutions for fluid-saturated elastic porous media with compressible constituents, *Rev. Geophys. Space Phys.*, **14**, 227-241.
- Rice J.R., W. Rudnicki and D.A. Simons, 1978, Deformation of spherical cavities and inclusions in fluid-infiltrated elastic materials, *Int. J. Solids. Struct.*, **14**, 289-303.
- Rowe R.K. and H.H. Armitage, 1987, Theoretical solutions for axial deformation of drilled shafts in rock, *Can. Geotech. J.*, **24**, 114-125.
- Rowe R.K. and E.H. Davis, 1982a, The behaviour of anchor plates in clay, *Géotechnique*, **32**, 9-23.
- Rowe R.K. and E.H. Davis, 1982b, The behaviour of anchor plates in sand, *Géotechnique*, **32**, 25-41.
- Rowe R.K. and P.J.N. Pells, 1980, A theoretical study of pile-rock socket behaviour, *Proc. Int. Conf. On Struct. Founds. On Rock*, **1**, 253-264.
- Samaha H.R. and K.C. Hover, 1992, Influence of micro-cracking on the mass transport properties of concrete, *ACI Mat. J.*, **89**, 416-424.
- Sandhu R.S., H. Liu and K.J. Singh, 1977, Numerical performance of some finite element schemes for analysis of seepage in porous elastic media, *Int. J. Rock Mech. Min. Sci. Geomech. Abstr.*, **1**, 177-194.
- Sandhu R.S. and E.L. Wilson, 1969, Finite element analysis of flow in saturated porous media, *J. Engng. Mech. Div.*, ASCE, **95(EM3)**, 641-652.
- Schiffman, R.L., 1984, *Fundamentals of Transport Phenomena in Porous Media*, (J. Bear and M.Y. Corapcioglu, Eds.), 619-669.
- Schiffman R.L., A.T-F Chen and J.C. Jordan, 1969, An analysis of consolidation theories, *J. Soil Mech. and Found. Div.*, ASCE, **95(SM1)**, 285-312.
- Schiffman R.L. and A.A. Fungaroli, 1965, Consolidation due to tangential loads, *Proc. of the Sixth Int. Con. on Soil Fdn. Engng.*, Montreal, Canada, **1**, 188-192.

- Schrefler B.A. and L. Simoni, 1987, Non-isothermal consolidation of unbounded porous media using mapped infinite elements, *Comm. Appl. Numer. Meth.*, **3**, 445-452.
- Schulze O., T. Popp and H. Kern, 2001, Development of damage and permeability in deforming rock salt, *Engng. Geol.*, **61**, 163-180.
- Selvadurai A.P.S., 1976, The load-deflexion characteristics of a deep rigid anchor in an elastic medium, *Géotechnique*, **26**, 603-612.
- Selvadurai A.P.S., 1978, The response of a deep rigid anchor due to undrained elastic deformation of the surrounding soil medium, *Int. J. Numer. Anal. Meth. Geomech.*, **2**, 189-197.
- Selvadurai A.P.S., 1979 a, *Elastic Analysis of Soil-Foundation Interaction*, Elsevier Pub., Amsterdam, The Netherlands.
- Selvadurai A.P.S., 1979 b, The elastic displacements of a rigid disc inclusion embedded in an isotropic elastic medium due to the action of an external force, *Mech. Res. Commun.*, **6**, 379-385.
- Selvadurai A.P.S., 1980a, The eccentric loading of a rigid circular foundation embedded in an isotropic elastic medium, *Int. J. Numer. Anal. Meth. Geomech.*, **4**, 121-129.
- Selvadurai A.P.S., 1980b, Asymmetric displacement of a rigid disc inclusion embedded in a transversely isotropic, elastic medium of infinite extent, *Int. J. Engng. Sci.*, **18**, 979-986.
- Selvadurai A.P.S., 1981, The behaviour of anchor plates embedded in creep susceptible geological media, *Proc. Int. Symp. Weak Rock*, Tokyo, Japan, A.A. Balkema Pub., 769-775.
- Selvadurai A.P.S., 1984, Elastostatic bounds for the stiffness of an elliptical disc inclusion embedded at a transversely isotropic bi-material interface, *J. Appl. Math. Phys. (ZAMP)*, **35**, 13-23.
- Selvadurai A.P.S., 1993, The axial loading of a rigid circular anchor plate embedded in an elastic half-space, *Int. J. Numer. Anal. Meth. Geomech.*, **17**, 343-353.
- Selvadurai A.P.S., 1994, Analytical methods for embedded flat anchor problems in geomechanics, *Computer Methods in Geomechanics*, Siriwardane and Zaman (eds.), 305-321.
- Selvadurai A.P.S. (Ed.), 1996, *Mechanics of Poroelastic Media*, Kluwer Academic Publications, A. A. Dordrecht, The Netherlands.

- Selvadurai A.P.S., 2000 a, *Partial Differential Equations in Mechanics*, Vol. 1, Springer, Berlin, Germany.
- Selvadurai A.P.S., 2000 b, *Partial Differential Equations in Mechanics*, Vol. 2, Springer, Berlin, Germany.
- Selvadurai A.P.S., 2000 c, An inclusion at a bi-material elastic interface, *J. Engng. Math.*, **37**, 155-170.
- Selvadurai A.P.S., 2001, On some recent developments in poroelasticity, *IACMAG 2001, Proc. 10<sup>th</sup> Int. Conf. On Comp. Meth. Adv. Geomech.*, (C.S. Desai *et al.* Eds.) , Tucson, Arizona, Vol. 2, 1761-1769, A.A. Balkema, The Netherlands.
- Selvadurai A.P.S., 2003, On certain bounds for the in-plane translational stiffness of a disc inclusion at a bi-material elastic interface, *Mech. Res. Commun.*, **30**, 227-234.
- Selvadurai A.P.S., 2004, Stationary damage modelling of poroelastic contact, *Int. J. Solids Struct.*, **41**, 2043-2064.
- Selvadurai A.P.S. and M.C. Au, 1986, Generalized displacements of a rigid elliptical anchor embedded at a bi-material geological interface, *Int. J. Numer. Anal. Meth. Geomech.*, **10**, 633-652.
- Selvadurai A.P.S. and M.C. Au, 1991, Damage and visco-plasticity effects in the indentation of a polycrystalline solid, *Proc. Plasticity 91: 3<sup>rd</sup> Int. symp. Plasticity Current Appl.*, J.P. Boehler and A.S. Khan (Eds.), Elsevier Applied Science, London, 405-408.
- Selvadurai A.P.S. and K.R. Gopal, 1986, Consolidation analysis of the screw plate test, *Proc. 39<sup>th</sup> Can. Geotech. Soc. Conf.*, Ottawa, Canada, 167-178.
- Selvadurai A.P.S. and J. Hu, 1995, The axial loading of foundations embedded in frozen soils, *Int. J. Offshore. Polar Engng.*, **6**, 96-103.
- Selvadurai A.P.S. and A.T. Mahyari, 1997, Computational modelling of the indentation of a cracked poroelastic half-space, *Int. J. Fracture*, **86**, 59-74.
- Selvadurai A.P.S. and T.S. Nguyen, 1995, Computational modelling of isothermal consolidation of fractured porous media, *Comp. Geotech.*, **17**, 39-73.
- Selvadurai A.P.S. and R.K.N.D. Rajapakse, 1985, On the load transfer from a rigid cylindrical inclusion into an elastic half space, *Int. J. Solids Struct.*, **21**, 1213-1229.



- Selvadurai A.P.S. and B.M. Singh, 1984a, Some annular disc inclusion problems in elasticity, *Int. J. Solids Struct.*, **20**, 129-139.
- Selvadurai A.P.S. and B.M. Singh, 1984b, On the expansion of a penny-shaped crack by a rigid circular disc inclusion, *Int. J. Fracture Mech.*, **25**, 69-77.
- Selvadurai A.P.S. and Z.Q. Yue, 1994, On the indentation of a poroelastic layer, *Int. J. Numer. Anal. Meth. Geomech.*, **18**, 161-175.
- Senjuntichai T. and R.K.N.D. Rajapakse, 1993, Transient response of a circular cavity in a poroelastic medium, *Int. J. Numer. Anal. Meth. Geomech.*, **17**, 357-383.
- Shanker N.B., K.S. Sarma and M.V. Ratnam, 1973, Consolidation of a semi-infinite porous medium subjected to surface tangential loads, *Proc. of the Eighth Int. Conf. Soil Mech. Fdn. Engng.*, **1.3**, 235-238.
- Shao J.F., G. Duveau, N. Hoteit, M. Sibai and M. Bart, 1997, Time dependent continuous damage model for deformation and failure of brittle rock, *Int. J. Rock Mech. Min. Sci.*, **34**, 385, Paper No. 285.
- Shao J.F., A. Giraud, N. Ata and D. Soukup, 1998, Modelling elastic damage in unsaturated porous rock, *Proc. the 4<sup>th</sup> Inter. Workshop Key Issues Waste Isol. Res.*, Barcelona.
- Shao J.F., D. Hoxha, M. Bart, F. Homand, G. Duveau, M. Souley and N. Hoteit, 1999, Modelling of induced anisotropic damage in granites, *Int. J. Rock Mech. Min. Sci.*, **36**, 1001-1012.
- Shao J.F., Lydzba D., 1999, Un modele d'endommagement poroélastique pour milieux poreux saturés, *C. R. Acad.Sci. Paris*, t. **327**, Séries II b, 1305-1310.
- Shiping L., L. Yushou, L. Yi, W. Zhenye and Z. Gang, 1994, Permeability-strain equations corresponding to the complete stress-strain path of Yinzhuang Sandstone, *Int. J. Rock Mech. Min. Sci. Geomech. Abstr.*, **31**, 383-391.
- Shirazi A., A.P.S. Selvadurai, 2002, Indentation of a poroelastic half-space susceptible to damage, *30<sup>th</sup> CSCE Conference*, June 1-4<sup>th</sup>, Montreal, QC, Canada, GES 020, 1-10.
- Sidoroff F., 1980, Description of anisotropic damage application to elasticity, *Int. The. Appl. Mech. Symposium Senlis, France, Physical Nonlinearities in Structural Analysis*, (J. Hult and J. Lemaitre, Eds.), Springer-Verlag, Berlin Heidelberg, New York, 237-244.
- Simo J.C. and J.W. Ju, 1987, Strain- and stress-based continuum damage models-II. Computational aspects, *Int. J. Solids. Struct.*, **23**, 841-869.
- Siriwardane H.J. and Desai C.S., 1981, Two numerical schemes for nonlinear consolidation, *Int. J. Numer. Meth. Engng.*, **17**, 405-426.

- Skempton A.W., 1954, The pore pressure coefficients A and B, *Geotechnique*, **4**, 143-147.
- Skoczylas F. and J.F. Shao, 1996, Endommagement de granites: Mesures de perméabilité sous chargement déviatorique, *Scientific Report, RS 96/02*, LML-ANDRA (in French).
- Small J.C. and J.R. Booker, 1987, The time-deflection behaviour of a rigid under-reamed anchor in a deep clay layer, *Int. J. Numer. Anal. Meth. Geomech.*, **11**, 269-281.
- Smith I.M. and D.V. Griffiths, 1988, *Programming the Finite Element Method*, John Wiley & Sons, N.Y.
- Sodeberg L.O., 1962, Consolidation theory applied to foundation pile time effects, *Geotechnique*, **12**, 217-225.
- Souley M., F. Homand, S. Pepa and D. Hoxha, 2001, Damage-induced permeability changes in granite: A case example at the URL in Canada, *Int. J. Rock Mech. Min. Sci.*, **38**, 297-310.
- Spooner D.C. and J.W. Dougill, 1975, A quantitative assessment of damage sustained in concrete during compressive loading, *Mag. Conc. Res.*, **27**, 151-160.
- Stormont J.C. and J.J.K. Daemen, 1992, Laboratory study of gas permeability changes in rock salt during deformation, *Int. J. Rock Mech. Min. Sci. Geomech. Abstr.*, **29**, 325-342.
- Tang C.A., L.G. Tham, P.K.K. Lee, T.H. Yang and L.C. Li, 2002, Coupled analysis of flow, stress and damage (FSD) in rock failure, *Int. J. Rock Mech. Min. Sci.*, **39**, 477-489.
- Terzaghi K., 1923, Die berechnung der durchlässigkeitziffer des tones aus dem verlauf der hydrodynamischen spannungserscheinungen, *Ak. Der Wissenschaften, Sitzungsberichte mathematisch-naturwissenschaftliche Klasse*, Part IIa, 132(3/4), 125-138.
- Terzaghi K., 1943, *Theoretical Soil Mechanics*, John Willey, N.Y.
- Tinawi R. and F. Ghrib, 1994, An anisotropic damage model for the response of concrete gravity dam, *Dam Fracture and Damage International Workshop*, Chamberry, France, 21-30, A.A. Balkema.
- Turska E. and B.A. Schrefler, 1993, On convergence conditions partitioned solution procedures for consolidation problems, *Comput. Meth. Appl. Mech. Engng.*, **106**, 51-63.
- Valliappan S., I.K. Lee and P. Boonlualohr, 1974, *Finite Element Methods in Flow Problems* (J.T. Oden Ed.), Univ. Alabama Press, 741-755.

- Valliappan S., M. Yazdchi and N. Khalili, 1996, Earthquake Analysis of gravity dams based on damage mechanics concept, *Int. J. Numer. Anal. Meth. Geomech.*, **20**, 725-752.
- Valliappan S., M. Yazdchi and N. Khalili, 1999, Seismic analysis of arch dams-a continuum damage mechanics approach, *Int. J. Numer. Meth. Engng.*, **45**, 1695-1724.
- Verruijt A., 1965, Discussion, *Proc. the Sixth Int. Conf. Soil Mech. Fdn Engng.*, **3**, 401-402.
- Vesic A.S., 1971, Breakout resistance of objects embedded in ocean bottom, *J. Soil Mech. Found. Div., ASCE*, **97**, 1181-1206.
- Vesic A.S., 1972, Expansion of cavities in infinite soil mass, *J. Soil Mech. Found. Div., ASCE*, **98**, 265-290.
- Voyiadjis G.Z., J.W. Ju and J.L. Chaboche (Eds.), 1998, *Damage Mechanics in Engineering Materials, Studies in Applied Mechanics*, **46**, Elsevier Science, Amsterdam, The Netherlands.
- Wang P.T., 1977, *Complete Stress-Strain Curve of Concrete and Its Effect on Ductility of Reinforced Concrete Members*, Ph.D. Thesis, University of Illinois at Chicago Circle.
- Wang H.F., 2000, *Theory of Linear Poroelasticity with Applications to Geomechanics and Hydrogeology*, Princeton University Press, Princeton, NJ.
- Wang J.-A. and H.D. Park, 2002, Fluid permeability of sedimentary rocks in a complete stress-strain process, *Engng. Geol.*, **63**, 291-300.
- Whitaker S., 1986, *Transport in Porous Media*, **1**, 3-25, 105-125, 127- 154.
- Whitworth L.J. and A.J. Turner, 1989, Rock socket piles in the Sherwood sandstone of central Birmingham, *Proc. Int. Conf. On Piling and Deep Foundations*, London, Balkema, Rotterdam, 327-334.
- Wohua Z. and S. Valliapan, 1998 a, Continuum damage mechanics theory and application, Part I- Theory, *Int. J. Damage Mech.*, **7**, 250-273.
- Wohua Z. and S. Valliapan, 1998 b, Continuum damage mechanics theory and application, Part II- Application, *Int. J. Damage Mech.*, **7**, 274-297.
- Wong T.T., G.D. Fredlund and J. Krahn, 1998, A numerical study of coupled consolidation in unsaturated soils, *Can. Geotech. J.*, **35**, 926-937.

- Xu K.J. and H.G. Poulos, 2000, General elastic analysis of piles and pile groups, *Int. J. Numer. Anal. Meth. Geomech.*, **24**, 1109-1138.
- Yue Z.Q. and A.P.S. Selvadurai, 1994, On the asymmetric indentation of a consolidating poroelastic half space, *Appl. Math. Model.*, **18**(4), 170-185.
- Yue Z.Q. and A.P.S. Selvadurai, 1995, On the mechanics of a rigid disc inclusion embedded in a fluid saturated poroelastic medium, *Int. J. Engng. Sci.*, **33**, 1633-1662.
- Yue Z.Q. and A.P.S. Selvadurai, 1995, Contact problem for saturated poroelastic solid, *J. Engng. Mech., ASCE*, **121**(4), 502-512.
- Zhang L. and M.B. Dusseault, 1997, Evaluation of formation damage from a constant-head borehole test, *Int. J. Rock Mech. Min. Sci.*, **34**, 561, Paper No. 360.
- Zhou Y., R.K.N.D. Rajapakse and J. Graham, 1998, Coupled consolidation of a porous medium with a cylindrical or a spherical cavity, *Int. J. Numer. Anal. Meth. Geomech.*, **22**, 449-475.
- Zhu W. and T.-F. Wong, 1997, Transition from brittle faulting to cataclastic flow: Permeability evolution, *J. Geophys. Res.*, **102**, 3027-3041.
- Zienkiewicz O.C. and R.L. Taylor, 2000, *The Finite Element Method*, Volume 1, 5<sup>th</sup> edition, Butterworth-Heinemann, Oxford.
- Zoback M.D. and J.D. Byerlee, 1975, The effect of micro-crack dilatancy on the permeability of Westerly Granite, *J. Geophys. Res.*, **80**, 752-755.
- Zureick A.K., 1988, Transversely isotropic medium with a rigid spheroidal inclusion under an axial pull, *J. Appl. Mech.*, **55**, 495-497.

## MAIN ACHIEVEMENTS OF THE THESIS

The work presented in this thesis introduces a new three-dimensional iterative finite element procedure has been developed to examine the influence of the isotropic damage-dependent alterations in both the elasticity and fluid transport characteristics of the damage-susceptible poroelastic geologic media. The computational scheme proposed in this research can also examine the influence of stress state-dependency on the evolution of damage. The detail related to the three-dimensional finite element program used in this research is available in Appendix A.

The computational developments have been applied to a range of problems of interest to geomechanics and civil engineering. The computational simulations indicate that the damage-induced alterations in hydraulic conductivity has a greater influence on the time-dependent response of the damage susceptible poroelastic medium.

The stress state-dependency of the damage process can also influence the time-dependent response of a damage-susceptible poroelastic medium.

## APPENDIX A

### THREE-DIMENSIONAL FINITE ELEMENT PROGRAM USED IN THE RESEARCH

The three-dimensional finite element program developed for the research can examine the coupled behaviour of damage-susceptible poroelastic media. The program performs an incremental non-linear analysis using the classical theory of poroelasticity developed by Biot (1941) with updated poroelastic parameters at each increment. The program has been written in FORTRAN 90. A twenty-node isoparametric element is used and the displacements within the element are interpolated as functions of the twenty nodes, whereas the pore pressures are interpolated as functions of only the eight corner nodes. This configuration allows less spatial oscillations in the computational results at early times. The poroelastic parameters are updated using the damage variables determined at twenty seven Gauss integration points of each element.

The program can also accept the finite element discretization and boundary conditions, generated by stress analysis software COSMOS 2.5 M developed by *Structural Research and Analysis Corporation*, as input data and apply the proposed computational scheme through this research to the three-dimensional domain.

The finite element program determines the nodal displacements and pore pressures solving the system of equations through Gauss back substitution method. Any person interested to have access to the three-dimensional finite element program developed in this research can contact with Professor A.P.S. Selvadurai, William Scott Professor in department of civil engineering and applied mechanics, McGill University or Mr. Ali Shirazi.